An investigation into the biology and function of protein Icb-1

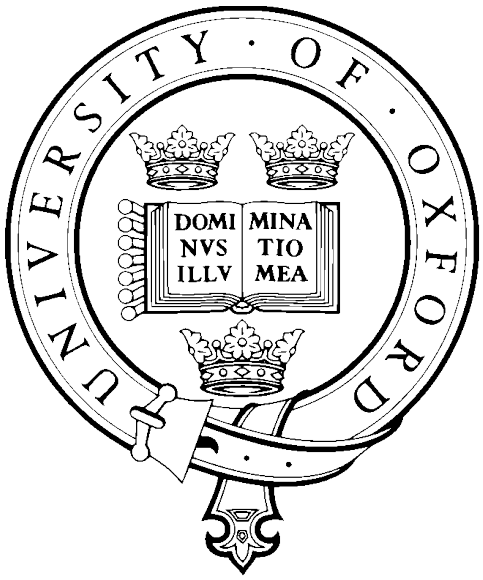

A thesis submitted for the
Doctor of Philosophy Degree

Daian Cheng

October 2012

Supervised by Professor Richard Cornall

Acknowledgement

I would first like to thank my supervisor, Professor Richard Cornall for accepting me for this intriguing project and his insightful help all the way through. My thanks also go to my funding bodies, the Wellcome Trust and Clarendon Fund, as well as Oxford University and Lincoln College for enabling this opportunity. I thank my colleges who provided assistance and inspiration in many aspects of my research life, especially Tanya, Delphine, Katherine, Sophia and Consuelo who directly contributed to the project.

I would full heartedly thank my parents who have made everything possible and supported me with all they could. I would also give thanks to Hedge, who has always been empathising, encouraging and helpful, even at the toughest times.

Summary

In this thesis I describe an investigation into the function of the protein Icb-1, a homologue of Themis1 in B cells and monocytes. Themis1 is important for T cell positive and negative selections. Yet its function in T cell development is not clear. Although it shows characteristics of an adaptor protein and involvement in TCR-induced signalling, the exact signalling defects in Themis1$^{-/-}$ T cells remain obscure. Icb-1 is similar to Themis1 in sequence, function and binding partners. It has been studied in human tumour and macrophage cell lines, leading to limited conclusions. Its role in B cells has never been published. Given the link with Themis1, it is of great interest to investigate the function of Icb-1.

My study has been focused on the comparison between Icb-1 knockout mice with wild-type controls. I characterised the B cell development in Icb-1$^{-/-}$ mice, either naturally born or produced as mixed adult bone marrow chimeras reconstituted from WT and Icb-1$^{-/-}$ donor cells. I examined the possible compensation and redundancy of Themis1 and Icb-1, by characterising Thems1/Icb-1 double knockout mice. The Ig-HEL mouse models were used to examine the change in B cell repertoire due to negative and positive selections. The mice were challenged with SRBCs or NP-CGG to examine the germinal centre response to foreign antigen when Icb-1 is absent. *In vitro* stimulation of B cells with soluble and membrane-bound antigens was used to investigate early B cell responses in detail and to give insights into the defects found in *in vivo* challenges. Finally, I examined the BCR-induced phosphorylation of key signalling molecules and Ca^{2+} flux in splenic B cells.

The study revealed largely normal B cell development with subtle selection impairments, but a partially defected B cell immune response to antigens in

Icb-1$^{-/-}$ mice. The marginal zone B cell population was enlarged in the absence of Icb-1, while the positive selection of B1 B cells induced by intracellular self-antigen was impaired. The deficient mice showed a reduction in germinal centre B cell generation. The defects are associated with impaired BCR-induced cell signalling to low abundance and/or low avidity antigens. In particular, Ca^{2+} flux and Erk1/2 phosphorylation were clearly reduced under certain conditions.

The results shine a light on the function of protein Icb-1, and also improve our knowledge of Themis1 and the Themis family. They provide a new avenue of investigation into the regulation of BCR signalling, especially in Ca^{2+} flux induction and Erk1/2 activation. They also provide insight into how differential signalling is controlled within cells during activation and differentiation in response to antigens that vary in terms of affinity, avidity and frequency.

Abbreviations

APC, antigen presenting cell

B6, C57BL/6

BAM32, B-lymphocyte adaptor molecule of 32 kDa

BCAP, B-cell adapter for PI3K

BCR, B cell receptor

BLNK, B-cell linker

BM, bone marrow

BSA, albumin from bovine serum

Btk, Bruton's tyrosine kinase

CABIT, cysteine-containing, all-β in Themis

CD, cluster of differentiation

CFSE, 5(6)-carboxyfluorescein diacetate N-succinimidyl ester

CLP, common lymphoid progenitors

CRAC, Ca^{2+}-release-activated Ca^{2+}

DAG, diacylglycerol

DC, dendtritic cell

DN, double negative

DNA, deoxyribonucleic acid

DP, double positive

DZ, dark zone

EGFR, epidermal growth factor receptor

ELISA, enzyme-linked immuno-sorbent assay

ELP, early lymphoid progenitor

ENU, ethyl-N-nitrosourea

ER, endoplasmic reticulum

FCS, foetal calf bovine serum

FDC, follicular dendritic cell

FO, follicular

FOXO, forehead box class O

Gads, Grb2-related adaptor downstream of Shc

GC, germinal centre

GEF, guanine nucleotide-exchange factor

Grb2, growth factor receptor bound protein 2

Grap, Grb2-related adaptoer protein

GSK3, glycogen synthase kinase-3

H9, HyHEL9

HBSS, Hanks' balanced salt solution

HC, heavy chain

HEL, hen egg lysozyme

HSC, hematopoietic stem cell

Ig, immunoglobulin

IKK, IκB kinase

IL, interleukin

IP_3, inositol-(1,4,5)-trisphosphate

ITIM, immuno-receptor tyrosine-based inhibitory motif

ITT, immunoglobulin tail tyrosine

LC, light chain

LPS, lipopolysaccharides

LT, lymphotoxin

LZ, light zone

MBL: mannose-binding lectin

MLN, mesenteric lymph node

MZ, marginal zone

NFAT, nuclear factor of activated T cells

NFkB1, nuclear factor-κB1

NK, natural killer

NLS, nuclear localization sequences

PBS, phosphate buffered saline

PCR, polymerase chain reaction

PDBu, Phorbol 12,13-dibutyrate

PH, pleckstrin homology

PI3K, phosphatidylinositol-3 kinase

PIP2, phosphatidylinositol-(4,5)-bisphosphate

PIP3, phosphatidylinositol-(3,4,5)-trisphosphate

PIRB, immunolglobgulin-like receptor B

PKC, protein kinase C

PMCA4, plasma membrane calcium-ATPase 4

RasGRP, Ras guanine nucleotide-releasing proteins

RNA, ribonucleic acid

SEM, standard error of mean

SFK, src family kinase

SH2, Src homology 2

SHIP, SH2-domain-containing inositol polyphosphate 5' phosphatase

SHP1, SH2-domain-containing protein tyrosine phosphatase 1

SMH, somatic hypermutation

SNP, single nucleotide polymorphism

SOCE, store-operated Ca^{2+} entry

SP, single positive

Spl, spleen

SRBC, Sheep red-blood cell

Syk, spleen tyrosine kinase

T1, transitional stage 1

TBM, tingible-body macrophage

TCR, T cell receptor

TD, T cell dependent

TdT, terminal deoxynucleotidyl transferase

Tfh, follicular helper T cell

Themis, thymus-expressed molecule involved in selection

TI, T cell independent

TLR, toll-like receptor

Treg, regulatory T cells

WB, western blot

Table of contents

ACKNOWLEDGEMENT **2**

SUMMARY **3**

ABBREVIATIONS **5**

TABLE OF CONTENTS **9**

CHAPTER ONE INTRODUCTION **12**

1.1. Themis1 and Icb-1 (Themis2) **12**
1.1.1. Themis1 and the Themis family 13
1.1.2. Previous studies on Icb-1 16

1.2. B cell development in the pre-immune repertoire **21**
1.2.1. Overview 21
1.2.2. B cell development in the bone marrow 22
1.2.3. B cell development in the periphery 24

1.3. B cell tolerance **26**
1.3.1. Tolerance during B cell development 26
1.3.2. Tolerance during immune responses 28

1.4. B cell in immunity **30**
1.4.1. B cells in humoral immune response 30
1.4.2. The germinal centre 34

1.5. B cell receptor signalling **40**
1.5.1. Overview of Signalling downstream of BCR 40
1.5.2. Ca^{2+} flux 45
1.5.3. BCR-induced Erk1/2 signalling 48
1.5.4. Grb2 in BCR signalling 51

CHAPTER TWO MATERIALS AND METHODS **55**

2.1. Reagents **55**
2.1.1. Antibodies 55
2.1.2. Buffers and other reagents 56

2.2. Animal keeping and procedures **62**
2.2.1. Mouse keeping and breeding 62
2.2.2. Genotyping of transgenic mice 62
2.2.3. Procedures involving live animals 64

2.3. General procedure **66**
2.3.1. Western blot and related 66
2.3.2. Flow cytometry and related 68
2.3.3. Sandwich ELISA 71
2.3.4. Cell culturing 73

2.3.5. Whole-genome sequencing 76
2.3.6. Real-time PCR 77

CHAPTER THREE B CELL DEVELOPMENT IN THE PRE-IMMUNE REPERTOIRE IN ICB-1 KNOCKOUT MICE 80

3.1. Introduction 80

3.2. Icb-1 expression in wild-type mice and the examination of knockout mice 81

3.3. Lymphocyte Development 86
3.3.1. Icb-1$^{-/-}$ mice 86
3.3.2. Mixed chimera 93

3.4. Icb-1$^{-/-}$Themis1$^{-/-}$ mice 96

3.5. B cell development in Icb-1$^{-/-}$ Ig mice 104
3.5.1. Icb-1$^{-/-}$ Ig mice 104
3.5.2. Selection of B cells reactive towards membrane-bound self-antigen 106
3.5.3. Selection of B cells reactive towards soluble self-antigen 111
3.5.4. Positive selection of B1 B cells reactive towards intracellular self-antigen 114

CHAPTER FOUR THE RESPONSES OF ICB-1$^{-/-}$ B CELLS TO FOREIGN ANTIGENS 118

4.1. Introduction 118

4.2. *In vivo stimulation* 118
4.2.1. SRBCs 118
4.2.2. NP-CGG 121
4.2.3. NP-Ficoll 123

4.3. *In vitro* stimulation 125
4.3.1. Soluble antigens 125
4.3.2. Membrane-bound antigens 127
4.3.3. IL-2 production 129
4.3.4. Proliferation 130

CHAPTER FIVE B CELL RECEPTOR SIGNALLING IN ICB-1$^{-/-}$ B CELLS 135

5.1. Introduction 135

5.2. Phosphorylation of signalling molecules down-stream of BCR 135

5.3. Ca^{2+} flux in Icb1$^{-/-}$ B cells 139

CHAPTER SIX DISCUSSION AND FURTHER WORK 141

6.1. Summary of observations 141

6.2. Analysis and hypothesis 147
6.2.1. Themis1 and Icb-1 147
6.2.2. Icb-1 in BCR-induced signalling 149

6.3. Summary and future work 152

APPENDIX **154**

A.1 **154**

A.2 **154**

A.3 **156**

A.4 **157**

REFERENCE **162**

Chapter One Introduction

1.1. Themis1 and Icb-1 (Themis2)

The interest in the protein Icb-1 in my group is a continuation from the studies in its T cell homologue Themis1, by previous student Andy Johnson who published the results on Themis1-deficient mice generated by ethyl-N-nitrosurea (ENU) mutagenesis[1].

As will be described in more details in later sections, Themis1 deficiency in mice caused a T cell developmental block at the double positive (DP, $CD4^{+}CD8^{lo}$) stage. There was evidence to suggest that Themis1 is an adaptor protein involved in T cell receptor (TCR) signaling, yet few and obscure defects were found in TCR signalling in Themis1-deficient T cells. As a Themis1 homologue, Icb-1 was shown to have a similar sequence, functions and binding partners. Judging by the homology, Icb-1 was also suggested to be involved in signalling and cell selection. It had been identified in human cancer cells and was later studied in macrophage cell lines, but its function remained unclear and studies in B cells have never been published.

This study aims to characterise mice deficient in Icb-1 and in doing so, investigate the function of the protein. The directions of the study were influenced by the homology and current findings of Themis1. It is hoped that the result of my investigations will shine light on the function of Themis1 and the other novel Themis family proteins.

1.1.1. Themis1 and the Themis family

Several studies on Themis1 were first published in 2009[1-4]. The name Themis is short for *T*hymus-*E*xpressed *M*olecule *I*nvolved in *S*election, and coincidentally is also the name of an ancient Greek Titaness who is the embodiment of divine order, law and custom.

One of the ways to gain new understanding of the processes involved in lymphocyte selection and antigen receptor signalling is to look for naturally-occurring or ENU-induced mutant mice with defects in these processes. Using this approach, a previous student in my group, Andy Johnson, identified a mouse strain with a block in T cell development in the thymus[1], which was later found to have a nonsynonomous mutation in the Themis1 gene. At the same time, Fu *et. al.* and Lesourne *et. al.* identified the Themis1 gene in searches for genes that affect T cell development[2,3].

The expression of Themis1 was found in lymphoid tissues and was the highest in the thymus. Its expression is the highest in double positive T cells and is down-regulated in the single positive (SP, $CD4^+CD8^-$ or $CD4^-CD8^+$) T cells. Themis1 knockout ($Themis1^{-/-}$) mice showed normal numbers of double negative (DN) T cells, enlarged DP T cell populations and much reduced numbers of SP T cells, especially that of $CD4^+$ SP T cells. Other subpopulations of mature T cells were normal, except for a slightly enlarged regulatory T cell (Treg) population.

Detailed studies showed that the T cell maturation was blocked at the earliest stage of positive selection in $Themis^{-/-}$ mice. By using genetically modified mouse models, it was shown that both the positive and negative selections of $Themis1^{-/-}$ T cells could be defective. These effects were believed to be a

result of attenuated TCR signalling. But the results from studying the detailed down-stream pathways in these reports were not in agreement.

Themis1$^{-/-}$ T cells were found to have normal amounts of surface expressions of TCR, CD3, CD5 and CD69 at different developmental stages. Theims1 protein was phosphorylated very quickly (within 30 seconds) after TCR cross-linking. It was also shown to bind to the adaptor protein Grb2 constitutively and the binding increased after TCR stimulation. This association was shown to be specific and possibly via the SH2 and/or SH3 domain of Grb2. Fu *et. al.* showed normal phosphorylation of Zap70, PLCγ1 or Itk (LAT) in Themis1$^{-/-}$ T cells[3]. In contrast to the other groups, they observed impaired Ca^{2+} flux and Erk1/2 phosphorylation in Themis1$^{-/-}$ T cells following TCR stimulation. The phosphorylation of the kinases Raf, Mek and JNK were not affected.

Phylogentic analysis revealed two other mammalian genes related to Themis1, Icb-1 (Themis2), which is expressed in B cells, dendritic cells and macrophages) and 9130404H23Rik, which is principally expressed in the intestine. Combined with structural prediction and comparison, Johnson *et.al.* defined a conserved protein domain that was named the CABIT domain (for '*C*ysteine-containing, *A*ll-*β* *I*n *T*hemis')[1]. They then defined an enlarged Themis-related family, including Icb-1 and 9130404H23Rik, throughout Metaxoans, in which all members contain the CABIT domain and the conserved proline-rich regions (Figure 1.1).

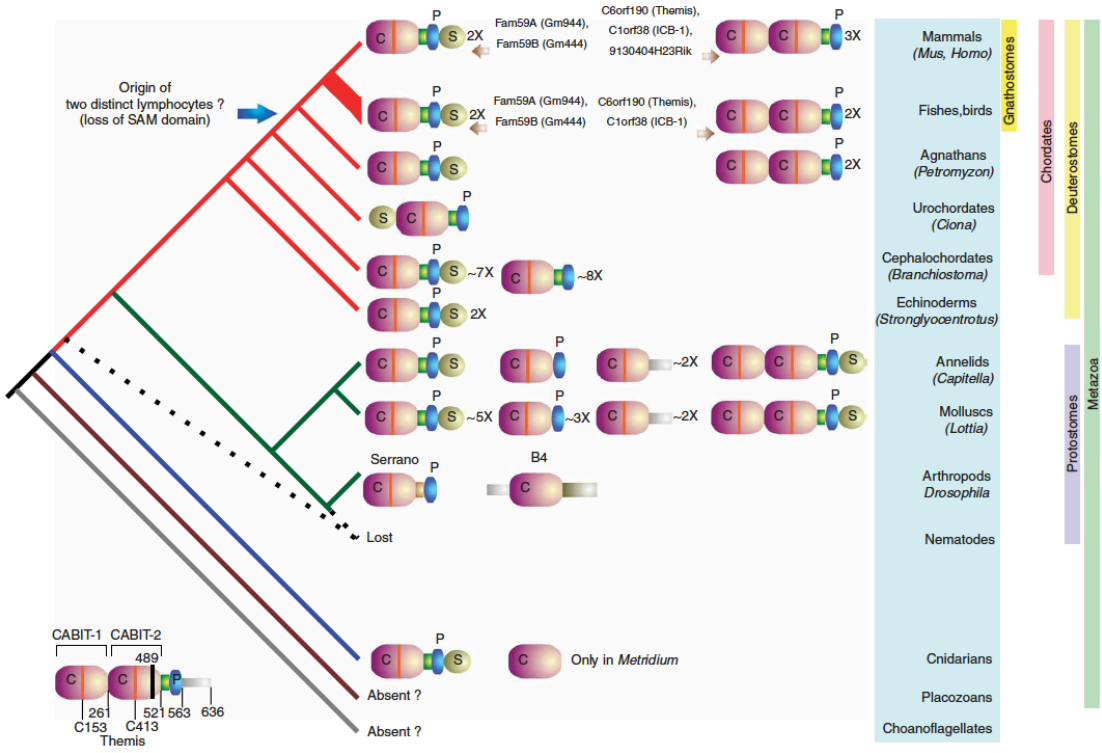

Figure 1.1 Figure and caption taken from publication of Johnson et. al.. Reprinted by permission from Macmillan Publishers Ltd: Nature Immunology[1], copyright 2009. Domain architectures and evolution of the CABIT domain. Bottom left, Themis structure, including two globular CABIT domains (CABIT-1 and CABIT-2; purple), a proline-rich region (blue), a conserved helical segment (green), conserved cysteine motifs (orange bars), the site of the substitution (black bar) and the location of key amino acid residues. Main image, superimposition of similar domain architectures for all CABIT domain–containing proteins on the animal phylogenetic tree (right margin, principal animal groups): C, CABIT domain; S, SAM domain; P, low-complexity proline-rich stretch; green elements, conserved helical elements preceding the proline-rich region; gray elements, extensions unique to particular proteins; orange bar, conserved cysteine in the CABIT domain (those representatives lacking it are presumed to be inactive versions of the domain). Numbers of family members are presented as 2X–8X, and for gnathostome vertebrates and insects, ortholog names are also included.

Lesourne *et. al.* followed up their original observations on Themis1 and showed interchangeable functions of Themis1 and Icb-1 in T cells[5]. They demonstrated that the transgenic expression of either protein could rescue the T cell developmental defects in Themis1$^{-/-}$ mice. Both proteins were found in the nucleus and cytoplasm despite their differences in putative nuclear localization sequences (NLS). Slight difference in their proline-rich regions resulted in no difference in binding to Grb2 following TCR engagement. Lesourne *et. al* also reported impaired phosphorylation of Vav1, Erk1/2 and p38 in Themis1$^{-/-}$ SP T cells (but not in DP T cells), which could be corrected by the expression of either Themis1 or Icb-1 transgene. This study is the first

to demonstrate functional similarities of the members of the Themis family and provides more inspiration and grounds for the study of Icb-1.

1.1.2. Previous studies on Icb-1

The human Icb-1 gene was first identified and isolated by Treeck *et. al.*, and was found to be up-regulated when the human endometrial adenocarcinoma cell line HEC1B responded to reconstituted basement membrane[6]. It was hence named 'induced on contact with basement membrane 1'. Over the years, the same group published data on studies of Icb-1 in human cancer cell lines. They found the mRNA levels of two Icb-1 isoforms, Icb-1α and β, increased in a time-dependent manner during the differentiation of HL-60 cells[7]. (The 11 currently known human Icb-1 splicing variants are shown in Figure 1.2.) The expression of Icb-1 was found to increase after the treatment of three breast cancer and one ovarian cancer cell lines with IFNγ[8].

Reduction in Icb-1 expression resulted in lower cell numbers after IFNγ-induced proliferation. In a similar study published in 2008, Icb-1 was estrogen-responsive in an ERα-dependent manner[9]. A recent clinical study tested 323 breast cancer patients and an equal number of healthy women for single nucleotide polymorphisms rs1467465 (Figure 1.2, marked in green) and rs12048235 (Figure 1.2, marked in blue)[10]. The patients showed higher frequency in carrying the A allele of SNP rs1467465 than healthy women, while the frequency of carrying either the A or G allele of rs12048235 was very similar between the two groups. Thus, the A-allele frequency of polymorphism rs1467465 can be associated with an increased risk of breast cancer.

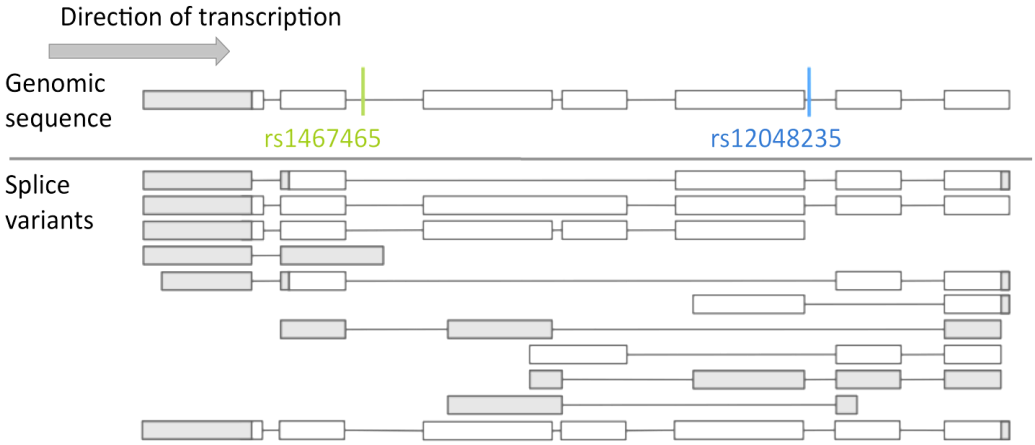

Figure 1.2 Illustrations of human Icb-1 gene (C1orf38) and the 11 known splice variants, as well as the locations of the two SNPs studied in relation to breast cancer risk. The information on the genomic DNA and splice variants was obtained from Ensemble; the information on the locations of the two SNPs were from NCBI's SNP database. The clear boxes show coding DNA sequence or transcrips; the grey boxes show nontranslated region or noncoding transcripts; lines show introns.

Studies on Icb-1's functions in murine immune cells started after the recognition of its similarities to Themis1. The relevance of the two proteins was based on both sequence similarities and structure predictions (hence it is also called Themis2 The genomic sequence and protein structure of mouse Icb-1 is shown in Figure 1.3a. They share 29% identity and 65% homology at the amino acid level. The two proteins were found to have no active sites but conserved tandem CABIT domains, as well as conserved sequence patterns that could be used in phosphorylation, SH2 and SH3 domain interactions. These findings provided clues on Icb-1's function and mechanism in line with those of Themis1.

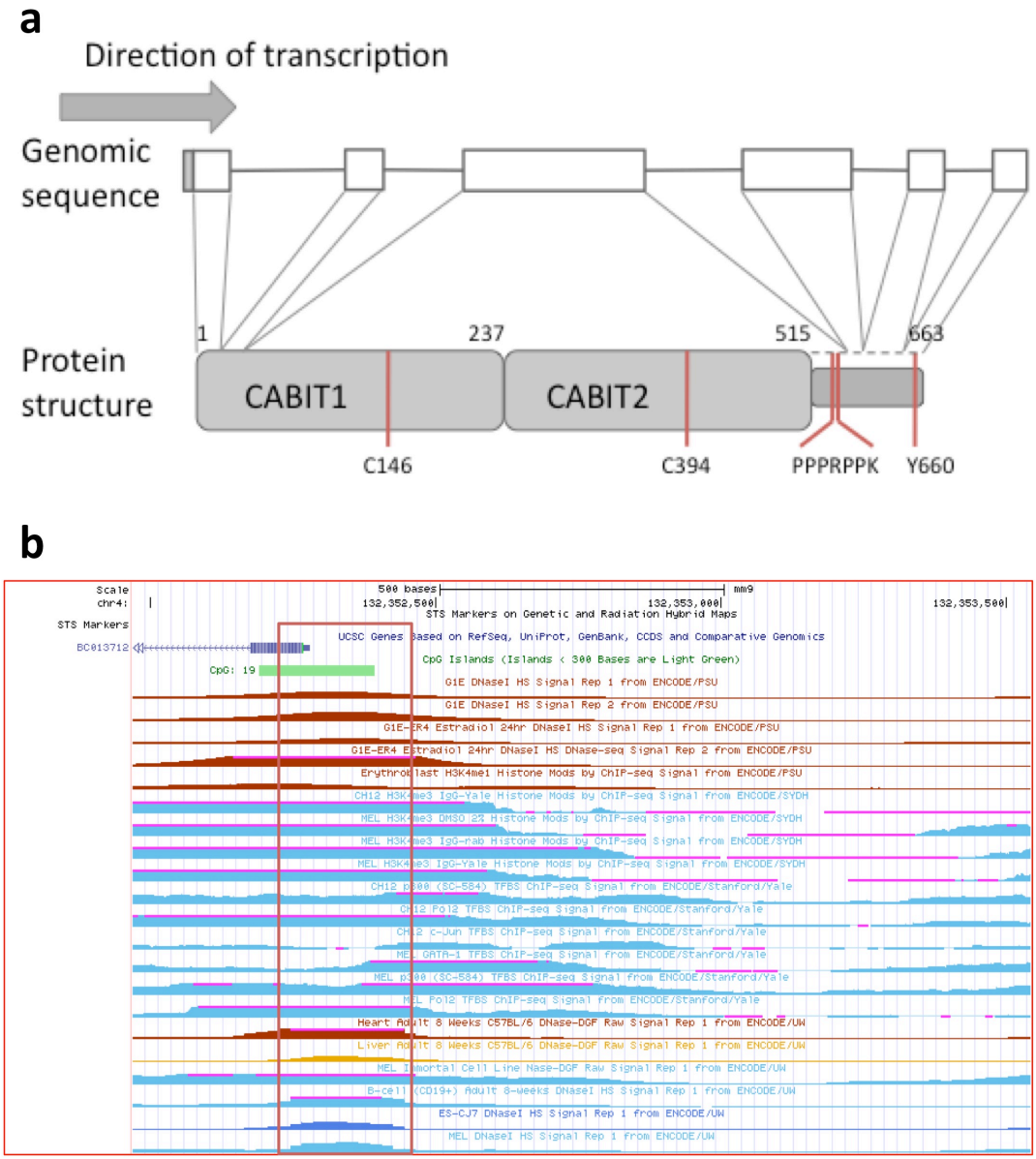

Figure 1.3 a) Illustraion of the genomic sequence and protein structure of Icb-1. For the genomic sequence, the clear boxes show extrons and the lines show introns. In the illustration of protein structure, the two prediced CABIT domains are shown, together with key amino acids: two highly conserved cyctein residues within the CABIT domains, a proline-rich region and a tyrosin residue that was shown to be phosphorylated upon cell stimulation. b) Picture from USCS showing selected ChIP-seq result peaks around the initiation of the icb-1 gene.

There has been no detailed study any other features of the icb-1 or themis1 genes. Murine *icb-1* gene contains 6 exons (Figure 1.3a). Current ChIP-seq data from ENCODE (USCS) showed a CpG island region containing 203 bps and 19 CpG islands, immediately upstream of Exon 1 (Figure 1.3b, in bright green). This region also extensively coincides with peak regions containing

DNase I, pol II and p300. However, the CpG island region marked in Figure 1.3b covered much of Exon 1 and hence unlikely to be reliable. An exact promoter region of the gene is yet to be defined. A search of predicted transcription factor binding sites was done using sequence 500bp upstream of the start of the *icb-1* gene (sequence shown in Appendix, Section A.1). Among all the online tools used, data from http://trap.molgen.mpg.de/cgi-bin/home.cgi and from http://www.cbrc.jp/research/db/TFSEARCH.html (using TFSEARCH Version1.3) were the easiest to understand. The former search gave 27 possible binding transcription factors with p-values smaller than 0.05, while the latter gave 20 with an arbitary score over 80. The result is enclosed in Apendix (Section A.2). Transcription factors appear in both sets are highlighted. More accurate information on transcription factors affecting Icb-1 expression requires further experimentation.

Peirce *et. al.* studied Icb-1's involvement in toll-like receptor (TLR) downstream signalling using the macrophage cell line RAW 264.7[11]. They demonstrated that both the phosphorylation of Icb-1 after TLR4 stimulation induced by LPS, as well as that Icb-1 over-expression resulted in enhanced TNF production. In the downstream pathways, Erk1/2 and p38 were shown to be affected, while the activation of JNK, IRF3 and NF-kB p65 remain unchanged. Icb-1's binding to Lyn, Vav and Grb2 was shown in expression cell lines and was shown to be subject to the intact and phosphorylated Tyrosine 660 residue and the proline-rich sequence of Icb-1.

Commercially available Icb-1 knockout mice (on C57BL/6 background) have been produced by the International Knockout Mouse Consortium and a testing result could be found from the Sanger institute[12,13]. It is reported that the knockout mice showed normal behaviour and physiology (in various tissue tests), including normal haematology. Data on plasma immunoglobulin tests were not available. The knockout mice were also found to be normal in

bacteria infection challenges using both *Salmonella Typhimurium* (*i.v.*) and *Citrobacter rodentium* (oral). The only defect was observed in the micronucleus test, which may indicate chromosomal instability of these mice.

1.2. B cell development in the pre-immune repertoire

1.2.1. Overview

Broadly speaking, there are three types of mature B cells in the pre-immune repertoire: follicular (FO) B cells, marginal zone (MZ) B cells and B1 B cells. FO B cells and MZ B cells are also collectively called B2 B cells. FO B cells are the most abundant B cell population.

These three mature B cell populations have distinct localizations in the body[14] as well as specialized functions related to their locations and properties. FO B cells reside in the B cell follicles of secondary lymphoid organs, circulate the body and return to the BM as re-circulating mature B cells. In their naïve state they do not proliferate but persist for several months. MZ B cells, as their name suggests, localize in the marginal zones of the spleen, where antigens are filtered and scavenged from the blood[15]. B1 B cells are mainly found in the peritoneal and pleural cavities. A small number of them can be found in the spleen. They are predominantly replaced by self-renewal rather than from newly-formed bone marrow B cells[16,17].

In terms of function, MZ B cells and B1 B cells share some similarities in immune responses and may in part constitute a form of natural memory. Their receptors are biased towards bacterial cell-wall constituents and senescent self-components. Their locations mean that they get in contact with antigens directly and at early stages. They initiate fast T cell independent (TI) reactions to foreign antigens by becoming plasma cells. They are both sensitive to blood-born particulate antigens and are placed to react to local infections[15]. B1 B cells also produce the majority of natural antibodies in circulation. In contrast, FO B cells are believed to be mainly involved in the T cell dependent (TD) response, the formation of germinal centres (GC) and the subsequent generation of long-lived plasma and

memory B cells. Their location in the spleen follicles enables them to contact T cells easily. There is also evidence that MZ B cells contribute to the formation of the germinal centre, at least at the early stage, and possibly in the role of antigen transportation[18].

The development of B cells, or at least B2 B cells, starts in the bone marrow. When they reach the immature B cell stage, they leave the bone marrow and enter the periphery where they develop further and differentiate into mature B cells. B1 B cells predominantly originate from the foetal liver and fewer B1 B cells are produced when BM becomes the site of B cell production shortly after birth. This is related to the fact that B1 B cells are self-renewing[17]. However, the maturation of B1 B cells is strongly subject to BCR signalling, suggesting a common selection process of B1 B cells and B2 B cells[19,20].

1.2.2. B cell development in the bone marrow

The description of B cell development could start from the hematopoietic stem cells (HSCs). They can be broadly considered as cells with abilities of self-renewal and potential to develop into all blood-cell lineages. Before the cells express B220 or other markers specific to the B cell lineage, they undergo a series of differentiation steps, which are best described as a step-wise yet continual re-balancing of lineage potentials. Epigenetic studies have provided many characteristics on the chromosomal or RNA level among these stages[21], yet the cause of these changes can still only be described in terms of “environmental cues”. The localized niches formed by stromal cells provide the stem cells with cellular and soluble factors which regulate fate choices[22]. The mechanism of this regulation is largely unknown. Nevertheless, some signals have been shown to influence B cell lineage choices[23,24].

The separation and identification of different developmental stages before clear lineage commitment are challenging. The HSCs can be identified by the surface expression of high levels of CD117 (c-kit, a stem cell factor receptor) and the absence of other lineage molecules. Yet this $CD117^{hi}Ln^{neg}$ population is heterogeneous. Within it, there are early lymphoid progenitors (ELPs), that can be identified by the expression of transcription factors Ikaros, PU.1, E2A, and EBF1[25]. They express lymphocyte-restricted genes, such as terminal deoxynucleotidyl transferase (TdT), which is involved in antigen receptor recombination. Activation of the lymphocyte-restricted recombinase activating genes, particularly Rag-1, in a fraction of the TdT^+ ELPs, makes them particularly lymphoid biased[26] and develop into common lymphoid progenitors (CLPs), which start to express IL-7R (CD127). MicroRNA may play some roles in this development step[27,28]. CLPs have the potential to develop into B, T, natural killer (NK) and dendritic cells (DC), yet some have B cell bias[29,30], and there is evidence of extensive immunoglobulin (Ig) heavy chain (HC) DJ rearrangement in the CLPs[31]. These cells start to express cell surface B220 and can be recognised as early (pre-pro) B cells.

In the pro-B cells stage, B cells rearrange the Ig heavy chain gene in the order of D-J and V-DJ. These heavy chains are paired with germ-line encoded surrogate light chains (LC) to form pre-BCRs[32,33]. Cells expressing a functional pre-BCR express the IL-7 receptor and undergo proliferation as large pre-B cells, before turning on Rag gene expression and rearranging light chain genes. At least in adults, immature cells with complete BCRs pass through a negative selection point where self-reactive B cells undergo rounds of light chain editing to remove or reduce self-reactivity[34]. The result is non-self-reacting immature B cells, clonal depletion or anergic B cells. (Also see later Section 1.3 for B cell tolerance.)

With the invention and rapid development of flow cytomery, cells at different developmental stages can be distinguished using surface molecules[35]. The bone marrow B cells can be first separated into mature/recirculating B cells (IgD^{+}) and developing B cells (IgD^{neg}). Within the latter, IgM^{+} cells are late-pre-B cells or newly formed immature B cells. Before the completion of HC rearrangement, B cells express surface CD45R (B220) and CD43, which are used to identify early stage B cells. Hence $B220^{+}Ig^{neg}$ cells are pre- and pro-B cells. They can be further separated according to expressions of CD43, CD24[35], CD117, CD127 (IL-7Rα), CD25 (IL-2Rα)[36] and CD93[31]. Heterogeneity and the co-existence of multiple lineage potentials, makes it difficult to separate early developmental stages clearly.

1.2.3. B cell development in the periphery

Newly formed B cells leave the bone marrow and enter the periphery. They are called “transitional B cells”, which can be further divided into T1-T3 stages according to their surface expressions of CD93, CD23 (low affinity IgE receptor) and IgM[37]. Due to the heterogeneity and the transient nature of these stages, there are debates about the division with transitional B cells. An alternative model does not include the T3 stage. There are also suggestions of MZ B cell precursors, also referred to as FO-II cells[38,39]. I shall not discuss this in detail here. At this stage, cell fate is largely dependent on the encounter of antigens and BCR signalling. It was shown in B cells expressing only the cytoplasmic domains of CD79αβ (Igα) and CD79β (Igβ) that tonic BCR signals can retain survival but further signals are needed for differentiation[40]. The survival of B2 B cells, but not their differentiation also depends on BAFF and BAFF receptors [41]. It was shown that BCR stimulation can increase the expression of BAFF receptors in B cells at T2 and T3 stages[42,43].

BCR signalling is important in determining B cell differentiation into follicular, marginal zone or B1 B cells[44]. There is no definitive route for any populations and BCR signalling is not the only factor in making this decision. Evidence suggests that intermediate BCR singling leads to follicular B cell production, strong signals select for B1 B cells and weaker BCR signalling favours MZ B cells[44]. For example, Btk-deficient mice showed reduced Ca^{2+} flux and PKC activation and produced more MZ B cells than follicular or B1 B cells[45]. Removal of positive regulators of BCR signalling, such as BLNK or CD19, led to the absence of B1 B cells[46-48], while increased B1 B cell populations were found in mice deficient in negative regulators such as CD22 and PIRB[49,50].

Due to the different localizations of the three mature B cell populations, distinct signals, in addition to those from BCR, contribute to the development. Cytokine signalling is important for the homing and as a result, the differentiation of MZ B cells[51,52]. Microbial products and TLR activation may induce the productions of MZ and B1 B cells[53]. MZ B cell maturation uniquely requires Notch2 signalling[54,55]. BAFF signalling is also more important for MZ B cell development[56]. The cellular location of self-antigen may be another important variable. In the hen egg lysozyme (HEL) and anti-HEL Ig transgenic model, intracellular HEL antigen positively selects B1 B cells, whilst the same antigen that is surface-bound or secreted leads to self-tolerance by receptor editing, deletion or anergy, respectively[57].

1.3. B cell tolerance

A large proportion of newly formed B cells are to some degrees self-reactive[58]. The formation of BCR is through random VDJ rearrangement. The somatic hypermutations (SMH) in the germinal centres are also random. These processes generate BCRs with broad affinities and specificities. Unavoidably, the random nature of the processes also generates reactivity towards self-antigens. Yet the occurrence of autoimmunity is low. The tolerance towards self-antigens is achieved through selections of immune cells. The development and function of B cells heavily depend on the BCR. It is hence the main target of B cell immune tolerance. At the checkpoints, the B cells that manage to successfully produce functional BCRs are positively selected. Those that bind to self-antigens must be modified in a way that balances their risk against potential benefit. The most autoreactive B cells must be eliminated.

1.3.1. Tolerance during B cell development

The formation of the BCR in developing B cells occurs in steps, during each of which, appropriate BCR signals enable survival and/or differentiation. Before becoming immature B cells, the BCRs are fully developed. At this stage, self-reacting B cells are negatively selected depending on the abundance of self-antigen and the avidity and affinity of their interactions with the antigen. The self-reactive cells can undergo apoptosis in clonal deletion, or may have the chance in secondary VDJ gene recombination to alter the binding specificity[59]. Some cells are allowed to enter the periphery in an anergic state (also referred to as 'by ignorance')[60]. These processes ensure the production of a diverse B cell repertoire retaining well-regulated low-level self-reactivity, which is reserved for an immune response and wider functions[61].

There is good evidence that receptor editing is the fate of most of the self-reacting B cells, and that clonal deletion is the last resort when receptor editing cannot eliminate or at least reduce the self-reactivity to an acceptable level[61,62]. It has been shown that about 50% of immature B cells express multiple light chains after receptor editing, and occasionally express multiple heavy chains[63]. This so-called "allelic inclusion", indicates a "dilution" strategy of weakly self-reactive immature B cells to escape central tolerance. This leads to poly-reactivity and self-reactivity early in B cell development[64,65].

Anergic B cells in the periphery have a short life span. The state of anergy is one of unresponsiveness in B cells[66], characterized by low surface IgM expression, a block in proximal BCR and NFkB signalling and constitutive signalling by Erk1/2 and NFAT dependent pathways, inhibition of NFkB-dependent signalling by co-receptors (notably TLRs) and increased dependence on the survival factor BAFF by increasing expression of the death factor, Bim[66,67]. They are identified in the T1 population in mice[68], and un-mutated $IgM^{neg}IgD^{+}$ population in humans. Failure of anergy is a common mechanism leading to the activation of self-reactive B cells. Anergic B cells can be recruited into the immune response when an encounter with a cross-reacting high avidity foreign antigen overcomes the BCR blockade and generates vigorous T cell help. Access to excess free BAFF, as might occur in immunodeficiency, can also rescue anergic B cells. This is another demonstration of the body trading in the danger of weak self-reactivity to the potential for defence under severe immune attack.

Transgenic mice have been very useful in the study of B cell tolerance. In mice expressing membrane bound, high avidity self-antigens, such as MHC Class I in 3-83 mice[69] and hen egg lysozyme in MD4 mice[70], the self-reactive B cells undergo apoptosis at early stages of bone marrow development, or shortly after entering the periphery. With soluble HEL at a dose higher than

20 ng/mL, anergy is triggered in MD4 B cells, while a lower dose (<10 ng/mL) of sHEL is below the detection limit of tolerance and the self-reactive B cells escape[57].

Tolerance of B1 B cells is less well studied. Some of the BCRs of B1 B cells and the antibodies they secrete are auto-reactive, but apparently not pathogenic[71]. As described already, the selection for B1 B cells is favoured by strong BCR signalling, possibly induced by self-antigens, which may pre-decide the low-level autoreactive nature of this population.

1.3.2. Tolerance during immune responses

Somatic hypermutation during the formation of the germinal centre is random and also has the chance of creating self-reactive B cells. The selection mechanism in the GCs is in the most part achieved by severely limiting T cell help and survival factors, such as IL-21 secreted by follicular helper T cells (Tfhs). In this way, the mechanism of selection is thought to discriminate between B cells according to the amount of antigen they have bound from the follicular dendritic cells in competition with other somatically mutated B cells and presented by MHC class II. According to one model, self-reactive B cells are less competitive by virtue of binding to self-antigens. Tfh cells are not responsive to self-antigens. In the more likely case of multi-reactive cells, the up-take of self-antigens equivalently dilutes the total “usable” antigens. In other cases, the interaction with antigen bound to FDC provides the B cells with survival signals, perhaps meduated by integrin-dependent signals. These are not available from self-antigens that are not bound by complement or Ig. The injection of soluble antigen can lead to the elimination of cognate GC B cells undergoing affinity maturation against the same antigen on FDC. A similar process could eliminate self-reactive B cells that have been induced to bind self-antigens following affinity maturation.

Tingible-body macrophages (TBMs) are also believed to be important in preventing autoimmunity by actively removing large numbers of dying cells, which are potentially immunogenic. More details on TBMs can be found in Section 1.4.

In localized or tissue-specific environments, there are tolerance mechanisms, which do not change the repertoire but act in a fail-safe capacity in reducing the responsiveness of mature B cells[60,63]. These include the regulation of B cell numbers, the dependence of humoral immunity on interactions with the complement pathway, the effects of soluble molecules (such as cytokines and anti-idiotypic antibodies) and negative influences from T cells[72-74].

1.4. B cell in immunity

1.4.1. B cells in humoral immune response

It is increasingly clear that B cells play a wide variety of important roles in immune responses, including some which do not depend on antigen specificity, such as the transport of antigens within lymphoid follicles[18]. However, their primary functions are to generate antigens that neutralise invading pathogens. The B cell encounter with antigen typically occurs in the secondary lymphoid organs and leads to B cell activation. Some antigens initiate a primary B cell response without T cell participation, generating low-affinity antibodies of the IgM and IgG subtypes. These are called T cell-independent (TI) antigens and generally contain repeated regions that are recognised by multiple surface receptors. TI antigens can be divided into Type I (TI-I) and Type II (TI-II) antigens, depending on their requirement of co-receptors for activation. TI-I antigens such as LPS contain mitogenic moieties and activate B cells by BCR-TLR co-stimulation. TI-II antigens, on the other hand, are large molecules that display highly repetitive epitopes on their surface and can directly cross-link BCRs without co-receptors. Antibody responses to protein antigens require both T and B cells and produce high-affinity antibodies and immune memory. These T cell-dependent antigens do not have repetitive epitopes and may rely on the binding to existing antibodies and complement components to crosslink receptors on the B cells. They are then internalized, processed and their epitopes raised as peptides by MHC Class II molecules. T helper cells can recognise these antigens and become activated. The subsequent T-B interaction may lead to the production of various molecules from T cells, which may lead to a different fate of the B cells, including clonal expansion, isotype switching, affinity maturation and differentiation into memory cells. These processes are crucial parts of the adaptive immunity and will be the focus of this section.

1.4.1.1 The complement system

The complement system is part of the innate immune system, and contributes to the adaptive immunity. The system consists of a network of plasma proteins, which are capable of cleaving off components upon activation and regrouping into effector units that carry on the signal. The overall effect of the complement system is to clear pathogens and cell debris, and amplify inflammation and haemostasis[75].

The mechanism and regulation of the complement system is well established. Three pathways have been charaterized: the classical pathway, the lectin pathway and the alternative pathway. The classical pathway is activated by antigen-bound IgM and IgG complexes. The lection pathway is similar to the classical pathway but is activated by binding of mannose-binding lectin (MBL) to mannose residues on the pathogen surface. The alternative pathway is continuously activated at a low level, as a result of spontaneous hydrolysis of C3 and the formation of C3b molecules in an aqueous environment, and does not rely on antigen binding. C3b molecules produced this way are capable of covalently binding to pathogens and altered self-cells and trigger a positive feedback loop, which can also amplify the complement activation after C3b is generated through the other pathways. The activation of the alternative pathway is limited to host cells by regulators such as membrane cofactor protein, decay accelerating factor, CD59 and the anticoagulant and complement inhibitory molecule thrombomodulin. Pathogens generally lack the complement regulatory proteins and are exposed to the attack of accumulative C3b binding.

Various components generated in the complement pathways can attack pathogens by forming a membrane attack complex, assisting inflammation,

acting as chemoattractants for phagocytes or enhancing the phagocytosis of antigens.

Complements are now believed to assist B cell activation. B cells express complement receptors CD21 and CD35, which can form a co-receptor with signalling protein CD19 and the CD81 (TAPA-1). The co-ligation of the co-receptors (to the complement elements coating the antigen) with BCR (to the antigen) significantly lowers the threshold of B cell activation[76,77]. In his 2004 review, Carroll listed the impact of co-ligation of antigen and complement receptors in B cell selection, activation and survival[78]. The enhancement by the co-ligation promotes the positive selection of B-1 B cells and enhances the elimination of auto-reactive B cells. Co-receptor cross-linking protects naïve B cells from apoptosis after encountering of T cell-dependent antigens. In the germinal centre, the complement coated antigens are presented to B cells by FDCs. The co-ligation of BCR and co-receptors is required for the survival of GC B cells.

1.4.1.2 T cell-dependent activation

Early studies showed that the affinity of antibodies increased with time and after repeated immunisations[79] and that the memory of the immune response was retained. Once a B cell is stimulated by foreign antigens, it can either proliferate in the extra-follicular area and produce short-lived plasma cells, or enter B cell follicles and undergo further receptor editing and produce higher affinity BCRs. The mechanisms for this fate decision remain uncertain, but BCR affinity to the antigen, its availability and the amount of T cell co-stimulation are considered important[80,81].

The location of B cells is crucially linked to their later fate, and is controlled by ligand-receptor attractions, mostly involving chemokines[82]. B cells express CXCR5, whose ligand is CXCL13, produced by the follicular stroma cells and follicular dendritic cells. They also express CCR7 to a lesser extent than T cells, which is attracted to CCL19 and CCL21 produced by stroma in the T cell zone. In contrast, T cells are low in CXCR5 and high in CCR7 and are bound to the T cell zone instead. Within the GC, the division of the light zone and dark zone is also governed by chemokines and their receptors, including CXCR5 and CXCR4[83].

From the initial interaction with the antigen to the initiation of germinal centre, a timely and specially controlled mechanism is in place. Hours after antigen engagement, B cells enter the G1 phase of the cell cycle and migrate to the T-B border with the assistance of increased surface CXCR7 expression[84]. They upregulate CD86, which binds to CD28 on T cells and promotes T cell secretion of survival cytokines. Prolonged antigen stimulation suppresses CD86 and CXCR5. Self-antigens are in general more abundant than foreign antigens. Hence, self-reactive B cells fall into this fate, drift to the B-T boundary with decreased ability to receive T cell help and die[85,86]. Other B cells redistribute to regions rich in $CD11c^{hi}$ mature dendritic cells (DC)[87]. These DCs are antigen-presenting cells and also provide survival signals BAFF and APRIL. B cells actively interact with antigen recognizing $CD4^{+}$ T cells at this stage[84]. The relocation to the $CD11c^{hi}$ region is facilitated by the increased expression of EBI-2 in the B cells[88,89].

The initial decision towards plasma cell or GC cell differentiation is made around 3 days after the first antigen encounter. Opposite to the plasma cells, GC cells express high Bcl-6, depressing Blimp-1 and EBI-2[90-93]. Blimp-1 has the effect of repressing CXCR5[90] and induces CXCR4. This pattern of expression ensures the correct homing of both the plasma cell and germinal

centre populations[94]. BCR affinity for the antigens is not thought to be important in the decision-making process that leads to plasma or GC cells. Lower affinity B cells are only outcompeted later in the GC process, which is due to an increased rate of apoptosis[95].

1.4.2. The germinal centre

1.4.2.1. Structure and players

Somatic mutation was first described by Weigert *et. al.* in 1970[96]. The amino acid replacements in the antibody variable region as a result of this process are low in short-lived plasma cells, but high in GC B cells[97,98], indicating GC's role in affinity maturation. The fact that mice unable to form GCs still have antibodies with certain degree of affinity maturation[99,100] indicates that GCs are probably the most efficient but not the sole site for this process. Long-lived plasma cells and memory B cells show a high degree of somatic mutation, indicating their possible GC origins[101,102].

In the early studies, GCs were identified as a unique structure in the spleen after antigen immunisation[103]. It was divided into the light zone (LZ) and dark zone (DZ) based on histological differences. The dark zone almost entirely consists of B cells with a high nucleus-to-cytoplasm ratio. The light zone contains fewer B cells travelling within the follicular dendritic cell (FDC) framework. The light zone is well positioned in the secondary lymphoid organs to receive foreign antigens[104]. The FDCs at this location have the ability of capturing and retaining large amounts of antigens[105]. Early pulse-chase experiments showed that labelled B cells first appeared in the DZ before appearing in the LZ[104,105]. This evidence suggested that the dark zone is designated to somatic mutation and proliferation before the cells travelling to the light zone to be selected[106]. The B cells residing in the light and dark

zones, referred to as centrocytes and centroblasts, respectively, were considered different in morphology.

Data from real time imaging and flow-cytometry revealed few differences between centrocytes and centroblasts. On the other hand, GC B cells are different from native follicular B cells, being activated, large, highly polarised, very motile and fast dividing[107,108]. In terms of surface molecules, they express more Fas-receptor (CD95) and GL-7; they express low levels of IgD, and they bind to peanut agglutinin[109]. They down-regulate EBI-2, and upregulate SIP2[110] and Bcl-6[111], which are important in the initiation and maintenance of the GC. In addition, Bcl-6 also has the important function of silencing anti-apoptotic Bcl-2 and establishing the GC B cell state, repressing transcription factors such as p53 and ATR, so enabling the dividing cells to tolerate DNA damage caused by a high mutation rate, thereby depressing mediators of BCR and CD40 signalling, to fine-tune the response pattern[112].

In terms of the sequence of the events, the B cells cross the boundary between the two zones in both directions. This is different from the previous 'DZ-LZ-release' model. The B cells are equally fast-moving in both zones[107,108,113]. Flow cytometry cannot distinguish a "larger" B cell population in one zone by forward and side scatters[114,115], and pulsed BrdU experiments indicate very similar amounts of cells in the S phase in both zones, although a higher ratio of cells in the G2/M phase has been found in the DZ[113]. The difficulty faced by real-time imaging is the low sample number and short observation period, making it impossible to apply accurate mathematical models or make generalised conclusions. Separation using flow cytometry, on the other hand, has been limited by reliable surface markers that are expressed differently in the two proposed cell types – CD77 was used but was proven unreliable[116,117]. Recently, Victora *et.al.* published results on *in*

situ photactivation which extended the observation period and enabled them to calculate that less than 10% of cells travel from DZ to LZ, while 50% made the reverse journey, making a net 30% return of LZ B cells to DZ[83]. They also identified multiple new surface markers that can clearly separate the LZ and DZ B cells, including CD83 and CD86[83]. Together with CXCR4, which is believed to guide the localization in the DZ[118], they separated the DZ and LZ B cells and discovered that although cells enter the S phase in the LZ, they complete the proliferation (G2/M phase) in the DZ. Their findings strongly support the idea that the two zones have distinct roles - cells divide in the DZ and are selected in the LZ. These data also support the suggestions of step-wise affinity maturation and cyclic selection[119,120].

The other cells in the GC that are vital to the process include FDCs, Tfhs and TBMs.

FDCs reside in the LZ and are able to retain antigens in intact forms on their surfaces for extended periods[121] in the form of iccosomes[122], which are immune complex coated bodies. They also secrete or express other molecules, including chemokines (such as CXCL13), cytokine and integrin ligands (such as ICAM-1 and VCAM-1[123]) and cytokines (such as IL-6 and BAFF[124,125]). FDCs obtained their name from the dendritic morphology. Their cellular origin is unclear, however, they are known to require TNF-α and lymphotoxin (LT) to develop{Pasparakis:1996vy}{LeHir:1996ts}. Due to difficulties, such as the inability to isolate the pure cell populations, and a lack of transgenic mice, the functions of FDCs are still under debate. Nevertheless, they are believed to be important in maintaining the architecture of B cell follicles and the germinal centre, and in capturing and retaining antigens for presentation to B cells[128]. Other roles suggested include rescuing selected B cells from apoptosis and removal of debris. The

absence of LT, and to a lesser extent TNF-α, stopped the development of FDCs and resulted in disrupted lymphoid organisations. B cells produce the most of LT in the follicles, and are attracted by CXCL13 produced by the FDCs. The dendrites of the FDCs can form strings of iccosomes, immune-complex-coated bodies, where they trap and retain unprocessed antigen[129]. The immume complexes are formed through Fc receptors such as FcγRIIb (CD32) and FcεRII (CD23) and complement receptors, such as CR2 (CD21) and CR1 (CD35). Immune complexes attached to FDCs were shown to be much more effective in activating B cells and T cells, than the soluble form, possibly because of their ability to cross-link the B cell complement receptor[130].

Folicular helper T cells are CD4+ T cells that also express surface molecules such as CXCR5, PD-1, SAP (SH2D1A), and ICOS, and are high in transcription factor Bcl6[131], [127,128]. They are essential for the formation and maintenance of germinal centers. The early differentiation of Tfh cells relies on the expression of Bcl6, as well as the lack of Blimp-1. Their maintenance and further differentiation require interaction with activated B cells in the follicle and germinal centre. The surface expression of CXCR5 on Tfh cells ensures the correct localization, and SAP and ICOS are required for adhesion to B cells. In the germinal centre, the Tfh cells express higher levels of Bcl6 and CXCR5 and are more active in providing signals for B cells. It has been shown that GCs fail to form or develop with a deficiency or dysfunction of Tfhs[132,133]. Tfh cells provide GC B cells with survival signals via multiple pathways, including CD40L, IL-4, IL-21, PD-1 and BAFF. These compete with the Fas-FasL interaction, which leads to B cell apoptosis. IL-21 is also a potent inducer of plasma cell differentiation.

Other T cells that reside within the GC with less clear functions are $CD8^+$ T cells[134], Th17[135] and $Foxp3^+$ regulatory T cells[136].

Tingible body cacrophages (TBMs) are named after the large number of tingible (stanable) bodies that they contain, which consist of the engulfed dying B cells or B cell debris[106]. The TBM are found in both zones without bias[113]. The large quantity of tangible bodies reflects the high death rate of B cells in the GC, which is a result of selection. It has been shown that the dying B cells retain their nuclei until they are taken up by the TBM. This is considered as a mechanism of preventing the release of nuclear antigens and the formation of high affinity anti-nuclear antibodies[137]. Deficiency or lack of function in TBM in humans leads to systemic lupus erythematosus or lupus-like phenotypes[134,135].

1.4.2.2. The selection process for high affinity clones

The classical view of the process of affinity maturation is that the high affinity B cells are selected directly by their more stable and prolonged engagement with Tfh cells, which provides them with sufficient and competitive amounts of signals for survival and proliferation[138]. However, modern live imaging showed that the GC B cells are very motile and are very unlikely to form stable interactions[107,108,113]. The current model suggests that T cell availability is the limiting factor, in the sense that the Tfh cells only make contact with B cells that present the largest amount of antigens[139,140]. T cell preference for cells with high surface peptide has been shown *in vitro* and *in vivo*[141-143]. This model is directly supported by the fact that in mice lacking immune complexes on FDCs, the initial formation of GCs were not affected[144,145].

Other clues can be drawn from the characteristics of the GC B and T cells. Compared to naïve follicular B cells, GC B cells show characteristics of highly activated antigen processes and presentations. In comparison, they express high levels of MHC II, CD80 and CD86[146], as well as performing faster internalization and process of antigens for MHC II presentation[147]. With high expression of surface CD95 (Fas receptor, the Fas-FasR interaction is proapoptotic)[148] and low levels of Bcl-2, GC B cells are pro-apoptotic, leaving them the default fate of death unless they are rescued selectively. T cells consist 5-20% of total GC cells and can only interact with one B cell at any time[147]. In addition, these T cells have elevated MHC-peptide recognition threshold, partly by expressing high levels of PD-1[149] and CTLA-4[150] , and hence limit the GC size[151,152]. The B-T interaction is also observed to be very short and may not provide sufficient signal[107,108,113]. It has been suggested that in this crowded environment, a B cell scrapes the surface of any cell it reaches and tries to interact with the antigens on the cell surfaces[153]. Higher affinity BCRs will then enable the B cells to obtain more antigens to present as MHC II peptides. They in turn have a better chance in competing for the limited T cell interactions.

By contrast, the role and importance of BCR signalling in this process is unclear. The main difficulty lies in that BCR signalling is required for both activation and survival. However, in models such as mice deficient in CD19, it was shown that BCR signalling still ensures optimal affinity maturation[154].

1.5. B cell receptor signalling

1.5.1. Overview of Signalling downstream of BCR

As already mentioned, BCR signalling is crucial not only in B cell immunity, but also in B cell development and selection. At each development stage following the formation of the heavy chain, B cell survival depends on an adequate level of BCR signalling. Its affinity to self-antigen also determines the cell's fate at negative and positive selection checkpoints[155,156]. For instance, mice lacking the key BCR-related protein tyrosine kinase (PTK) Syk showed developmental block as early as the pre-B cell stage[157,158]. Mature B cells also require basal BCR signalling for their maintenance before antigen encounter[159,160].

The membrane-bound BCR complex consists of a pair of identical, covalently linked heavy and light chains, plus the signalling components Igα (CD79α, mb-1) and Igβ (CD79β, B29), which are non-covalently connected[161]. Upon the encounter with antigen, BCR molecules, co-receptors and regulatory molecules form organized clusters[162] similar to the immunological synapse that has been so well characterized in T cells[163]. The engagement of BCR and the formation of immunological synapse trigger down stream signalling pathways. A simplification of current models is illustrated in Figure 1.4.

Within the cell, kinases activate in progression and trigger a network of signalling pathways, eventually lead to transcriptional changes. After BCR stimulation, Igα and Igβ undergo structural transformations, from a closed to an open conformation[161]. This process is phosphorylation-dependent, and is promoted by proteins bound to the inside of the cytoplasmic membrane, most likely Lyn[164], a member of the src family kinases (SFKs).

The phosphorylated cytoplasmic tails of Igα and Igβ provide binding sites for SH2 domain-containing proteins, including spleen tyrosine kinase (Syk), which is itself further activated by phosphorylation[165]. The activated Syk binds to adaptor protein B-cell linker (BLNK)[166]. Parallel to Syk, activated SFKs also phosphorylate and activate Bruton's tyrosine kinase (Btk). Syk and Btk together are required for the full phosphorylation and activation of PLCγ2[167]. This process is assisted by BLNK, which provides binding sites and scaffolding for Syk, Btk and PLCγ2. Activated PLCγ2 hydrolyses PIP_2 (phosphatidylinositol-(4,5)-bisphosphate) to generate IP_3 (inositol 1,4,5 trisphosphate) and diacylglycerol (DAG). From here, multiple pathways initiate.

IP_3 binds to its receptor (IP_3R) on the endoplasmic reticulum (ER) membrane and triggers the release of Ca^{2+} into the cytoplasm from the Ca^{2+} store within the ER. The reduction of Ca^{2+} within the ER activates molecules that cause the Ca^{2+} influx from outside the cell[168]. Details of Ca^{2+} influx are described later in Section 1.5.2. Cytosolic Ca^{2+} sensor calmodulin binds the ion by its two EF arms and activates the serine/threonine phosphatase calcineurin, which targets nuclear factor of activated T cells (NFAT)[169]. In resting cells, NFAT is heavily phosphorylated. Calcineurin de-phosphorylates NFAT, which enables it to enter the nucleus and carry out gene transcriptions. This pathway is considered important for cell-cell interactions, which are required for immune responses and lymphocyte development[169,170].

DAG recruits and activates Ca^{2+}-dependent protein kinase C (PKC)[171], which activates the NFκB pathway. PKCβ, in particular, phosphorylates CARMA1, which then recruits BCL-10 and MALT1 into a signalling complex[172]. The complex's functions are tightly regulated by the phosphorylation at different positions[173]. The positive outcome is the activation of IκB kinase (IKK), which

consists of two catalytic subunits (IKKα, IKKβ) and a regulatory subunit (IKKγ, or NEMO). Activated IKK phosphorylates, ubiquitinates and degrades IκB, promoting the release of nuclear factor-κB1 (NFκB1) and its transit to the nucleus. NFκB1 induces the expression of anti-apoptic genes such as c-Myc, Bcl-2, Bcl-XL and A1[174,175] and is important for cell survival and activation[176].

DAG activated PKC also activates the Ras-Raf-Erk pathway, although other routes following both Ca^{2+} mobilization and Sos activation can also lead to Ras activation. This will be discussed in more detail in Section 1.5.3. Erk1/2 is a component of the canonical MAPK pathway and is phosphorylated in many cell types following growth factor engagement. Its downstream transcription factors control the survival and proliferation of the cell, but it may also be associated with BCR-induced apoptosis[177]. Current evidence suggests it can transduce qualitatively different outcomes depending on subtle balances of signal characteristics, especially in strength and duration. This is relevant and important from the perspective of conventional assays of lymphocyte activation. Erk1/2 activation also transduces signals leading to the transcription of activation markers such as CD69[178].

The B cell specific co-receptor CD19 contributes to BCR signalling in multiple ways. The CD19-CD21 complex binds to the complements and can assist BCR's engagement of complement-tagged antigens, significantly lowering the threshold of B cell activation[76,77]. The recruitment of CD19 to the BCR-microcluster has been suggested to enable the phosphorylation of CD19, which can then be bound to SH2-containing proteins including Vav and phosphatidylinositol-3 kinase (PI3K)[179].

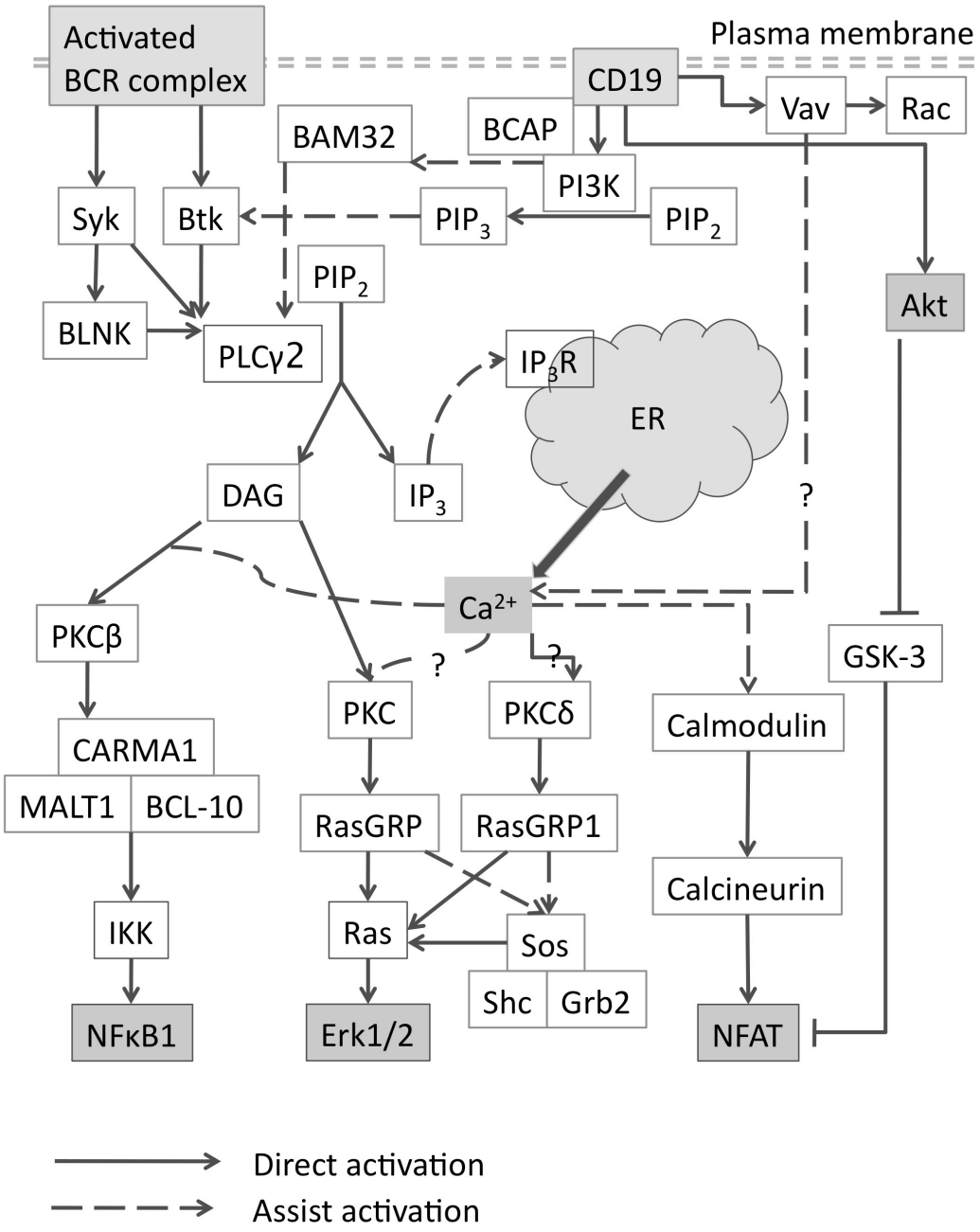

Figure 1.4 Simplified model of BCR-induced down stream signalling. This scheme demonstrates the sequence of the events and the relationship between molecules. The special and structural features are not realistic.

Vav family proteins are guanine nucleotide-exchange factors (GEFs) for Rac/Rho molecules[180]. They provide the major link to the Rho family of GTPases, which mediates actin polymerization. Vav is thought to be an important regulator of early events after BCR-antigen engagement[181], possibly in virtue of its regulation of cytoskeletal structure through Rac[182]. However, Vav's roles independent of GEF activities are not entirely clear, since it is believed to contribute to Ca^{2+} mobilization[183,184]. Mice lacking all three Vav proteins fail to activate the NFκB pathway[185], due to a completely disrupted antigen-dependent Ca^{2+} signalling[186].

Binding of the p85 subunit of PI3K to CD19 leads to the activation of its p110 subunit. Activated and membrane-bound PI3K catalyses the conversion of PIP_2 to phosphatidylinositol-(3,4,5)-trisphosphate (PIP_3). PIP_3 contains binding sites for pleckstrin homology (PH) domains found in enzymes such as PDK1/2, Akt, Btk and PLCγ2[187]. The recruitment to the membrane by PIP_3 is crucial for their activation. The B-cell adapter for PI3K (BCAP) also associates with the SH2 domain of PI3K p85 subunit, and defects in BCAP function result in impaired PI3K and Akt activations[188]. Genetic ablation of both CD19 and BCAP leads to a complete block in BCR-mediated Akt activation, as well as severe defects in the generation of mature B cells[189].

The Akt-dependent signalling pathway is linked to cell survival and proliferation processes[190]. Activated Akt can phosphorylate glycogen synthase kinase-3 (GSK-3)[191], which suppresses GSK-3's kinase activity and reduces its phosphorylation of NFAT. Hence, the activation of Akt may result in the activation of the NFAT pathway. Akt can also inactivate forehead box class O (FOXO)[192], which are transcription factors that activate the genes of proapoptotic and antiproliferative proteins such as Bim, p27kip and Rbl2[193-195].

BCR activation-induced down-regulation of FOXO mRNA involves PI3K, Btk, BLNK and PLCγ2[196].

B-lymphocyte adaptor molecule of 32 kDa (BAM32) binds to PLCγ2 and regulates its activation[197,198]. The membrane recruitment of BAM32 also depends on PI3K, creating a cross talk between the PLCγ2 and PI3K pathways. BAM32 expression is elevated in the germinal centre B cells, which is one example of how the expression of key adaptors varies during B cell development and function. It is likely that these changes influence the outcome of BCR-induced signalling and cell fate.

BCR signalling is negatively regulated by cell surface molecules containing immunoreceptor tyrosine-based inhibitory motifs (ITIMs), including paired immunologulin-like receptor B (PIRB) and FcγRIIB. These co-receptors recruit SH2-domain-containing protein tyrosine phosphatases 1 (SHP1) and SH2-domain-containing inositol polyphosphate 5' phosphatases (SHIP), which in turn reverse the phosphorylation carried out by kinases[199,200]. CD22 recruits adaptor protein Grb2, possibly to enhance the bindings of other molecules such as SHP1 and SHIP. Grb2 itself associates with Dok3 after BCR stimulation and restricts Btk activities[201]. More details on Grb2 functions will be discussed in Section 1.5.4.

1.5.2. Ca^{2+} flux

It is clear from the brief discussion already presented and from our understanding of the current literature that Ca^{2+} mobilization and influx have very widespread impacts on cellular physiology and signalling pathways[202]. Changes in the Ca^{2+} flux or in proteins associated with its function result in

alternations in B cell development, selection or the response to antigens. For these reasons, and to provide a framework for my results, I will now discuss these phenomena in more detail.

As described previously, the activation of BCR leads to a cascade of kinase activations. Activated PLCγ2 produces IP_3 and DAG from PIP_2. IP_3 binds to IP_3-receptor on the membrane of the ER, which triggers the release of Ca^{2+} from the ER to the cytoplasm. This is a rapid and transient increase of cytosolic Ca^{2+} concentration. Sustained increase of Ca^{2+} relies on the Ca^{2+}-release-activated Ca^{2+} (CRAC) channels in the plasma membrane. This process is referred to as store-operated Ca^{2+} entry (SOCE) and was first described in 1986[203-205].

The loss of Ca^{2+} in the ER lumen dissociates Ca^{2+} from the EF arms of Ca^{2+} sensor STIM1 and STIM2[206,207]. The current SOCE model is that free STIM molecules translocate to near the plasma membrane and form concentrated junctions[208,209]. At the same time, Orail1/2/3 (CRACM1/2/3) molecules move within the plasma membrane to the area near the STIM-rich junction. Orail molecules are transmembrane, pore-forming subunits of the CRAC channels. STIM molecules then associate with the Orail molecules to activate the Ca^{2+} channels.

Many of the signalling molecules already mentioned can affect the initiation of Ca^{2+} flux. CD19 enhances Ca^{2+} flux by lowering the BCR signalling threshold[76,77,210]. As described previously, activated CD19 leads to the production of PIP_3, which anchors Btk to the plasma membrane for its activation; and activated Btk is required for PLCγ2 activation and eventual Ca^{2+} release. CD22 and FcγRIIB1 negatively regulate Ca^{2+} flux via functions of SHIP and/or SHP1. Co-ligation of FcγRIIB1 and the BCR induces

dephosphorylation of PIP_3 to PIP_2 by SHIP and reduces the membrane translocation of Btk. SHIP also dephosphorylates CD19 and consequently reduces the activation of PI3K. Plasma membrane calcium-ATPase 4 (PMCA4) pumps Ca^{2+} out of the cytoplasm. CD22 has been suggested to physically associate to PMCA4 in a SHP1-dependent manner[211]. Grb2 is known to negatively regulate Ca^{2+} flux via its interaction with Dok3, but also by its association with SHIP and phosphorylated FcγRIIB1 and CD22. In the latter cases, its adaptor function can enhance the binding to the two molecules. It plays a similar role in binding to the cytosolic tails of IgG, though in this case, the effect is to enhance the signalling of the BCR[212,213]. The IgM BCR lacks the long cytosolic tail and the unique binding sites of IgG, so Grb2's positive influence on BCR signalling is not shown in IgM-induced stimulations.

Impairment in the function or the loss of Btk, BLNK or CD19 causes a reduction or absence of the BCR-dependent cytosolic Ca^{2+} flux[214]. These defects lead to changes in the B cell repertoire and human immuno-deficiency. On the other hand, functional impairment of the negative regulators of the Ca^{2+} flux, such as SHP1, CD22 and FcγRIIB1, leads to an augmented Ca^{2+} response, hyper-responsive B cells and autoimmunity[215-218]. Gain-of-function mutations in the *plcg2* gene show similar effects[219].

The impact of a sustained, rather than differential or transient, Ca^{2+} flux on B cells is manifest in the studies of SOCE components. Patients with mutations in ORAI and STIM genes show impaired immunity[220,221]. However, mice lacking both STIM1 and STIM2 in B cells show no B cell developmental defects[222], nor do they show impaired immune response to T cell dependent or T cell independent antigens *in vivo*, although the SOCE and proliferation are defective. Yet, SOCE may be crucial for the function of regulatory B cells.

Sustained Ca^{2+} flux was shown to be crucial for NFAT1 activation, which leads to IL-10 production in these cells[222]. Moreover, recent studies on STIM1 lead to the finding of Ca^{2+}-dependent Erk1/2 activation[223]. It has been suggested that this process is involved in BCR-induced apoptosis of immature and transitional B cells.

1.5.3. BCR-induced Erk1/2 signalling

One of the key features of BCR signalling is the activation of Ras and its downstream pathways[224,225], including the phosphorylation and activation of ERK1/2. This pathway influences many biological processes including cell survival, proliferation, growth arrest and differentiation[177].

Three pathways following BCR stimulation have been shown to lead to the activation of Ras and eventually Erk1/2 phosphorylation. Two of them are downstream of PLCγ2 and the third downstream of the guanine nucleotide exchange factor Sos. The dominance of PLCγ2-dependent pathways is evident that in the B cells of PLCγ2 knockout mice, where IkBα activity was found to be completely absent, and the Erk1/2 activation was almost, but not completely, abrogated[226].

Sos can be recruited to the membrane as part of an Shc/Grb2/Sos complex and be activated as a result. Activated Sos releases Ras from its inactive GDP-bound form to enable the formation of active Ras-GTP[227,228]. Importantly, Sos activity is significantly enhanced by its binding to Ras-GTP at an activation motif, which is separated from the enzyme active site[229]. This provides a positive feedback loop for Ras activation. Due to the sheer increase in Sos activity after binding to Ras-GTP, Sos may appear as a major component in the PLCy2-dependant Ras activation pathway, or might be

seen as redundant in some experiments. This amplification mechanism may be important in distinguishing real antigen-receptor signals, as well as in tuning the strength of the Ras signals, and influence the result of antigen encounter in terms of activation and cell fate decisions[230,231].

The PLCγ2-dependent activation of Ras can be DAG- or Ca^{2+}-dependent. DAG can associate PKC via its C1 domain. Together, they activate Ras guanine nucleotide-releasing proteins (RasGRPs) by recruiting them to the membrane[232,233], and phosphorylate RasGRP1 at Thr184, or RasGRP3 at Thr133. RasGRP then activates Ras and triggers the Ras-Raf-MAPK pathway.

A description of the Ca^{2+}-dependent Erk1/2 activation pathway has recently been published by Limnander *et. al.*[223]. IP_3 leads to the Ca^{2+} flux as described previously. The Ca^{2+}-dependent activation of PKCδ and its phosphorylation of RasGRP has been shown to be essential for the Ca^{2+}-dependent Erk1/2 activation, probably via the phosphorylation of a further activating motif at Ser332 on RasGRP1.

Deletion of RasGRP1 and RasGRP3 saves B cells from antigen-induced apoptosis. The interconnection and fine-tuning of these pathways are yet to be fully explored, but have potentially important and interesting implications for positive and negative B cell selection. For example, developing B cells contain less DAG than mature B cells, due to increased DAG-kinase activity, but have stronger and more sustained Ca^{2+} influx[234-237]. They are also more prone to apoptosis after BCR engagement with self-antigen. Both RasGRP and PKC have been shown to mediate proapoptotic signals in B cells[238,239]. Together, these findings may imply that sustained high intensity signalling via the Ca^{2+}-dependent MAPK pathway assists the negative selection in

immature B cells; whereas, the DAG-dependent pathway may promote positive selection or proliferation in mature B cells.

Most of the pioneering work on Erk1/2 signalling in lymphocytes has been done in T cells. During T cell development in the thymus, MHC-peptides leading to positive or negative selection induce different patterns of Ras/MAPK signalling[240]. Negatively selected T cells show strong, fast and transient effects, whilst positively selected T cells show weaker, slower and more sustained Ca^{2+} flux and phosphorylation of Erk1/2. This is reflected in different intracellular localisation of the key signalling molecules: membrane localisation of Raf-1, RasGRP and Ras is associated with strong and rapid signals that cause negative selection, while positive selection is associated with localisation of signalling molecules at the Golgi or intracellular vesicles. Phospho-Erk is membrane-localised in negatively selected T cells, but is dispersed throughout the cytoplasm in positively selected T cells. In contrast, the localisation of phospho-JNK shows no difference[240].

The compartmentalized Ras/MAPK signalling has been studied and was summarised by Mor and Philips[241]. At steady-state, a substantial proportion of Ras resides on the Golgi apparatus[242], mainly from the cell membrane, through the acylation/deacylation cycle[243]. The activation of Erk1/2 at this site is carried out in a complex held by scaffolding molecules called Sef[244]. It was shown that phospho-Erk1/2 is retained in the complex rather than moving into the nucleus. This indicates that the activation at the Golgi limits the effect of phospho-Erk1/2 on its cytosolic substrates. Nuclear substrates such as Elk-1 could not be activated, illustrating one way in which compartmentalization of the signalling response can affect cell fate. Interestingly, Ca^{2+} and RasGRP1 were shown to be responsible for the Golgi mechanism[245]. The kinetics of Golgi activation has been shown to be delayed and sustained, compared with the fast and transient pathway at the cell membrane[246]. These kinetics

and localization characteristics fit the positive selection patterns in T cells shown by Daiels *et. al.*[240].

Few signalling defects have been reported in Themis$^{-/-}$ thymic T cells and these have been disputed. Fu *et. al.*, but not other groups, demonstrated slight defects in Ca^{2+} influx and phosphorylation of Erk1/2 following TCR cross-linking. The Erk1/2 phosphorylation in Themis$^{-/-}$ thymocytes was weaker and more transient than in WT in their results. The authors attributed these findings to the developmental defects in Themis$^{-/-}$ mice. As discussed above, less sustained Erk1/2 phosphorylation may lead to a failure in positive selection. In addition, it is widely accepted that sustained signals favour CD4 SP T cell selection[247]. Indeed, the reuction in CD4 SP T cells is more severe than the reduction in CD8 SP T cells in the absence of Themis1. However, the same results were not reported by any other groups. Lesourne *et. al.* recently published that Themis$^{-/-}$ CD4 SP T cells showed weaker phosphorylation of Erk1/2 after 1 minute stimulation with anti-CD3 and anti-CD4. But the same was not found in Themis$^{-/-}$ DP T cells, which are subject to selection. It was also suggested that the role of Themis1 lies in sustaining TCR signalling. Future studies on the kinetics and/or the location of Erk1/2 signalling would be valuable in discovering the function of Themis1.

1.5.4. Grb2 in BCR signalling

Finally I wish to discuss Grb2, a key adaptor protein in BCR signalling and a binding partner of Themis1 and Icb-1. Although my study so far has not covered Grb2, its potential involvement in the functions of Themis1 and Icb-1 provides important insights.

Grb2 was identified as one of the proteins that bound to the tyrosine-phosphorylated epidermal growth factor receptor (EGFR)[248] and was named growth factor receptor bound protein 2. It was also identified in an independent cDNA screen for mammalian SH2 domain-containing proteins[249]. It is related to adaptor proteins Grb2-related adapter protein (Grap)[250] and Grb2-related adaptor downstream of Shc (Gads, or GrpL, Mona, GRID, Grf40, Grap-2)[251-256]. Grb2 is highly conserved throughout evolution and has an apparent molecular weight of 25-30 kDa. It is widely expressed in B cells, at an almost uniform level.

X-ray crystallography has revealed that it contains a central SH2 domain flanked on either side by SH3 domains[257]. Solution phase structure measurements revealed extensive flexibility facilitating ligand recognition[258]. The SH2 domain of Grb2 uniquely tolerates the ligand motif pYRNM[259], which gives advantages and specificity to the Grb2 functions. Its N-terminal SH3 domain interacts with the typical motif PxxPxR[260], while the C-terminal SH3 domain can associate with atypical motifs lacking the PxxP core with high affinity and remarkable versatility[261].

In signalling, Grb2 binds to pYXN motifs in the cytosolic tails of cell surface receptors. Its binding to FcγRIIB and CD22 is believed to enhance the binding of SHIP and SHP1, respectively[262,263] via the SH3 domain of Grb2. In addition, Grb2 was suggested to reduce Ca^{2+} mobilization by the association with hematopoietic adapter protein downstream of kinase-3 (Dok-3)[264]. Dok-3 is tethered to the lipid rafts through its N-terminal PH domain and contains YXN sites for Grb2 binding. It is phosphorylated by Lyn following BCR activation[201]. The complex suppresses Btk function with an unknown mechanism.

On the other hand, Grb2 also binds to the pYXN site of CD19[265], where it can recruit and reinforce the binding of BCAP to CD19, which presumably places BCAP at a favourable position to be activated. By a similar mechanism, Grb2 has been suggested to assist the localization in lipid rafts and the activation of Vav[266]. IgG and IgE type BCRs have very long cytosolic tails which contain immunoglobulin tail tyrosine (ITT) sites that have been shown to recruit Grb2 following stimulation[213]. The association of ITT and Grb2 boosts Ca^{2+} mobilisation and proliferative responses[212]. The detailed mechanism of the enhancement is unclear, but is likely to rely on the adaptor activity of Grb2 in recruiting and assisting the activation of signalling molecules.

Grb2's functions can be dampened by NTAL[267], which permanently resides in the lipid rafts and associates with Grb2 via one or more pYXN sites. This recruitment of Grb2 prevents its involvement in other activities. Although Grb2 is uniformly expressed in different B cell subsets, NTAL is differentially expressed[267]. Its expression correlates to the signal strength of Ca^{2+} in immature and mature B cells[236,268]. NTAL's T cell homologue, LAT, performs similar roles[269]. This is an example of fine tuning BCR signalling by altering the expression of adaptor proteins.

Recently, Ackermann *et al.* published data obtained from mice with B cell specific deletion of Grb2 (Grb2-KO-B)[270]. These B cells mount a stronger Syk phosphorylation and Ca^{2+} response after BCR stimulation, findings that are in line with the negative regulatory role of Grb2. The Grb2-KO-B cells showed strongly reduced Akt activation, which is probably a reflection on Grb2's association with CD19 and the enhancement of BCAP activation[271]. Interestingly, the authors found normal Erk1/2 and p38 phosphorylation, while that of JNK was attenuated. The authors attributed these findings to the different activation thresholds of Erk1/2 and JNK[272], which was shown in T cells[273]. In agreement with Grb2's role in enhancing BCR signalling in IgG

activation, mice containing Grb2-KO-B cells showed a strong secondary IgG defect in *in vivo* challenge.

B cell specific Grb2 knockout mice also showed early B cell developmental defects in the bone marrow, as well as containing fewer transitional B cells and a reduced number of mature B cells. Both immature and mature Grb2-KO-B cells were slightly more susceptible to spontaneous apoptosis *in vitro*. Transitional Grb2-KO-B cells failed to upregulate BAFF-R, which is important for survival at this stage[43] and may contribute to the reduced mature B cell numbers.

These findings in a large part confirm the functions of Grb2 in BCR signalling. They also demonstrate the complex and finely tuned roles of adaptor proteins like Grb2. The net result of these changes is to alter the development of B cells; but precisely how they influence the development processes – by protein sequestration, by limiting in the recruitment of positive and negative regulators or by some other undefined mechanism, is not yet clear.

Chapter Two Materials and methods

2.1. Reagents

2.1.1. Antibodies

Antibodies for flow cytometry surface staining

Target	Other name	Clone	Supplier
B220	CD45R	RA3-6B2	eBioscience
CD117	c-kit	2B8	BD Pharmingen
CD19	-	eBio1D3	eBioscience
CD21	CD35	7G6	BD Pharmingen
CD23	FcRII	B3B4	BD Pharmingen
CD24	HSA	M1/69	eBioscience
CD25	-	PC61.5	eBioscience
CD3	-	145-2C11	eBioscience
CD4	-	GK1.5	eBioscience
CD43	Ly-48	eBioR2/60	eBioscience
CD44	-	IM7.8.1	BD Pharmingen
CD45.1	$Ly5^a$	A20	eBioscience
CD5	Ly-1	53-7.3	BD Pharmingen
CD69	-	H1.2F3	eBioscience
CD8	-	53-6.7	eBioscience
CD86	B7.2	GL1	eBioscience
CD93	AA4.1	AA4.1	eBioscience
CD95	FasR	15A7	eBioscience
GL-7	Ly-77	GL-7	eBioscience
HyHEL9	-	HyHEL9	In-house
IgD	-	11-26c.2a	BD Pharmingen
IgD^a	-	AMS9.1	BD Pharmingen
IgG1	-	P3	eBioscience
IgM	-	II/41	eBioscience
IgM^a	-	DS-1	BD Pharmingen
Live/dead indicator	-	-	Invitrogen
MHC II	I-A	M5/114.15.2	eBioscience

Table 2.1. List of antibodies used in flow cytometry surface staining.

Antibodies for flow cytometry intracellular staining for phosphorylated proteins

Target	Host	Clone	Target site	Supplier
p-p38	Rabbit IgG	3D7	pThr180/pTyr182	C.S.6908
pAkt	Rabbit IgG	193H12	pSer473	C.S.4058
pAkt	Rabbit IgG	C31E5E	pThr308	C.S.3375
pBLNK	Mouse IgG	J117-1278	pTyr84	BD 558443
pErk1/2	Rabbit IgG	D13.14.4E	pThr202/pTyr204	C.S.4284
pSyk	Mouse IgG	17A/P-ZAP70	pTyr319/pTyr352	BD 557817

Table 2.2. List of antibodies used in flow cytometry intracellular staining for phosphorylated molecules. C.S., Cell Signalling; pAkt, phosphorylated Akt and so on.

Antibodies for phosphorylation staining in western blot

Target	Target site	Conjugation	Host/type	Supplier
pAkt 308	pThr308	None	Rabbit IgG	Cell Signalling
pAkt 473	pSer473	None	Rabbit IgG	Cell Signalling
pErk1/2	pThr202/pTyr204	None	Rabbit IgG	Cell Signalling
pIκκα/β	pSer176/177	None	Rabbit IgG	Cell Signalling
pPLCγ2	pTyr1217	None	Rabbit IgG	Cell Signalling
pSyk	pTyr319/pTyr352	None	Rabbit IgG	Cell Signalling
Rabbit IgG	N/A	HRP	Goat	Promega

Table 2.3. List of antibodies used in western blot for phosphorylated molecules. N/A, not applicable; pAkt, phosphorylated Akt and so on.

Antibodies used for other western blot, B cell negative selection and ELISA

Target	Clone	Conjugation	Host/type	Supplier
Avidin	-	AP	-	Sigma A7294
CD11b	M1/70	Biotin	Rat IgG	ebioscience 13-0112
CD11c	N418	Biotin	Hamster IgG	ebioscience 13-0114-85
CD3	145-2C11	Biotin	Hamster IgG	eBioscience 13-0031
CD43	eBioR2/60	Biotin	Rat IgM	ebioscience 13-0431
Icb-1	N/A	None	Rabbit IgG	Love Group
IgM^a	DS-1	Biotin	-	BD Pharmingen
Ly76/Ter119	TER-119	Biotin	Rabbit IgG2b	eBioscience 13-5921
Mouse IgG1	-	AP	-	Southern Biotechnology 1070-04
Mouse IgG1	-	None	-	BD Biosciences 553445
β-Actin	AC-15	HRP	IgG1	Sigma A3854

Table 2.4. List of other antibodies used in western blot, cell purification and ELISA.

2.1.2. Buffers and other reagents

(Unless otherwise stated, chemicals mentioned were from Sigma-Aldrich or Fisher Scientific)

Agarose gel (2%), 1 g of agarose (Thistle AGR-500) was mixed with 50 mL TAE (see later entry for TAE) and heated in a microwave oven until the powder was completely dissolved. 3 μL of RedSafe (Chembio 21141) was added and a gel poured into gel cast to set.

Alum solution (9%), 9% (w/v) solution of aluminium potassium sulfate (12 hydrate, BDH 270855R), made with MilliQ water

Anti-Mouse IgM, μ-chain specific, from goat, Jackson Immuno research 115-005-075

Baytril, active ingredient: enrofloxacin, Biomedical Services 01250138, used at 1/1000 in drinking water

Beta-actin expression assay (RT-PCR), endogenous control, Applied Biosystems 4352341E

Beta-mercaptoethanol, 2-mercaptoethanol, Invitrogen 31350-010

Binding buffer (WB), 5% BSA in TBS (see later entry for TBS)

Blocking buffer (WB), 1% BSA in TBS

BSA, albumin from bovine serum, Sigma A7906-11

Carbonate buffer, pH 9.6, 50 mM Na_2CO_3, pH 9.8 (dissolved 1.59 g of Na_2CO_3 and 2.93 g of $NaHCO_3$ in 1 litre of MilliQ water)

Cell strainer, 70 micron, BD 352350

CFSE, 5(6)-carboxyfluorescein diacetate N-succinimidyl ester, Sigma 21888-25MG-F. Dissolved in sterile PBS at 10 mM, stored in small aliquots away from light at -20 °C

Chemiluminescence, SuperSignal West Pico Chemiluminescent Substrate, Promega 34087, used according to manufacture's instructions

Coating buffer (ELISA), eBioscience 00-0044, prepared according to manufacturer's instruction, 0.2 μm filter-sterilised before use

Complete media, RPMI1640 (Sigma) or DMEM (PAA Labs) medium supplemented with 10% FCS (see entry 'FCS'), 20 mM HEPES pH 7.4 (PAA

Labs), 100 μg/mL streptomycin (Sigma) and 100 U/mL penicillin (Sigma). RPMI complete media was also supplemented with 50 μM 2-mercaptoethanol and 20 mM sodium pyruvate (Sigma). Other medias named R0 and R2 with the number indicating the percentage of FCS added

Cytofix/Cytoperm buffer, BD Bioscience 555028

DNA ladder (agarose gel), 100 bp, NEB N3231S

DNase I, amplication grade, with buffer, Invitrogen 18068-015

DNeasy Tissue Kit, Qiagen 69504

Ear-notch buffer, 50 mM Tris-HCl pH 8.0, 2 mM NaCl, 10 mM EDTA, 1% SDS

ELISA plate, 96-well, flat bottom, high binding, Greiner 655061

FACS tube, BD

FCS, foetal calf serum, ultra-low IgG, Life Technologies Ltd (Invitrogen division) 16250086. Heat-inactivated at 55 °C for 40 minutes, then stored in 10 mL and 50 mL aliquots at -20 °C

Film (WB), Kodak X-Omat LS film, Sigma F1149-50EA

Fura Red, AM, Life Technologies Ltd (Invitrogen division) F3021

Haemacytometer, VWR

HBSS, Hanks' balanced salt solution, Sigma H8264

HEL, Hen Egg Lysozyme, lyophilized powder, ⩾90 %, ⩾40,000 units/mg, Sigma L6876

HEPES saline solution, HBSS (Sigma) with 0.1% BSA, 1 mM $CaCl_2$, 0.5 mM $MgCl_2$ and 10 mM HEPES (Gibco)

Icb-1 expression assay (rt-PCR), TaqMan, assay ID: Mm 01180770_m1

ICE-T, 1% FCS, 1% milk powder (w/v), 0.1% (v/v) Tween20, 0.1% (w/v) NaN_3 in 1X PBS

IL-2 ELISA kit, eBioscience 88-7024

Ionomycin, calcium salt from *Streptomyces conglobatus*, Sigma-Aldrich I0634

LPS, lipopolysaccharides from Salmonella enterica serotype enteritidis, Sigma-Aldrich L7770

Loading buffer (WB, reducing), Thermal Scientific 39000

Lysis buffer (1x), 125 mM NaCl, 30 mM Tris HCl, 10 mM EDTA, 10 mM $Na_4P_2O_7$, 1% (v/v) Triton X-100, 3 mM Na_3VO_4, 10 mM NaF, phosphatase inhibitor cocktail 2 and 3 (Sigma P5726 and P0044), protease inhibitor cocktail (Sigma P8340)

MACS LS column, Miltenyi Biotec Ltd130-042-401

MACS magnet, Miltenyi Biotec Ltd 130-042-303

Mini Trans-Blot apparatus, Bio-Rad

Molecular microbeads, streptavidin coated, Miltenyi Biotec Ltd 130-048-102

NP(19)-CGG, Biosearch Technologies N-5055

NPP buffer, 50 mM Na_2CO_3, 0.5 mM $MgCl_2$, pH 9.8

PB, PBS, 0.5% BSA

PBE, PBS, 0.5% BSA, 2 mM EDTA

PBS, phosphate buffered saline, Fisher HYC-001-198F

PBS/Tw, 0.05% (v/v) Tween20 (Sigma) in PBS

PDBu, Phorbol 12,13-dibutyrate, Sigma-Aldrich P1269

Perm/Wash Buffer, BD Biosciences 554723

Plates (96-well), Greiner

Pluronic F-127, 20% solution in DMSO, Life Technologies Ltd (Invitrogen division) P3000MP

Primers (PCR), Sigma-Aldrich

Protein ladder (WB), multicolour broad range, Fermentas 26634

Protease K solution, 20 mg/mL (Roche), made up in PCR-grade water immediately prior to use

RNaseOUT, recombinant ribonuclease inhibitor, Invitrogen 10777-019

RNeasy kit, Qiagen 74104

SDS-PAGE gel (10%), for two separating gels, 2.5 mL ProtoGel buffer (Geneflow A2-0072), 3.3 mL acrylamide (BioRad 161-0125), 50 μL 10% ammonium persulphate, 20 μL TEMED (Sigma T9281) and 4.13 mL MilliQ water. For two stacking gels, 1.25 mL ProtoGel stacking buffer (Fisher Scientific ELR-210-020M), 650 μL acrylamide (BioRad 161-0125), 25 μL 10% ammonium persulphate, 10 μL TEMED (Sigma T9281) and 3.1 mL MilliQ water.

SDS-PAGE running buffer, Tris-Glycine-SDS Buffer (Sigma-Aldrich T7777, 10× concentrate). Stock was diluted to 1x buffer with 10% stock and 90% MilliQ water

Sigma[104], 4-Nitrophenyl phosphate disodium salt hexahydrate (NPP), Sigma 71768

Staining media (flow cytometry), HBSS (Sigma), 0.1% sodium azide, 2% FCS, 20 mM HEPES (Gibco), pH7.4

SRBCs, Sheep red-blood cells, Patricell C100-0210

Superscript II Reverse Transcriptase, Invitrogen 18064-022, including 25 mM EDTA, Random hexamers, 10 mM dNTPs, 10X RT buffer, 50 mM $MgCl_2$, 0.1 M DTT, superscript, nuclease-free water and RNaseH

TAC, 17 mM Tris Base, 140 mM NH_4Cl, pH7.2

TAE, Tris-Acetate Electrophoresis Buffer, 40 mM Tris-acetate, 1 mM EDTA

TaqMan Gene Expression Master Mix, Applied Biosystems 4369016

Themis1 expression assay, Applied Biosystems 4331182

TBS, 20 mM Tris pH 7.6, 137 mM NaCl in MilliQ water

TBST, TBS with 0.1% (v/v) Tween20

Transfer buffer (WB), Tris-Glycine Buffer (Sigma-Aldrich T4904, 10× concentrate). Stock was diluted to 1x buffer with 10% stock, 20% methanol and 70% MilliQ water

Trypan Blue, 0.4% Trypan Blue Solution (Sigma)

Transfer membrane, 100% nitrocellulose, 0.45 μm or 0.2 μm pore size, Fisher, BRD-110-155 or BRD-110-145

Trypsin-EDTA, Sigma T3924

Tween20, Sigma P1379, 10% (v/v) stock was made with MilliQ water and used according to dilution

WBCCF, while blood cell counting fluid, 0.5% methyl violet, 1.5% acetic acid in distilled water

2.2. Animal keeping and procedures

2.2.1. Mouse keeping and breeding

All animals were housed in specific-pathogen free (SPF) conditions at the Oxford University BMSU, JR Hospital, and provided with food and water *ad libitum*. Animal experiments were approved by the Oxford University Ethical Review Committee, and were performed under Home Office license.

Litters were separated from parents 3 weeks after birth and were put into single-sex cages of up to 7 animals per cage. Ear notching was used for identification and genotyping. Breeders were at least 6 weeks of age. Animals used in any procedure were also at least 6 weeks of age.

2.2.2. Genotyping of transgenic mice

Genotyping of transgenic mice was performed using PCR by Tanya Cheetham. The genomic DNA of each mouse to be screened was produced from the ear notching. Ear notches were collected in 0.6 mL eppendorfs and stored at -20 °C until processing. 150 μL of freshly prepared proteinase K solution was mixed with 2.85 mL of Ear-notching Buffer, and 20 μL of the mix added to each sample. The tubes were incubated at 55 °C for 40 minutes, vortexing twice to break-up the tissue. 180 μL of PCR-grade water was added per tube and the tubes heated to 100 °C for 5 minutes to inactivate proteinase K. The DNA was stored at 4 °C.

Primer sequences and product sizes of all transgene screens are listed in Table 2.5

Icb-1	
ICB-g2	GGG AAG AAC AGA CGA TGT TC
ICB-s5	CCA AAG AGC CAG GGT ATC AA

NEO-s2	CTT GGG TGG AGA GGC TAT TC
NEO-a5	ATG GGT CAC GAC GAG ATC AT
WT band	400bp
KO band	550bp

Themis1	
TLAP-R3	GTA GGA CAG CCC TAA GGT GGG
gCA-S1	ACT GTC TCC TGC CTA TTC TC
Neo3-1	AAG TGC CAG CGG GGC TGC TA
WT band	125bp
KO band	250bp

Ig-HEL	
IgH F1	GCGACTCCATCACCAGCGAT
IgH F2	CTGGAGCCCTAGCCAAGGAT
IgH R1	ACCACAGACCAGCAGGCAGA
HEL 3F	GAGCGTGAACTGCGCGAAGA
HEL 4R	TCGGTACCCTTGCAGCGGTT
Ig band	460bp
Control band	264bp
HEL band	<control band

MHCII kb	
Ea3'	CATAGCCCCAAATGTCTGACCTCTGGAGAG
K5'	CATGGGCATAGAAAGGGCAGTCTTTGAACT
Ea5'	AGTCTTCCCAGCCTTCACACTCAGAGGTAC
k band	210bp
b band	150bp

Table 2.5 List of primers and band sizes for mouse genotyping. Bp, basepair.

PCR reactions were carried out using Pltier Thermal Cycler (MJ Research). The products were separated by 2% agarose gel and the bands viewed using UVP AutoChemi System (Bioimaging system).

2.2.3. Procedures involving live animals

Adult bone marrow chimeras

Chimeras were generated by irradiation of CD45.1 ($Ly5^a$) allotype-marked B6 animals with two doses of 4.5 gray (Gy) gamma radiation 3 hours apart. The donor cells were from the leg bones of the donor mice. For mixed chimeras, donor cells from CD45.1 ($Ly5^a$) WT mice and CD45.2 ($Ly5^b$) mice with the appropriate genotypes were mixed and used. The donor cells were washed out of the leg bones by sterile R2. Each recipient mouse was injected intravenously with at least $5x10^6$ adult bone marrow cells in a volume of 200 µL. The mice were kept on Baytril for 3 week and analyzed 8-10 weeks after reconstitution.

Stimulation with sheep red-blood cells (SRBCs)

3.5 mL of SRBCs was washed in 45 mL of cold sterile PBS. The mixture was centrifuged at 500g for 10 minutes. The supernatant was carefully taken off, leaving around 5 mL of soft pellet containing most of the SRBCs. The remaining pellet was resuspended. Each mouse was injected intraperitoneally on both sides with a total of 200 µL washed SRBCs. The animals were sacrificed 7-9 days post stimulation.

Stimulation with NP-CGG coupled with alum

NP(19)-CGG was dissolved in PBS at 1 mg/mL. LPS was dissolved in PBS at 1 mg/mL. 9% stock of alum solution was diluted to 0.9% in PBS. 3.2 µL of NP(19)-CGG solution was mixed with 320 µL of LPS solution and 4.08 mL PBS. Then 3.2 mL of 0.9% alum solution was added dropwise while the mixture was being vortexed, resulting in a cloudy suspension. A final 2 mL

PBS was added at the end. Each mouse was injected intraperitoneally with 200 µL of the mixture. This gives each animal 50 µg NP(19)-CGG and 5 ug LPS coupled to alum. The animals were sacrificed on 7 and 14 days post stimulation.

Stimulation with NP-Ficoll

NP(25)-Ficoll stock solution was made in sterile PBS at 5 mg/mL. Prior to injection, the NP(25)-Ficoll was diluted to 250 µg/mL in sterile PBS. Each mouse was injected intraperitoneally with 200 µL of the solution (50 µg of NP(25)-Ficoll per mouse). Mice were bled from tail on days 7, 14, 21 and 28 after the injection. 50-100 µL of blood was taken before the bleeding was stopped by applying pressure.

2.3. General procedure

2.3.1. Western blot and related

Sample preparation for SDS-PAGE gel and western blot

Mouse spleens were harvested and pressed gently through 70 μm cell strainers to form single-cell suspensions. The samples were centrifuged at 250 g, 7 minutes at 4 °C, washed in ice-cold PBS, centrifuged and resuspended in ice-cold 1x lysis buffer. The samples were incubated on ice for 30 minutes before centrifugation at 13,000 g for 20 minute at 4 °C. The supernatant was harvested and frozen at -20 °C.

B separation by negative selection protocol

Spleen samples were prepared as described previously. Cells were centrifuge at 250 g for 7 minutes at 4 °C, and resuspended in 10 mL ice-cold PB. After centrifuging again, cells were resuspended in 1 mL PB and lumps were removed. 5 μL each of biotinylated anti-CD43, anti-CD3, anti-CD11c, anti-CD11b and anti-Ly76 was added to each cell suspension and incubated on ice for 15 minutes. Cells were washed by the addition of 14 mL of TAC and re-centrifuged and resuspended in 300 μL of PB per spleen before the addition of 15 μL of microbeads and then a 10-minute incubation on ice. During this incubation the MACS LS columns were washed twice with 4 mL of PBE and attached to the magnets. A further 300 μL of PB was added to the cells before they were loaded onto the columns. 4 mL of ice cold PBE was then added twice to the columns and the flow through collected.

B cell stimulation prior to WB analysis

Spleen samples were prepared and enriched for B cells by negative selection as described previously. The resulting samples were washed and resuspended at $1x10^8$ cells/mL in R0. Stimuli were made in R0 and used at 10x final concentration. Cells and stimuli were warmed in a 37°C water bath for 20 minutes. Stimulation began with the addition of 9 volumes of cells to 1 volume of 10x stimulus. After the time indicated, the cells were put into ice-cold 2x lysis buffer to lyse.

Running SDS-PAGE gel and western blotting

In preparation for SDS-polyacrylamide gel electrophoresis (SDS-PAGE), 1 volume of 5x reducing loading buffer was added to 4 volumes of sample. The mixtures were heated at 98 °C for 5 minutes before being loaded onto 10% SDS-PAGE gels. Gels were electrophoresed at 150 volts until the loading dye front reached the bottom of the gel.

Gels were soaked in transfer buffer for 10 minutes before the assembly of the transfer cassette, consisting of membrane, filter paper and Mini Trans-Blot apparatus (Bio-Rad). Transfer was carried out at 100 volts for between 45 minutes to an hour.

The transferred membrane (blot) was blocked in blocking buffer for typically 1 hour at room temperature or over-night at 4 °C. Antibodies were added to binding buffer at typically 1/2000, and incubated for 1 hour at room temperature or over-night at 4 °C. The blots were then rinsed once and washed 3 more times for 15 minutes each in TBST. Secondary antibodies coupled to HRP were diluted at typically 1/3000 in binding buffer and

incubated at room temperature for 1 hour, before the washes. Detection was by enhanced chemiluminescence. Film was exposed in the dark and developed by Xograph X4 (Xograph) film processor.

2.3.2. Flow cytometry and related

Preparing mouse cell samples for flow cytometry analysis

Cells from the peritoneal cavity were obtained by washing the cavity repeatedly with R2 and collecting the media. Blood was collected from the heart. For flow cytomery, approximately 100 µL of peripheral blood was transferred into 10 mL 1% EDTA/PBS at room temperature and mixed by reverting. For serum, blood was collected in 1.7 mL eppendorfs and left to clot. Samples were then centrifuged at 13,000 g for 5 minutes and the supernatant collected. This was repeated and the sera stored at -20°C. Thymus, spleen and mesenteric lymph nodes were taken into. Bones from the hind legs were taken and kept in 10 mL chilled R2 to obtain bone marrow cells.

25 gauge needles were used to flush the bone marrow from the shaft of the tibiae and femurs with ice-cold R2. The cells were then passed through the needle until a single-cell suspension was obtained. Spleen, lymph node and thymus cell suspensions were prepared in ice-cold media by gently pushing the organ through a 70 µm cell strainer. The cells were centrifuged at 250 g for 7 minutes, and the supernatant aspirated. Bone marrow, spleen, lymph node and thymus pellets were then resuspended in 5 mL, 10 mL, 2 mL and 10 mL of ice-cold R2 respectively. Blood samples in 1% EDTA/PBS were centrifuged and the red blood cells lysed by resuspending the pellets in 10 mL TAC at 37 °C for 10 minutes. After centrifuging at 250 g for 7 minutes, the

samples were aspirated and washed in 10 mL ice-cold R2. Cells were finally resuspended in 200 µL ice-cold R2. All cells were held on ice until staining for flow cytometry analysis.

Cell concentration was determined by counting a 1 in 10 dilution of cells in WBCCF, with a 0.1 mm haemacytometer (VWR) under Nikon Eclipse E400 Microscope.

General surface staining

The volume of each sample equivalent to 5 x 10^5 cells was transferred to a round-bottomed 96-well plate, and the wells filled to a volume of 200 µL with staining media. The plates were centrifuged at 800 g, 4 °C for 1 minute, and the media removed. Cells were then resuspended in 25 µL of staining mixture, containing appropriate antibodies, and incubated on ice, in the dark, for 20 minutes. Cells were washed twice with staining media before further staining or the transfer to FACS tubes for Flow Cytometric analysis. All antibodies used were titrated to optimize staining, and diluted in staining media immediately prior to use.

Cell stimulation and intracellular staining for phosphorylation

Spleen cells were processed as previously described and resuspended in room temperature R0. Cells were counted and resuspended at 2.5x10^7 cells/mL in R0 and then warmed in a 37 °C water bath for 30 minutes. 100 µL of 2x stimulus was added to each FACS tube and warmed for 5 minutes. The final concentration of stimulus is as indicated in the results figures. 100 µL of cell suspension was then added to each FACS tube containing the stimulus

and left to stimulate for exactly 5 minutes. The stimulation was stopped by adding 1 mL of Cytofix/Cytoperm buffer and incubating at 37 °C for 10 minutes. Cells were centrifuged at 500 g for 5 minutes and resuspended in 1 mL of Permwash buffer for 10 minutes at RT. Cells were divided into 5 x 10^5 cell aliquots and placed into round bottom 96 well plates for staining. Cells were washed once in Permwash buffer before being stained in Permwash buffer with the appropriate surface and intercellular antibodies and incubated at room temperature for 30 minutes in the dark. Finally cells were wased and resuspended in Permwash before analysis by flow cytometry.

Ca^{2+} flux monitored by flow cytometry

To monitor Ca^{2+} flux following BCR stimulation, spleen cells were prepared as already described. WT and KO cells were first stained separately for surface B220 coupled to different fluorochromes and live/dead indicator. The cells were mixed in equal parts and resuspended in HBSS containing 0.02% Pluronic F-127, 1 µg/mL Fura Red, AM, already warmed to 37°C. The cells were incubated at 37 °C for 30 minutes, before washing and resuspending at 1x10^7 cells/mL in HEPES saline solution.

For stimulation, a small volume of cells was warmed to 37 °C in water bath for 10 minutes before being acquired by flow cytometer. A base line was first established using cells without any stimulus. 1 volume of 10x stimulus was placed at the bottom of a new FACS tube and warmed to 37 °C. The acquiring tube was taken off the machine after 20 seconds and 9 volumes of cells were taken out and added to the stimulus tube. This tube was immediately returned to the flow cytometer to visualise the induction of Ca^{2+}

flux. Each sample was acquired for a total of 3 minutes. The final concentrations of stimulus are indicated in the result figures.

Data collection and analysis

Six-color flow cytometry data were collected on BD FACSCanto; Ca^{2+} flux was collected on BD LSRII. Data were analysed using FlowJo (Tree Star). Statistical analysis was done using Excel (MicroSoft) and Prism (GraphPad).

2.3.3. Sandwich ELISA

Sandwich ELISA was used to measure antibody titres and cytokine concentrations. IgM^a titres of Ig mice were measured using HEL-Ig capture ELISA. IgG1 titres of challenged mice were measured by anti-mouse IgG1 capture ELISA. The IL-2 concentration in the supernatant of cultured cells were measured by IL-2 ELISA kit (eBioscience)

Protocol of HEL-Ig capture ELISA:

96-well flat bottome ELISA plates were coated with 100 µL of 10 µg/mL HEL in carbonate buffer pH 9.6 (0.2 µm filter sterilised) and incubated at 37 °C for 2 hours or overnight at 4 °C. Plates were washed 3 times with PBS/Tw and then blocked with 200 µL of 1% BSA/PBS (0.2 µm filter-sterilised) at 37 °C for 2 hours or overnight at 4 °C. Plates were again washed 3 times with PBS/Tw and the serum samples added and serially diluted in 0.1% BSA/PBS before being incubated at 37 °C for 2 hours. After incubation, the plates were

washed 5 times with PBS/Tw and 50 µL of biotinylated anti-IgM^{a} in ICE-T was added to each well. Plates were then incubated for 2 hours at 37 °C or overnight at 4 °C. The plates were then washed 5 times with PBS/Tw before the addition of 50 µL of avidin-AP (1/3000) in 0.1% BSA/PBS and a final incubation of 1 hour at 37 °C. Lastly, the plates were washed 5x PBS/Tw, 2x PBS, 1x water and 1x NPP buffer. Plates were developed with 100 µL/well of 1 mg/mL SIGMA^{104}/NPP buffer, and absorbance measured at 405 nm with a model 550 Microplate Reader (BIO-RAD). The positive control used in this ELISA was serum from one WT Ig-inHEL mouse. The concentration of Ig titre of the standard, was measured using sera stored and measured by previous lab members The standard was used at in 1/3 serial dilutions starting from 1/30 of the original.

Protocol of IgG1 capture ELISA:

See previous ELISA protocol with the following changes. Plates were coated with 100 µL of 2 µg/mL anti-mouse IgG1 in ELISA coating buffer (0.2 µm filter-sterilised). An alkaline phosphatase conjugated anti-mouse IgG1 was used in replacement of a primary and secondary antibody and was diluted in 0.1% BSA/PBS.

Protocol of IL-2 capture ELISA:

The supernatant of cultured cell was separated from cells as described in Section 2.3.4. The IL-2 capture ELISA was performed using Mouse IL-2 ELISA Ready-SET-Go! Kit (eBioscience 88-7024). The protocol within was followed.

For sHEL stimulation, the supernatant was diluted at 1/10 for the highest sHEL concentrations, 1/5 or 1/2 for the intermediate ones and 1/1 for the lowest concentrations and media alone. For mHEL stimulation, the supernatant dilution was uniformly 1/5. These ratios were determined by trial experiments and ensured that multiple readings were within the range of the reference. The absorption at 450 nm was read and that at 570 nm was deducted, using Safire^2 (TECAN) and Magellan5.

Protocol of anti-NP IgM and IgG3 capture ELISA:

See ELISA protocol for HEL-Ig capture, with the following changes. Plates were coated with 100 µL of 5 µg/mL NP_{25}-BSA in ELISA coating buffer (0.2 µm filter-sterilised). Sera were used in 1/00 and 1/200 dilution and in duplicates. An alkaline phosphatase conjugated anti-mouse IgM and IgG_3 was used in replacement of a primary and secondary antibody and was diluted in 0.1% BSA/PBS.

2.3.4. Cell culturing

General conditions

The handling of cultured cells was under sterile conditions, within an extraction fume hood. All buffers were kept under sterile condition, handled within an operating hood, or filter-sterilised by 0.2 µm syringe filter. All items were wiped with 70% ethanol before entering the hood. The cells were kept in incubators at 37 °C with 5% CO_2.

Cell lines

NIH3T3 cell line was kept in complete DMEM media. The cell line clones used for mHEL stimulation grew at different rates and were passaged at least once a week. The division ratio was determined by inspection of the flask, as viewed under a microscope. The cells were passaged by first rinsing with warm PBS, followed by the addition on Trypsin-EDTA to detach the cells from the flask. The cells were then washed once with warm media before transferring to a fresh flask.

2G7.1 cells were kept in complete RPMI media (R10). The cells were passaged twice per week at 1/20 dilution. The appropriate volume was simply added to fresh media in a new flask.

In vitro stimulations

For over-night sHEL stimulation, spleen samples were first prepared as described in Section 2.3.1, but under sterile conditions. The cells were counted, centrifuged and resuspended at $4x10^7$ cells/mL in room temperature R10. 50 μL per well cell suspension was added in 96-well (round bottom) plates. 2x concentration HEL solution was made from lyophilized powder in R10. 50 μL/well of 2x sHEL solutions was added to the plate containing the cells, pipetting repeatedly to mix. a multi-channel pipette was used to ensure the accuracy of timing. The plates were incubated for 16 hours before the cells were washed in cold staining media and used for flow cytometry analysis.

For mHEL stimulation, the NIH3T3 clones were seeded up to 24 hours before stimulation, in 96-well (flat bottom) plates. $1x10^4$ cells were seeded in each

well in triplicates and incubated for at least 12 hours. Spleen samples were prepared as described for sHEL stimulation, but resuspended at $4x10^6$ cells/mL in R10. Supernatant was removed from the NIH3T3 cells, leaving 50 μL. Then 50 μL of spleen cells were added to each well. The plates were incubated for 24 hours. The next day, the plates were centrifuged and supernatant removed. Cold staining media was added to the plate and cells in suspension were washed off by repeated pipetting. Triplicates were combined for flow cytometry analysis

For IL-2 production assay, B cells were enriched in spleen samples, as described in Section 2.3.1 under sterile conditions. The preparation and plating of sHEL solution and mHEL clones were similar as above. 25 μL/well of 4x sHEL solutions was plated and 25 μL of media was left in each well of the NIH3T3 clones. 2G7.1 T cells were grown at large scales from 5 days previously and were divided 1/3 the day before. The T cells were counted, centrifuged and resuspended in warm R10 at 2.4x the concentration of spleen cells ($9.6x10^6$ cells/mL). Spleen samples were counted and resuspended at $4x10^6$ cells/mL. To assemble the stimulation plates, 25 μL/well of T cells were added to the antigens. Then 50 μL/well spleen samples were added to the wells. The plates were incubated for 16 hours. When the incubation ended, the plates were centrifuged and the supernatant retained and kept at -20°C until being used. The cells were washed in cold staining media and used in flow cytometry as described above.

In vitro proliferation

For proliferation, the cells were first stained for CFSE. Cells were washed twice in room temperature HBSS and resuspended in HBSS at $5x10^7$

cells/mL. CFSE was dissolved in PBS at 10 mM and stored away from light at -20°C. 10x solution was made in HBSS at 50 μM (final concentration at 5 μM). This was added to 9x the volume of cells and mixed immediately. The cells were kept at room temperature in the dark for 8 minutes, before the staining was quenched by adding at least 10 volumes of R10 to the cells at room temperature. The cells were washed 3x with 50 mL room temperature R10, counted and resuspended at $2x10^6$ cells/mL.

100 μL/well was plated in triplicates in 96-well (round bottom) plates. Stimulants were prepared at 2x and 100 μL/well was added on top of the cells, pipetting repeatedly to mix. 1/3 dilutions were used. The highest final concentration of ionomycin was 2 μM; PDBu, 2 μM; LPS, 20 μg/mL. In stimulations using both LPS and sHEL, the final concentrations were as indicated in the result section.

After the time indicated (48 hrs, 72 hrs or 4 days), the plates were centrifuged and supernatant removed. The cells were washed in cold staining media and analysed by flow cytometry.

2.3.5. Whole-genome sequencing

Genomic DNA preparation

Tails were taken from mice and stored frozen at -20 °C. DNA extraction was carried out according to Qiagen Isolation of Total DNA from Rodent Tails protocol using DNeasy Tissue Kit. The DNA concentration was measured using ND-1000 Spectrophotometer (NanoDrop). DNA quality was evaluated by the values of 260/280 and 260/230 absorptions. DNA was stored at -20 °C or 4 °C.

Data process and analysis

Sequencing was performed by the High-Throughput Genomics Group at the Wellcome Trust Centre for Human Genetics, Oxford, UK. The raw data from the whole-genome sequencing were processed by Dr Katherine Bull in my group. Briefly, the sequencing data were first mapped to the standard sequence of C57BL/6J (B6) using Stampy. Then variants were called by Platypus, an in house tool developed to call both single nucleotide variants and small indels. The variants were then filtered to remove known B6 variations, variants with low coverage or quality and those in repetitive regions of the sequence. The resultant variants were annotated against the mouse refseq gene set using ANNOVAR. This process resulted in a short list of variants. I examined all exonic nonsynonymous variants. The qualities of these variants were checked by hand using IGV. The number of reads containing the variants, allelic and strand bias and the position of variants in the gene and reads were some of the factors considered. The PolyPhen2 scores were obtained from the PolyPhen website (http://genetics.bwh.harvard.edu/pph2/index.shtml). Other programmes used during analysis included Excel and Prism.

2.3.6. Real-time PCR

Cells of populations indicated were sorted by flow cytometry at the Jenner Institute, Oxford, UK. Pre/pro, immature and mature B cells were from the bone marrow; follicular and marginal zone B cells were from the spleen; T cells were from the thymus; germinal centre and class-switched B cells were from the spleens of mice immunised by SRBCs 7 days previously. The organs were prepared and cells stained for surface antigens, as described

previously. The collected pure populations were kept in RNA-free eppendorfs on ice then centrifuged, resuspended in Buffer RLT (part of RNeasy kit) with β-mecapitoethanol, snap-frozen in liquid nitrogen and stored at -80°C until further processing.

Total RNA was extracted from the cells using RNeasy kit following the protocol within. To make cDNA, RNA concentration was first measured using ND-1000 spectrophotometer (NanoDrop). The same amount, and up to 8 μL of RNA, was used to produce cDNA together with 1 μL DNase 1, 1 μL DNase 1 buffer and nuclease-free water to a total volume of 20 μL. This was incubated at 25 °C for 15 minutes before the addition of 1 μL of 25 mM EDTA, and a further incubation at 65 °C for 10 minutes. The reaction was then cooled on ice for 2 minutes. The following was then added to the mixture: 1 μL Random hexamers, 1 μL 10 mM dNTPs, 2 μL 10x RT buffer, 2 μL 50 mM $MgCl_2$, 2 μL 0.1 M DTT and 1 μL RNase out. This was incubated at 25 °C for 2 minutes before the addition of 0.25 μL of superscript and 0.75 μL of nuclease-free water. Following this, the mixture was incubated for: 25 °C for 2 minutes, 42 °C for 50 minutes and 70 °C for 15 minutes. At the end of this incubation 1 μL of RNaseH was added and incubated at 37 °C for 20 minutes. The concentration and quality of the cDNA were measured using ND-1000 spectrophotometer (NanoDrop).

The cDNA was used in real-time reverse-transcript PCR (RT-PCR). Each RT-PCR reaction contained the following: 0.5 μL 20x Taqman Gene Expression Assay (Icb-1 or Themis1), 0.5 μL β -actin gene expression assay, 5.0 μL 2X Taqman Universal Master Mix, 3.0 μL Nuclease-free water and 1 μL of cDNA

template (0.5–50 ng). The sample plate was run on StepOnePlus Real-Time PCR System (AppliedBiosystems), using multiple wavelength detection for control and target.

Chapter Three B cell development in the pre-immune repertoire in Icb-1 knockout mice

3.1. Introduction

To investigate Icb-1, the B and monocyte-lineage homologue of Themis1, I obtained a previously uncharacterized gene-targeted null mouse (Icb-1$^{-/-}$ or KO) from the laboratory of our collaborator Dr Paul Love at the NIH. These animals carried a neomycin replacement cassette at the end of Exon 4 of the genomic Icb-1 sequence (chromosome 4: 132,338,272-132,352,279).

Icb-1 is expressed in B cells, macrophages and dendritic cells, as demonstrated by previous studies[1] and BioGPS (http://biogps.org). I focused my studies on B cells and first examined the expression of Icb-1 in different B cell subpopulations in wild-type (WT) C57BL/6 (B6) mice. I confirmed the deficiency of Icb-1 expression in KO and heterozygously knocked-out (HET) mice by western blot. Since the gene targeting had been performed on a 129 background, with backcrossing to C57BL/6, I also used low-coverage whole-genome sequencing to examine the genetic similarity between the knockout mice and B6 WT controls.

To identify the defects in B cell development, I compared B cell populations from un-manipulated adult KO, HET and WT mice. B cell populations were enumerated in the bone marrow, the spleen, the mesenteric lymph nodes and the peritoneal cavity. To create a more stringent test, I then compared B cell development in a competitive environment by creating mixed-chimeric mice reconstituted from WT and KO adult bone marrow cells. Finally I produced Icb-1$^{-/-}$Themis1$^{-/-}$ mice to investigate possible redundancy between Themis1 and Icb-1 proteins.

To be able to follow antigen-specific B cell clones and to explore the possible effects of Icb-1 on negative and positive selections, I crossed the KO mice with MD4 mice[70] that express IgM^a and IgD^a transgenes (derived from the HyHEL10 clones) with high affinity ($K_a=2x10^{10}$ M^{-1})[274] to hen egg lysozyme (HEL) (the 'Ig mice'). KO and WT Ig mice were investigated in the absence of HEL and then crossed to mouse strains expressing systemic membrane-bound HEL (mHEL, KLK), soluble HEL (sHEL, ML5), or intracellular HEL (inHEL, mHEL-KK)[57]. By this strategy, I created double transgenic mice expressing a systemic form of HEL as self-antigen with different availabilities but the same affinity. I was then able to explore the role of Icb-1 in negative and positive selections of different B cell populations by self-antigens.

3.2. Icb-1 expression in wild-type mice and the examination of knockout mice

As a prelude to examining the functional role of Icb-1, I confirmed the expression of Icb-1 in B cells of WT mice. To achieve this, I sorted B and T cell subtypes by flow cytometry, as indicated in Figure 3.1a, and determined the amounts of Icb-1 mRNA in each cell group using real-time PCR. The cell surface antibody marker used to distinguish the different cell types were also used in subsequent sections and are described in more detail therein. Briefly, pre/pro ($B220^+CD43^+$), and immature B cells ($B220^+CD43^{neg}$), were separated from bone marrow cell lymphocyte populations; follicular ($B220^{++}CD23^{++}CD21^+$) and marginal zone B cells ($B220^{++}CD23^{neg}CD21^{++}$) from naïve splenocytes. Germinal centre (GC $B220^{++}CD95^+GL\text{-}7^+$) and class-switched ($B220^{++}IgG1^+IgD^{neg}$) B cells were from the spleens of mice immunised with sheep red-blood cells; B1 B cells ($B220^{low}IgM^{++}IgD^{neg}FS^{high}$) were from the peritoneal cavity separated.

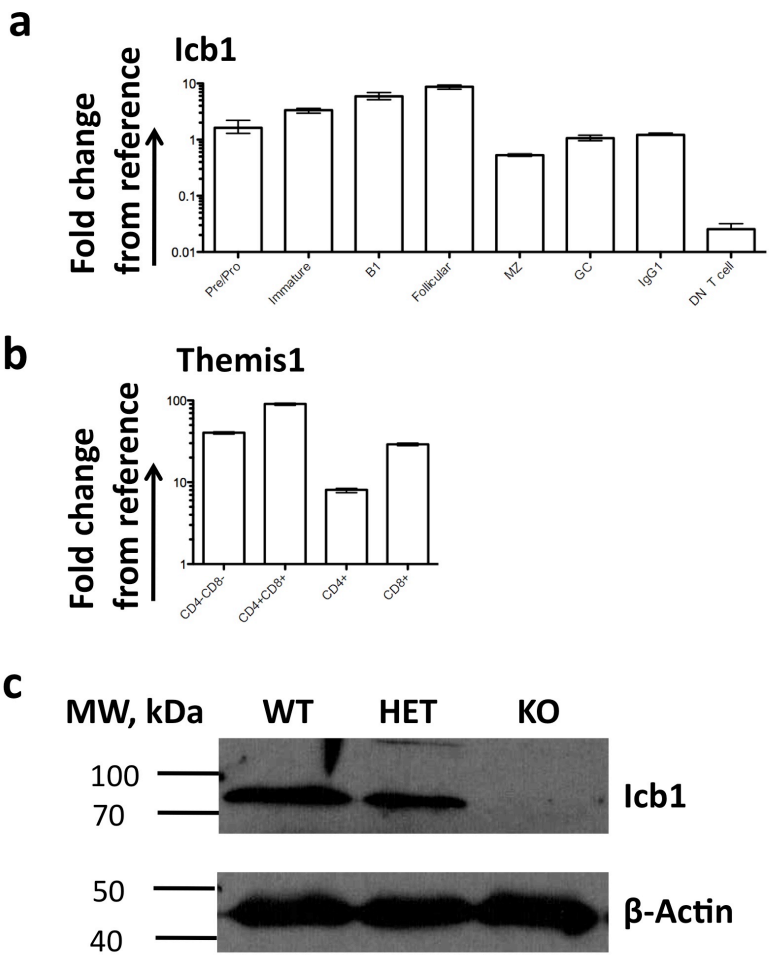

Figure 3.1 Icb-1 expression. a) Icb-1 expression in B cell sub-populations and double negative (DN) T cells. B cells were sorted and mRNA isolated. The expression was determined by real-time PCR and normalized to a common reference. Data show the mean and range of one sample (triplicated) and is representitive of three independent experiments. b) Themis1 expression in thymus T cell subpopulations. Data show the mean and range of one sample (triplicated) and is representitive of three independent experiments. c) Western Blot showing Icb-1 protein expression in spleen samples enriched for B cells (>95%). Icb-1 has a molecular weight (MW) of 72 kDa. β-Actin was used as loading control. Its molecular weight is 42 kDa.

The results showed that Icb-1 is expressed in all the B cell subpopulations studied, from bone marrow early precursors to peripheral mature B cells. The expression level increases gradually and in small amounts from pre/pro to follicular B cells and is relatively low in marginal zone B cells. To assess the expression in more differentiated cells, I stimulated mice with sheep red-blood cells (SRBCs) and purified germinal centre (GC) B cells and class-switched ($IgG1^+$) B cells 9 days post stimulation. These populations showed relatively low levels of Icb-1 expression compared with the other B cell subpopulations. In contrast, a very low level of Icb-1 mRNA was found in the thymus, as demonstrated in the double negative (DN) T cell population. It was not detectable in any other T cell populations in the thymus (the lowest detected value was 0.0215 in fold change).

The Icb-1 homologue Themis1 was found to be expressed at much higher levels in T cells than Icb-1 in B cells (Figure 3.1b). A common reference sample was used, extracted from a 1:1 mixture of wild-type thymocytes and splenocytes. All values shown were unified against this reference. In agreement with previous studies, the expression of Themis1 was the most highly expressed in double positive (DP) T cells and was reduced in single positive (SP) T cells[1,3]. It was not detectable in any of the B cell populations studied.

I then examined the expression of Icb-1 in the knockout mice. A western blot showed the loss of all Icb-1 expression in splenic B cells from KO mice (Figure 3.1c). HET mice showed intermediate expression between WT and KO mice.

An unknown number of backcrossing was performed before the mice arrived in my research group. Several differences have been described between

129S/J and C57BL/6 (B6) mice, therefore I performed low-coverage whole-genome sequencing to define the genetic background of the experimental mice. Two male mice were sequenced: Mouse A, representative of mice commonly used in my experiments, which have been backcrossed to B6 mice for three generations since the strain arrived; Mouse B, backcrossed to B6 mice for a further three generations (a total of six generations after arriving).

The two sets of data from the two mice showed the same coverage, with 88.2% of the genome read at least once (Figure 3.2a). I am grateful for the assistance from Dr Katherine Bull in performing the analysis of the raw data. The resultant group of variants ('variants' from here on) were plotted according to their positions in the chromosomes (Figure 3.2b). Both plots from Mouse A and B showed a single small area rich in variants in Chromosome 4, representing a signle congenic region around the Icb-1 genomic sequence (starting position shown as a horizontal bar). The variant-dense region in A covers 10.8479×10^6 bases, and in B covers 7.6391×10^6 bases.

When I combined the variants from the two data sets, 171 single-nucleotide polymorphisms (SNPs) were found in the 129 congenic region in Chromosome 4. Within these, 37 variants were exonic and nonsynonymous, in 20 out of 338 genes in this region (according to Ensembl at the time of writing).

In order to predict the impact of these SNPs on the coded proteins, I gathered information on these proteins, mainly by using databases Uniport and Gene Ontology. Details are listed in Appendix. I also considered HumDiv scores from PolyPhen2 as an estimate of the impact of damage due to the amino acid replacement.

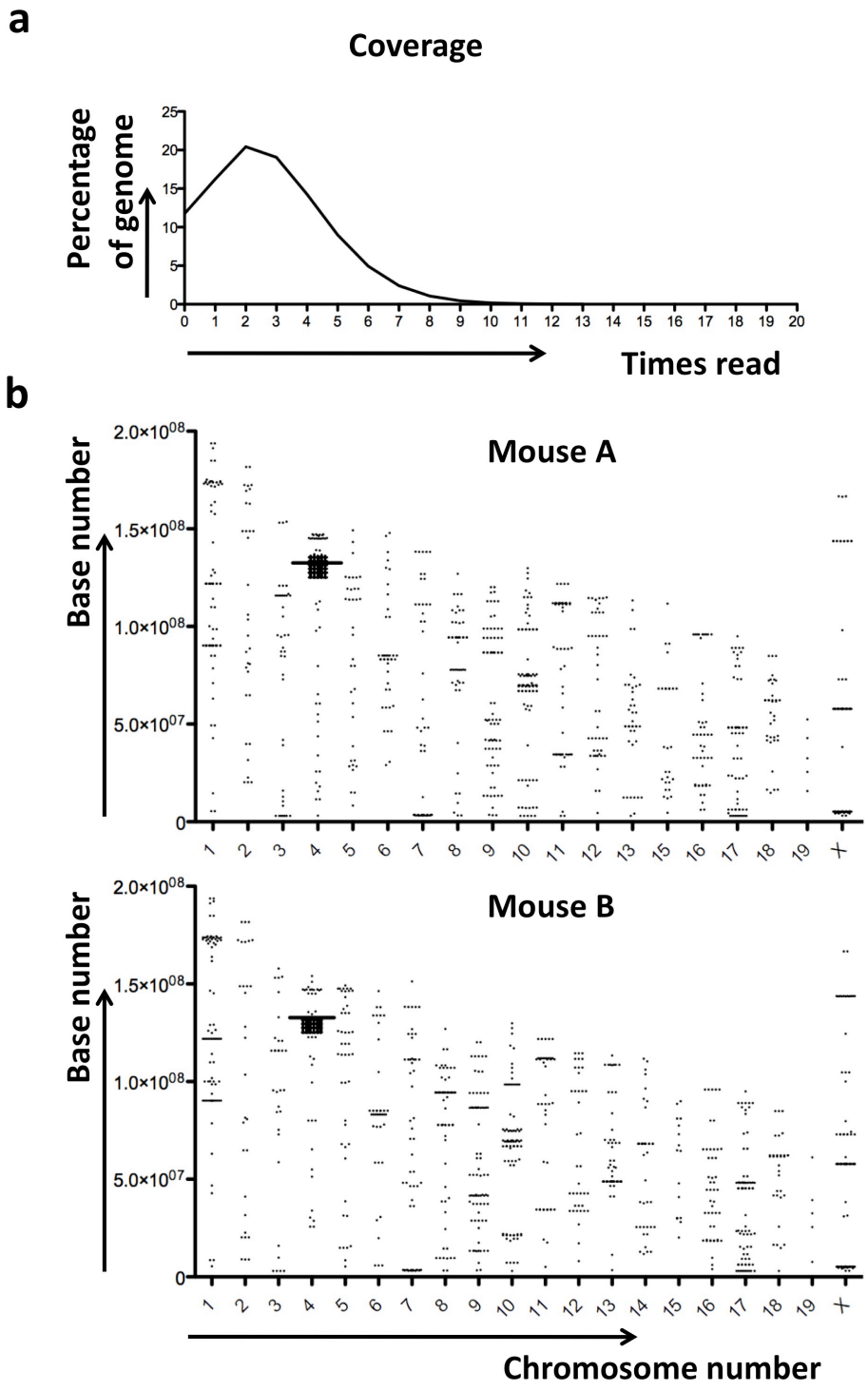

Figure 3.2 Low-coverage whole-genome sequencing to assess backcross. a) Coverage of the sequencing data presented as the percentages of the genome read at different levels of coverage (times read). b) Scatter plots showing the locations of variants according to chromosomal location (base number). Horizontal bars wider than the column indicate the starting position of Icb-1.

None of the variants listed stood out as likely to influence the phenotype of the KO mice on the basis of tissure-specific expression, known functions of the protein and the PolyPhen score of HumDiv (more suitable for non-disease-causing variants and cross-species comparisons). By these criteria, no variant was likely to be significant in my study due to one or more reasons. A table in the Appendix lists these reasons and possible first-stage investigations, if investigations of any of the proteins are needed. (Section A.3, details found on the genes are listed in Section A.4)

To summarize, I began by showing that Icb-1 is expressed in developing, peripheral and immunized B cells. Only a very small amount of Icb-1 mRNA was detected in double negative T cells. Conversely, Themis1 was detected in thymic T cells, but was undetectable in any B cell population studied. The deficiency of Icb-1 in KO mice was demonstrated in spleen B cells by western blot. The results from low-coverage whole-genome sequencing showed that the Icb-$1^{-/-}$ mice used in my experiments were near identical to B6 controls. The exonic, nonsynonymous variants differing from the B6 reference sequence clustered around the knockout cassette, and none of the variants were likely to affect immunological phenotypes. On this basis, I felt confident I could make meaningful comparisons between KO mice and B6 controls.

3.3. Lymphocyte Development

3.3.1. Icb-$1^{-/-}$ mice

Given the role of Themis1 in T cell development, it seemed highly possible that its homologue Icb-1 would have a similar role in B cell development. Therefore, I compared B cell development in the bone marrow and the

spleen of adult mice. HET mice were all littermates with KO mice and WT controls were either littermates or unrelated mice. In agreement with the genetic findings in Section 3.2, no difference was identified between WT siblings or unrelated mice in any of the experiments.

In the bone marrow, KO mice showed normal total (white blood cells), lymphocyte (B and T cells) and total B cell ($B220^{+}$) counts (Figure 3.3a). Two strategies were used in viewing B cell development stages in the bone marrow, by surface expressions of CD24 or CD43 in combination with B220 (Figure 3.3b). There was no difference between KO and WT mice in relative numbers or proportions of pre/pro-B cells ($CD43^{+}B220^{+}$), immature ($CD24^{+}B220^{+}$ or $CD43^{neg}B220^{+}$) or mature recirculating cells ($CD24^{mid}B220^{++}$ or $CD43^{neg}B220^{++}$) (Figure 3.3b and c). Similar results were found using cell surface IgM and IgD (not shown).

Total white blood cell, lymphocyte and B cell counts were also normal in the spleen (Figure 3.4a). The mature and immature B cells were separated by their respective negative and positive expression of surface CD93 (AA4.1) (Figure 3.4b, upper panel). Immature B cells were then separated into transitional stages T1 ($CD93^{+}IgM^{hi}CD23^{neg}$), T2 ($CD93^{+}IgM^{hi}CD23^{+}$) and T3 ($CD93^{+}IgM^{lo}CD23^{+}$) (Figure 3.4b, middle panel). Mature B cells were viewed as follicular ($CD23^{hi}CD21^{mid}$) and marginal zone B cells ($CD23^{lo}CD21^{hi}$) (Figure 3.4b, lower panel). No statistically significant difference ($p>0.05$) was found in the numbers in all three transitional stages, overall mature, or follicular B cells. However, the number of MZ B cells was slightly higher in the KO mice (Figure 3.4d). The difference was found to be small but consistent in all 5 experiments (as well as in experiments using chimeric mice, as shown later). In the experiment shown, the means and standard errors of mean

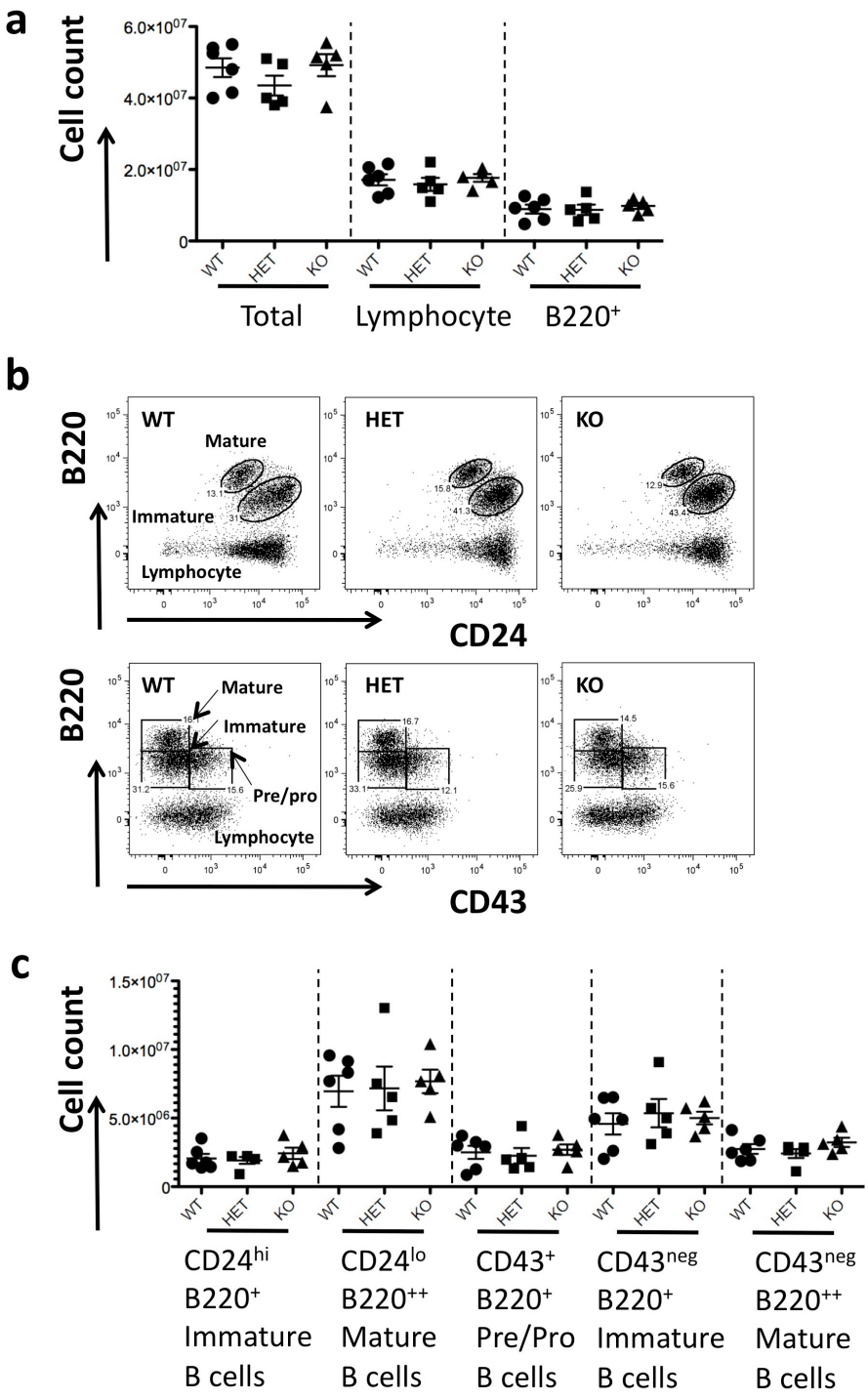

Figure 3.3 B cell development in the bone marrow. a) Total (white blood cells), lymphocyte and B cell numbers in the bone marrow of WT, HET and KO mice. b) Flow cytometry plots demonstrating B cell development monitored by cell surface expressions of B220, CD24 and CD43. c) Bone marrow cell counts of different gated populations shown in b, from WT, HET and KO mice. Data are presented as mean and standard error of mean (SEM); data points represent individual animals. p values are shown if $p \leq 0.05$.

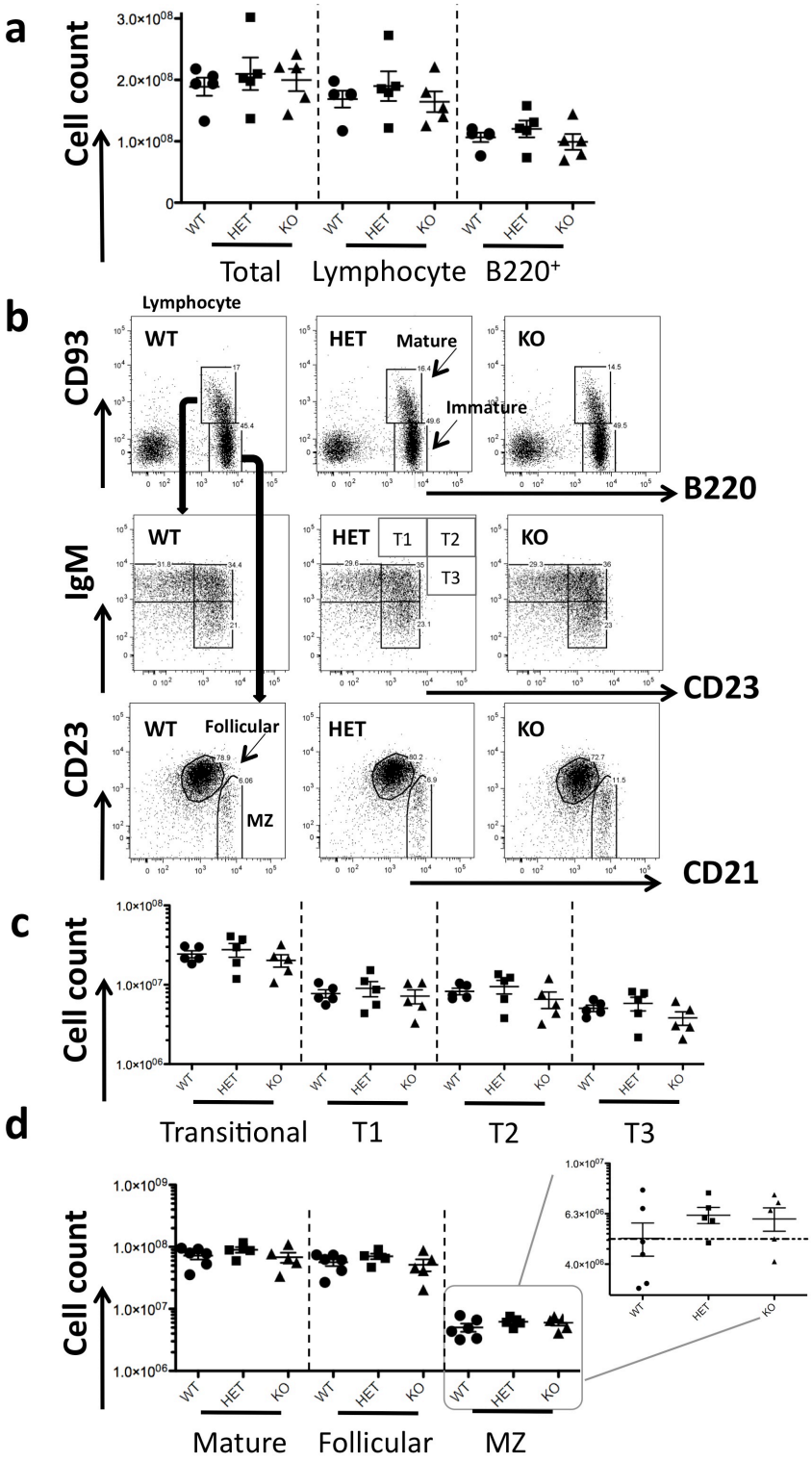

Figure 3.4 B cell sub-populations in the spleen. a) Total white blood cell, lymphocyte and B cell numbers in the spleens of WT, HET and KO mice. b) Flow cytometry plots demonstrating the separation of B cell sub-populations. Immature and mature B cells were classified as CD93 positive and negative B220 positive cells, respectively. Immature B cells were separated into transitional stages 1-3 according to IgM and CD23 expressions, and mature B cells into follicular and marginal zone B cells according to CD23 and CD21 expressions. c-d) Cell counts of spleen B cell sub-populations in WT, HET and KO mice. T1, transitional stage 1; MZ, marginal zone. Error bars show mean and standard error of mean (SEM); data points represent individual animals. p values are shown if $p \leq 0.05$.

(SEM) of WT, HET and KO mice were (5.038±0.756)x10^6, (6.225±0.458)x10^6 and (6.017±0.639)x10^6, respectively (p value of the WT-KO difference was 0.3604).

Lymphocyte and B cell counts were also normal in the mesenteric lymph nodes (data not shown).

KO mice showed a normal B1 B cell population ($B220^{lo}CD23^{neg}$, Figure 3.5a and b). The cell counts did not show consistent trends in all cases. Uncertainty about the absolute number of cells obtained from each mouse makd the interpretation difficult. The percentages of B1 B cells in lymphocytes were broadly similar among the three groups (Figure 3.5c). No consistent difference was found in absolute numbers or percentages of B1a ($CD5^+$) and B1b ($CD5^{neg}$) subsets, in comparisons with WT mice.

The one consistent difference I did observe was an increase in IgM expression in mature KO B cells, measured as the median of anti-IgM antibody staining in flow cytometry analysis. In the bone marrow, this difference was observed in the mature B cell population gated on $B220^{++}CD24^{lo}$ cells (Figure 3.6a, means and SEM of WT, HET and KO were 1090±88.78, 1330±59.73, 1349±20.17) or $B220^{++}CD43^{neg}$ cells (not shown). In the spleen (Figure 3.6b), there was little difference between KO and WT transitional B cells; but mature follicular B cells again showed clear differences (656.8±35.89, 735.0±21.55, 715.5±17.18). The IgM levels of follicular B cells were mirrored into those of total spleen B cells and mature spleen B cells, due to the dominant proportion of this cell type. Interestingly, the surface IgM expression of HET mice was also found to be high, without clearly being intermediate.

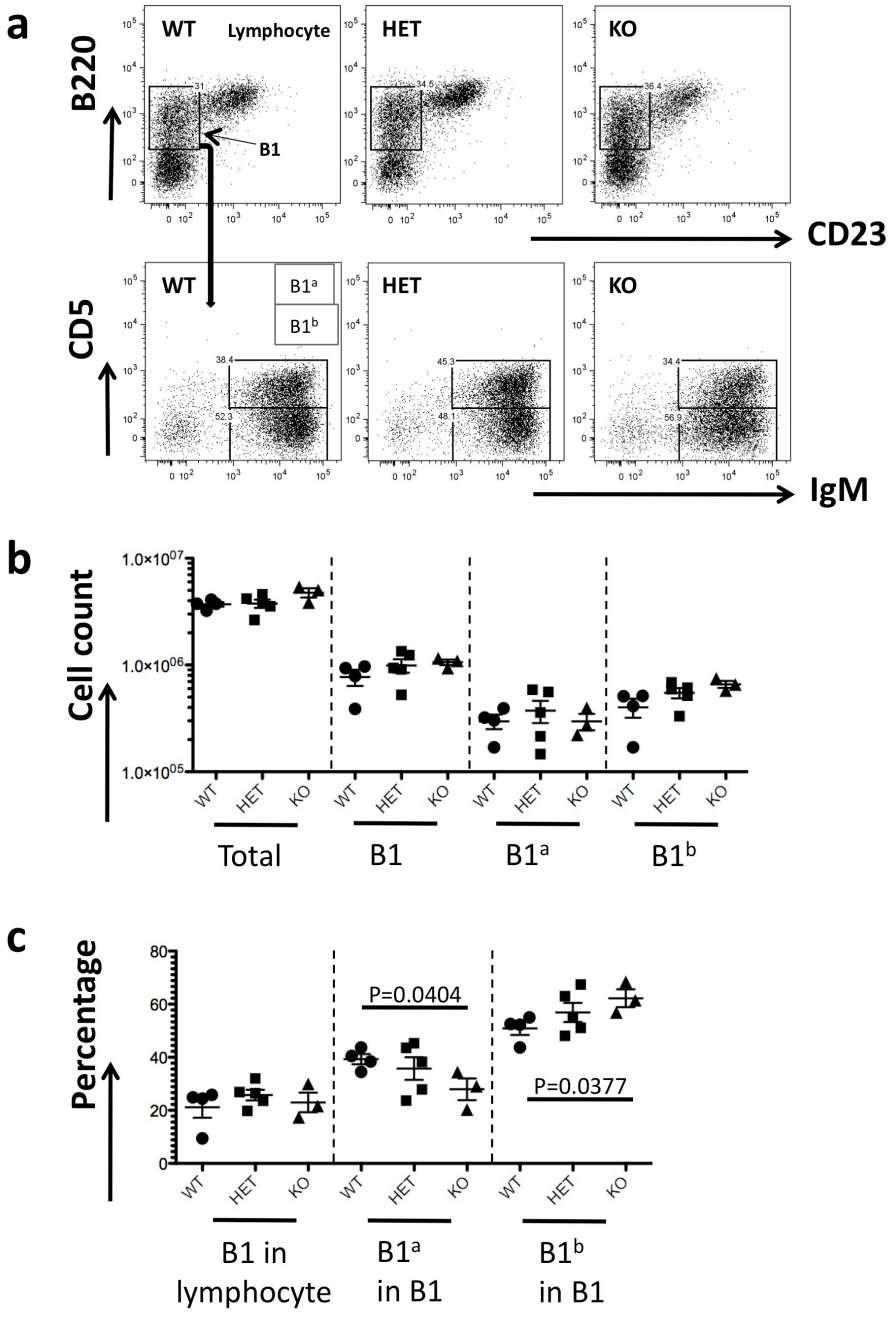

Figure 3.5 B cell sub-populations in the peritoneal cavity. a) Gating of B1 B cells as B220 positive, CD23 negative lymphocytes. The B1 B cells were then separated into $B1^a$ (CD5 positive, IgM high) and $B1^b$ (CD5 negative, IgM high) cells. b) Cell counts of the sub-populations shown in a, in WT, HET and KO mice. c) Percentages of B1, $B1^a$ and $B1^b$ cells in their respective parent populations as indicated. Error bars showing mean and standard error of mean (SEM); data points represent individual animals. p values are shown if $p \leq 0.05$.

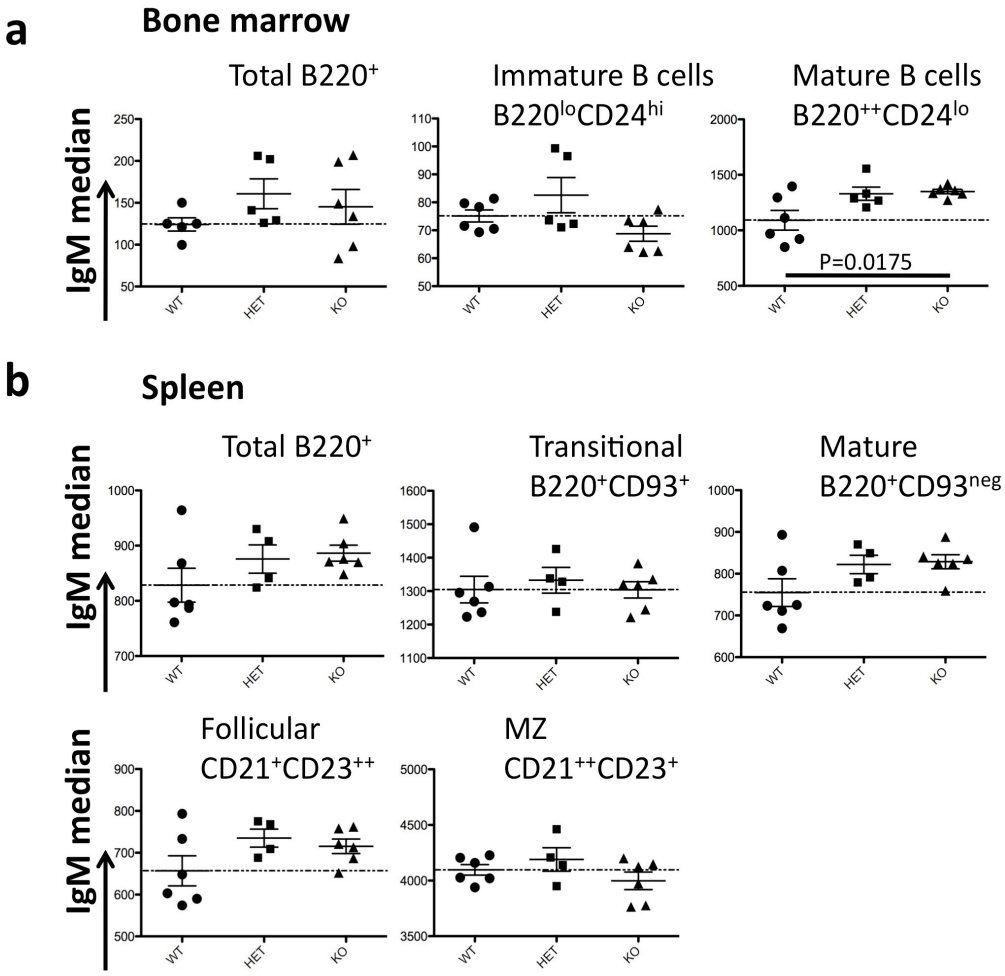

Figure 3.6 Surface IgM expression on mature B cells. a) Median values of IgM in bone marrow total B cells, immature B cells ($B220^{lo}CD24^{hi}$) and mature B cells ($B220^{hi}CD24^{lo}$), of the WT, HET and KO mice. b) Median values of B cell sub-populations in the spleen B cell sub-populations as indicated. Error bars showing mean and standard error of mean (SEM); data points represent individual animals. p values are shown if $p \leq 0.05$.

3.3.2. Mixed chimera

Deficiency in B cell development, shown as absolute numbers, could be compensated by the proliferation capacity of the lymphocytes. Therefore, to apply a more stringent test of development and measure intrinsic and extrinsic cellular effects of the knockout, I examined the KO B cell development in competition with WT B cells using mixed adult bone marrow chimeras.

Chimeric mice were generated by injecting a 50:50 mixture of bone marrow cells of CD45.1 WT and CD45.2 KO mice into lethally irradiated CD45.1 WT recipients. In this way, any background from radio-resistant cells would be identified as WT cells. Control mice were reconstituted with a 1:1 mixture of CD45.1 and CD45.2 WT donor cells, using the same pool of CD45.1 WT bone marrow cells. After reconstitution for 8 to 10 weeks, the fractions of CD45.1 and CD45.2 B cells were compared with those in the initial injected mixture. The CD45.2 donor cells reconstituted a higher proportion of the lymphocyte subsets in all mice, but the WT CD45.1 control cells were clearly visible (Figure 3.7a). In the bone marrow, B cell development was followed using expression of surface IgM and IgD to identify early ($IgM^{neg}IgD^{neg}$), immature ($IgM^{+}IgD^{neg}$) and mature/recirculating ($IgM^{+}IgD^{+}$) B cells. Spleen B cell subpopulations were assessed as previously described. As in non-chimeras, no convincing difference was found between the reconstitutions of CD45.2 WT and KO donor cells in the bone marrow. In the spleen, there were similar percentages of transitional and follicular B cell populations. However, Icb-1-deficient MZ B cells were again proportionately larger: WT CD45.2 cells accounted for 62.32±1.83% of reconstituted MZ B cells, while KO CD45.2 cells took up 82.02±0.49% of the population (mean±SEM, $p<0.0001$). The reconstitutions in the blood and the lymph nodes were similar

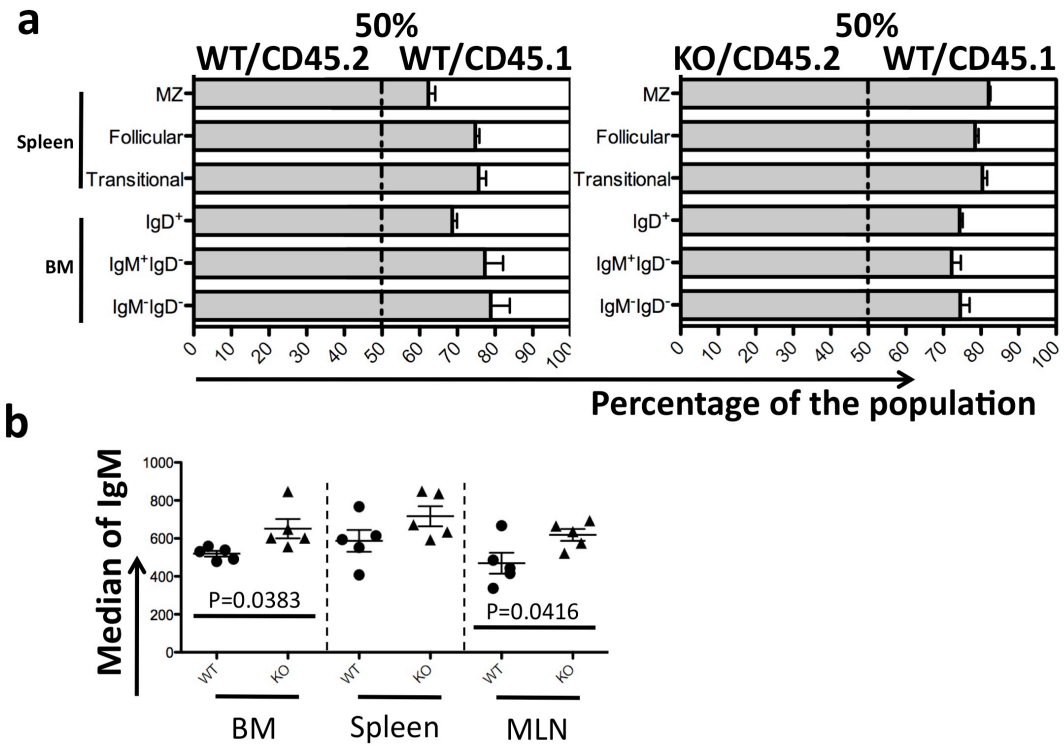

Figure 3.7 Mixed Chimeras. Mice reconstituted with 1:1 mixture of either CD45.2 WT and CD45.1 WT, or CD45.2 KO and CD45.1 WT adult bone marrow donor cells into irradiated CD45.1 WT recipients. Error bars showing mean and standard error of mean (SEM), n=5 in each group. a) Diagram showing the percentage of reconstituted cells originated from CD45.2 (grey) and CD45.1 (white) donor cells. The calculation of the values included the ratios of the initial mixtures. Shown on the left is the result of control mice, which were reconstituted with WT CD45.1 and CD45.2 cells. On the right, data from mice reconstituted from KO and WT cells. In the bone marrow, the B cells were separated by surface expressions of IgM and IgD. In the spleen, the data were shown for transitional, follicular and marginal zone B cells. b) The median values of B cell surface IgM of CD45.2 donors of WT or KO type, in the bone marrow, spleen and mesenteric lymph nodes. p values are shown if $p \leq 0.05$.

between WT and KO CD45.2 donors (not shown). Because B1 B cells generally do not reconstitute substantially from adult BM donor cells, these cells were not examined in these experiments. Once again, the surface IgM expression was higher in mature KO B cells (Figure 3.7b), showing that this is a cell intrinsic effect of Icb-1 deficiency.

From these findings I could conclude that normal numbers of Icb-1-deficient B cell subsets develop in the bone marrow and the pre-immune B cell repertoire, with the exception of slightly increased marginal zone B cells. However, at the same time, mature Icb-1-deficient B cells showed a higher constitutive level of surface IgM. This is a phenotype previously associated with decreased constitutive signalling[275,276].

Under competing conditions, similar results were found. This confirms the largely normal B cell development of Icb-1$^{-/-}$ mice, the increased marginal zone B cells and that the elevated surface IgM expression on KO B cells was intrinsic.

3.4. Icb-1$^{-/-}$Themis1$^{-/-}$ mice

The lack of an obvious phenotype in the absence of Icb-1 is strikingly different from the findings in Themis1$^{-/-}$ mice. I considered if this could be due to functional redundancy between Icb1 and Themis1. Recent experiments by Lesourne *et. al.* have shown that the expression of transgenic Icb-1 in T cells can fully compensate for the absence of themis1 and restore T cell development[5]. Although expression of the two proteins is likely to be distinct – in B and myeloid cells, and T cells respectively – low B cell specific expression of Themis1 might compensate for the loss of Icb-1. Conversely, it would also be interesting to see if Icb-1 deficiency would exacerbate the T cell deficiency in Themis-deficient mice. Therefore, Icb-1$^{-/-}$ mice were crossed to Themis1$^{-/-}$ mice to produce double-knockout mice, which were compared with WT mice, and mice only deficient in either one of the two proteins.

As reported before, Themis1$^{-/-}$ mice showed a developmental block in the T cell lineage with reduced CD4 and CD8 single positive (SP) T cells, in the thymus and periphery (Figure 3.8 and 3.9). The reduction in CD4 SP T cells was proportionately greater than that of CD8 SP T cells. In the results shown, the WT controls showed slightly higher total lymphocyte numbers in the thymus (Figure 3.8b). This is likely to be becuase the WT mice were nine days younger than the mutants (culled at age of 49 and 58 days respectively)[277,278]. To assess this, I conducted an experiment using four group of mice aged 7, 8, 9 and 10 weeks and examined their Tcell numbers in the thymus. This showed similar reduction in thymocyte cell numbers across the age range (Figure 3.8c).

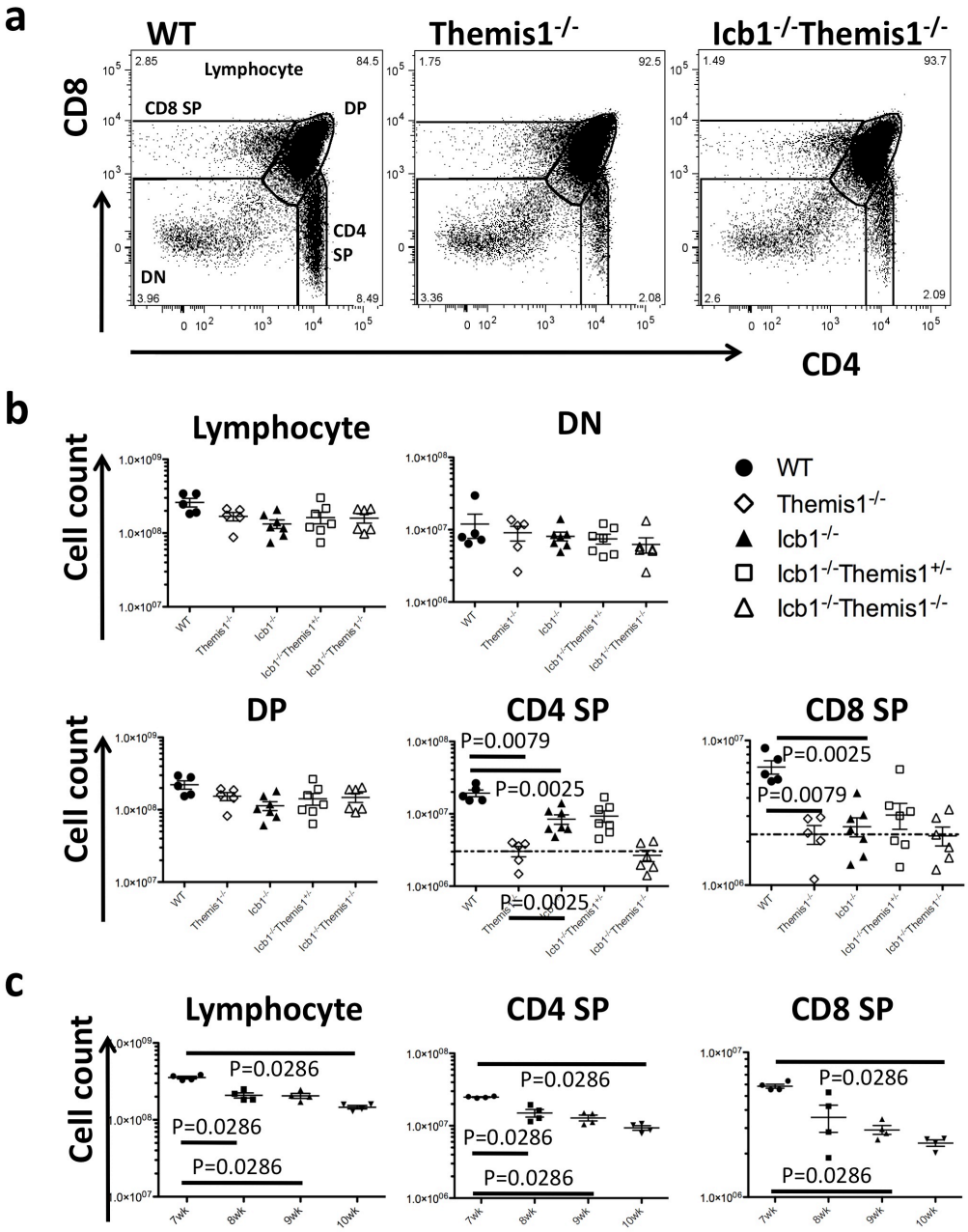

Figure 3.8 Analysis of Themis1/ Icb-1 double-knockout mice in the thymus. a) Flow cytometry plots showing the T cell developments in the thymae of WT, Themis1 knockout and Themist1/Icb-1 double-knockout mice. b) Cell counts of cell population indicated in the thymus, as shown in a, in mice with genotypes indicated. Dotted horizontal line showing the levels of Themis1$^{-/-}$ mice. c) Cell counts of populations indicated in the thymus of WT mice of different ages. Error bars showing mean and standard error of mean (SEM); data points represent individual animals. p values between WT and Themis knockout, WT and Icb-1 knockout or Themis1 and Icb-1 knockout are shown if $p \leq 0.05$.

All mutants showed normal DN and DP T cell percentages. Themis1$^{-/-}$ and Themis1/Icb-1 double-knockout mice showed reduced CD4 and CD8 SP T cells. The extent of these changes was similar between Themis1 single knockout and Themis1/Icb-1 double knockout mice (Figure 3.8b, Table 3.1).

		WT	Themis1$^{-/-}$	Icb-1$^{-/-}$	Icb-1$^{-/-}$ Themis1$^{+/-}$	Icb-1$^{-/-}$ Themis1$^{-/-}$
		Cell counts (x10^6)				
Thymus	DN	12.00±4.42	9.06±2.08	8.11±1.12	7.47±1.16	6.23±1.49
	DP	221.80±29.32	153.60±19.88	113.40±15.97	141.90±26.16	147.70±21.34
	CD4 SP	19.28±2.12	3.03±0.49	8.42±1.27	9.30±1.68	2.66±0.47
	CD8 SP	6.54±0.70	2.25±0.34	2.54±0.38	3.05±0.62	2.19±0.33
MLN	CD4	17.75±3.43	2.57±0.29	13.38±0.45	9.94±1.32	2.00±0.23
	CD8	7.79±1.09	3.69±0.38	5.95±1.16	6.01±0.84	4.66±1.99
Spl	CD4	23.02±1.83	4.84±0.70	26.77±3.02	19.46±2.19	5.98±0.76
	CD8	7.91±0.43	3.13±0.53	9.83±1.03	8.24±0.99	4.15±0.54

Table 3.1 Cell counts in millions (10^6) in the thymus, spleen and mesenteric lymph nodes. Each entry is the mean ± SEM of 6 samples. MLN, mesenteric lymph nodes; Spl, spleen.

Reductions in T cell proportions and numbers were apparent in the periphery (Figure 3.9, Table 3.1). Again, Themis1$^{-/-}$ and Themis1/Icb-1 double-knockout mice showed similar reductions.

For the possible interaction or redundancy in B cells, the same strategies in antibody staining were used in flow cytometry to separate B cell subpopulations (plots not shown). Normal numbers of cells were found in the bone marrow in all the single and double deficient lines (not shown). In the

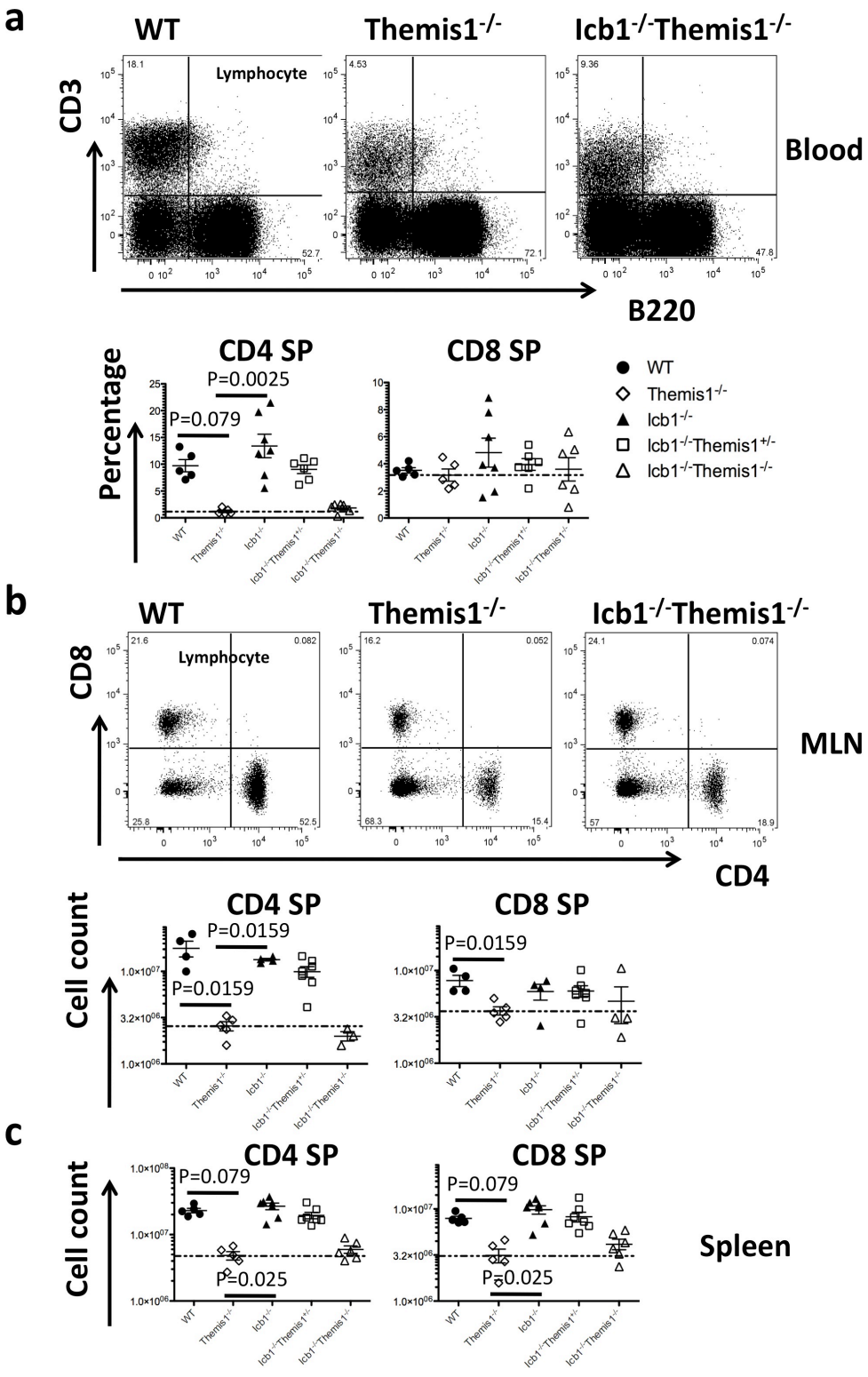

Figure 3.9 Analysis of CD4 and CD8 single positive T cell sub-populations in the periphery in double knockout mice. a) Flow cytometry plots showing the fractions of B and T cells in the periphery blood, in mice with genotypes indicated. The percentages of CD4 and CD8 single positive T cells in the $CD3^{+}B220^{-}$ population are summarized in two figures. b) Flow cytometry plots showing CD4 and CD8 staining in the mesenteric lymph nodes, with counts of T cell sub-populations. c) The counts of CD4 and CD8 single positive T cells in the spleen. Error bars showing mean and standard error of mean (SEM); data points represent individual animals. p values between WT and Themis knockout, WT and Icb-1 knockout or Themis1 and Icb-1 knockout are shown if $p \leq 0.05$.

spleen, the mutants showed normal lymphocytes numbers of immature and mature B cells, with the exception of the double knockout mice (Figure 3.10 a). The double knockout mice showed elevated B cell counts in immature, mature, follicular, and in particular, in the marginal zone B cell populations. The other three mutant lines showed almost identical cell counts in these populations, which were lower than those in the double knowckout mice. As before, all mutants lacking Icb-1 showed elevated cell surface IgM expressions in mature B cells, which were not seen in Themis1$^{-/-}$ mice (Figure 3.10b).

I then examined the phenotypes again in mixed chimeric mice to exclude possible compensatory effects, including effects that might cause apparent differences in the B cell compartment due to T cell deficiency. Mice reconstituted with Themis1 single knockout and Themis1/Icb-1 double knockout bone marrow cells showed similar losses of CD4 and CD8 SP mutant cells in the thymus and periphery, with normal DN T cell fractions and elevated DP fractions (Figure 3.11a). On the other hand, mice reconstituted with WT control or Icb-1$^{-/-}$ cells showed normal T cell populations (Figure 3.11a). In this case, no significant difference was found in B cell populations in mice reconstituted with any of the mutant cells (Figure 3.11b).

Overall, Themis1/Icb-1 double knockout mice showed developmental defects in T cells, comparable to the Themis1 single knockout mice. The double knockout mice showed elevated mature B cell numbers compared with either Themis1 or Icb-1 single knockout mice, but this effect was not seen in mixed chimeras. Importantly, the IgM expression levels were higher in all three strains lacking Icb-1, showing that this finding is cell intrinsic and specific.

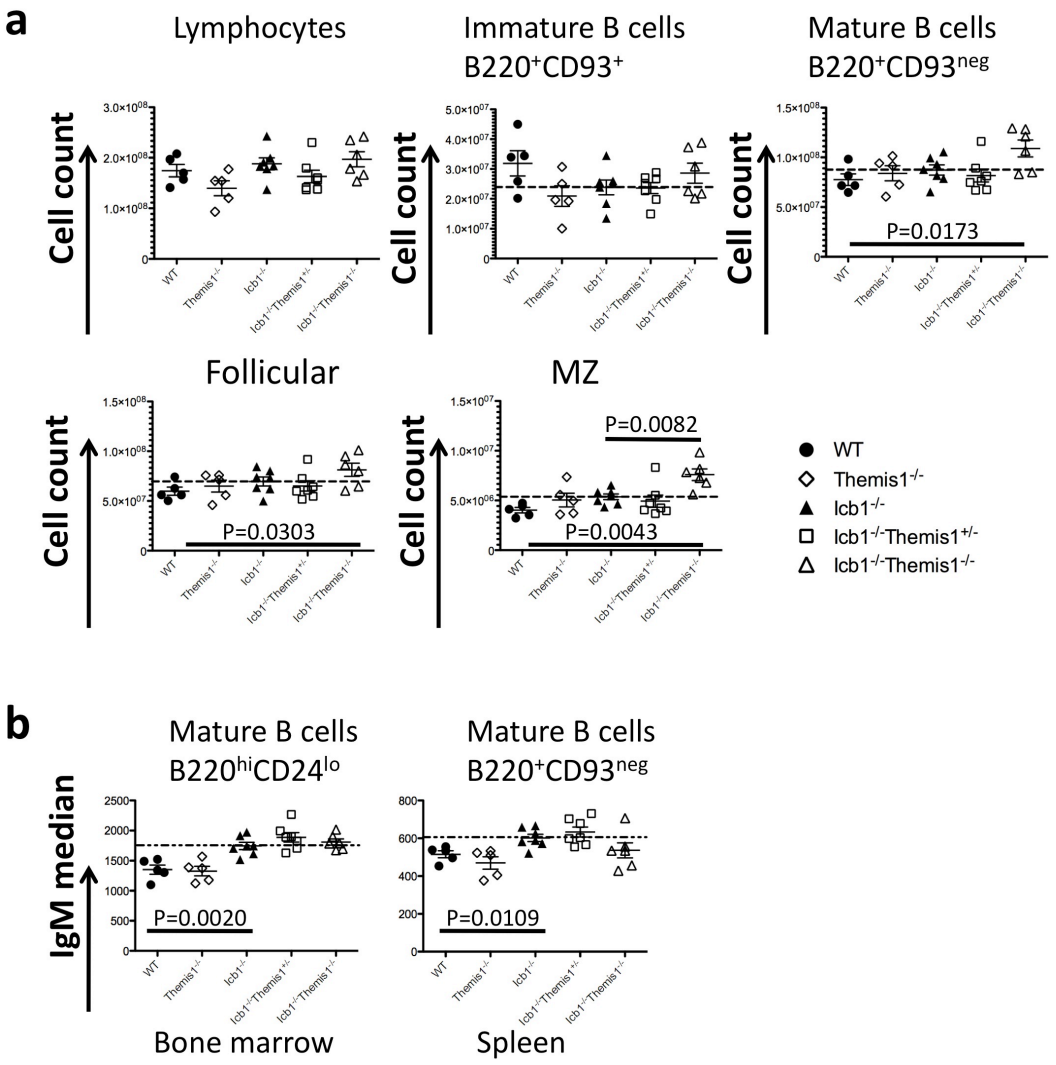

Figure 3.10 Analysis of B cell phenotype in the double knockout mice. a) Cell counts of lymphocytes and percentages of immature, mature, follicular and marginal zone B cells in lymphocytes, in the mice with genotypes indicated. b) Median values of cell surface IgM staining in mature B cell populations in the bone marrow and spleen. Error bars showing mean and standard error of mean (SEM); data points represent individual animals. . p values between WT and Themis knockout, WT and Icb-1 knockout or Icb-1 knockout and Themis1/Icb-1 double knowckout are shown if $p \leq 0.05$.

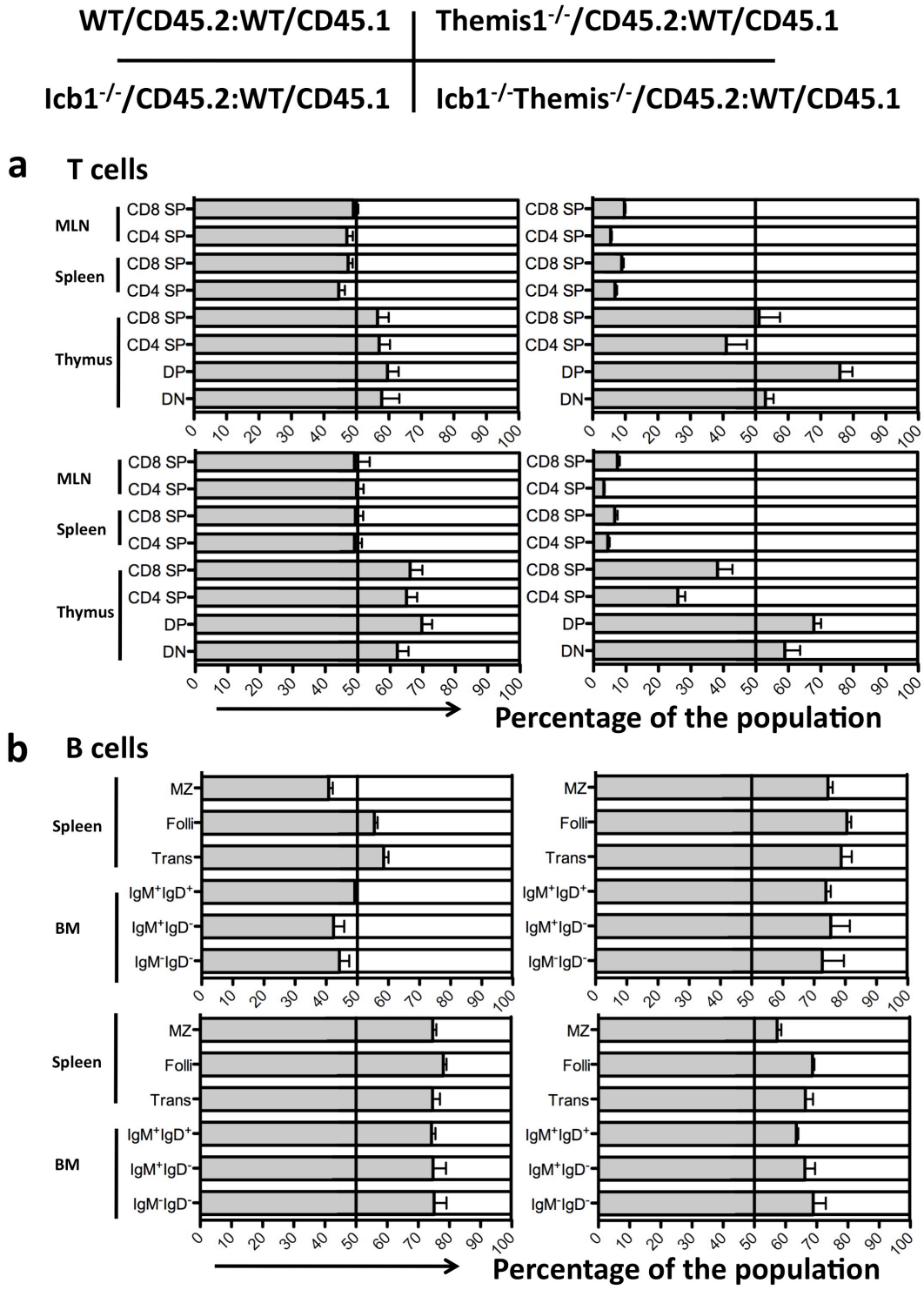

Figure 3.11 Mixed chimeras including double knockout mice. Analysis of chimeras reconstituted with mixtures of CD45.2 and CD45.1 bone marrow donor cells. The CD45.2 cells in each mixture were one of WT, Icb-1$^{-/-}$, Themis1$^{-/-}$ or Icb-1$^{-/-}$Themis1$^{-/-}$. a) The reconstitution of T cell populations in the thymus, spleen and mesenteric lymph nodes: CD45.2 populations in grey, CD45.1 in white. b) The reconstitution of B cell populations in the bone marrow and spleen. Error bars showing means and SEM, n=6 in each group. The order of figures is indicated at the top.

Hence there is little evidence for functional redundancy between the two proteins in knockout mice, despite the functional similarity shown by the capacity of Icb-1 to substitute for Themis1 in T cells. This is in agreement with the result of real-time PCR, which detected little or no mRNA expression of Icb-1 in thymic T cells, or no Themis1 in B cells.

3.5. B cell development in Icb-1$^{-/-}$ Ig mice

The last mechanism of compensation to be considered is the change in the repertoire as a result of the changes in B cell selection. To address this possibility and to be able to track antigen-specific B cells during development, I bred the Icb-1$^{-/-}$ alleles onto B6 MD4 mice that express high affinity IgM^{a}/IgD^{a} BCRs against hen egg lysozyme (HEL), to produce the Ig transgenic mice. This approach would allow me to look at negative and positive B cell selection induced by HEL expressed as transgenic self-antigen. The fate of the self-reacting Ig B cells could also be traced along developmental stages. (In this section, the mice used contain one copy of the Ig transgene. 'WT', 'HET' and 'KO' refer to the status of Icb-1; 'non' mice are without the Ig transgene.)

3.5.1. Icb-1$^{-/-}$ Ig mice

I first examined the B cells in the KO Ig mice. In the bone marrow, WT, HET and KO Ig transgenic mice showed similar cell numbers in lymphocytes, total B cells (B220^{+}), pre/pro B cells (B220^{+}IgM^{aneg}IgD^{aneg}), immature B cells (B220^{+}IgM^{a+}IgD^{aneg}) and mature B cells (B220^{+}IgD^{a+}) (Figure 3.12a and b). Using flow cytometry, I measured Ig binding to HEL by counter-staining with a separate anti-HEL antibody (HyHEL9) that binds to a non-overlapping HEL epitope[274] (Figure 3.12c). As expected, Pre/pro B cells mostly showed no HEL binding, except for a small population, presumably due to the overlapping of the gates (Figure 3.12c). Immature and mature B cells showed a step-wise increase in HEL binding. KO B cells showed a trend toward lower HEL binding (by both IgM^{a} and IgD^{a}) than WT or HET but less modulation on mature cells in the spleen and the median level of transgene

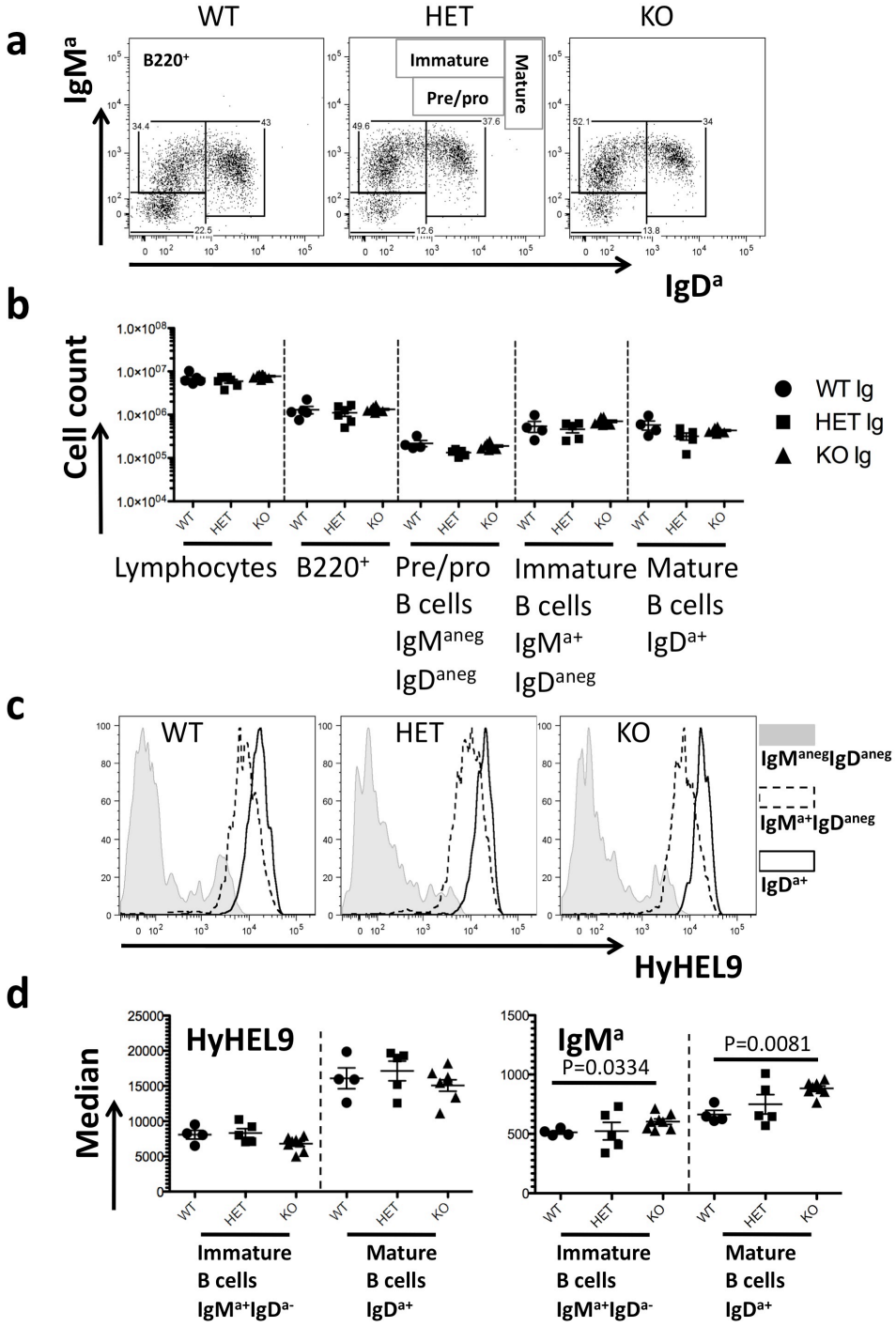

Figure 3.12 B cell populations in the bone marrow of WT, HET and KO Ig mice. a) B cell development in the bone marrow indicated by the cell surface expressions of IgM^a and IgD^a. b) Cell counts of cell populations indicated in the bone marrow. c) Histograms showing the binding of HEL (by HyHEL9 antibody staining) on pre/pro, immature and mature B cells in the bone marrow. d) Median values of HyHEL9 and IgM^a staining of immature and mature B cells in bone marrow. Error bars showing mean and standard error of mean (SEM); data points represent individual animals. .p values are shown if $p \leq 0.05$.

specific IgM^a was again higher on the mature recirculating KO B cells (Figure 3.12d).

In the spleen, KO mice showed normal B cell development, demonstrated by absolute cell counts of total B cells, immature ($IgM^{a+}IgD^{aneg}$), mature (IgD^{a+}), follicular and MZ B cells (Figure 3.13a, b and c). KO B cells showed lower HEL binding and lower IgM^a expression (Figure 3.13d). The data of total B cells are shown.

3.5.2. Selection of B cells reactive towards membrane-bound self-antigen

In mice expressing the Ig transgene and membrane-bound HEL (mHEL) under the class I promoter, the ubiquitous self-antigen triggers the elimination of the strongly self-reacting B cells at early stages in bone marrow development. In this model, the majority of B cells are unable to escape deletion by editing their BCR receptors to a non-autoreactive specificity. I used this system to examine the role Icb-1 in negative selection.

Mice expressing both transgenes were produced by injecting WT or KO CD45.2 ($CD45.1^{neg}$) Ig bone marrow cells into lethally irradiated CD45.1 recipient mice expressing mHEL systematically (Ig-mHEL mice). The number of surviving donor B cells ($B220^+CD45.1^{neg}$/$B220^+$CD45.2) that are capable of binding HEL provides a measure of self-tolerance. In the bone marrow of the Ig-mHEL mice, the $B220^+$ population consisted almost exclusively of donor cells (Figure 3.14a and b). The relative reconstitution of donor cells was

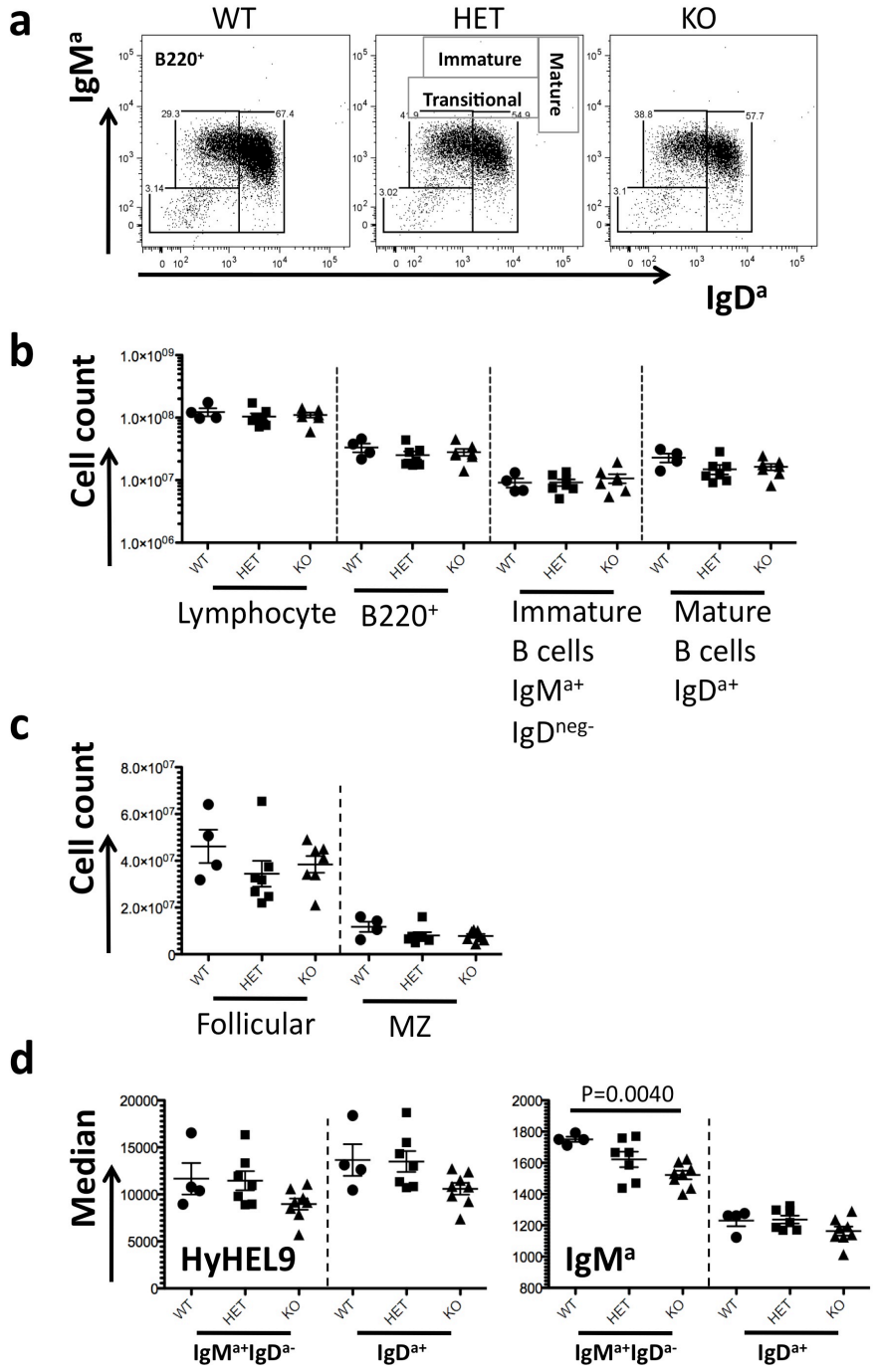

Figure 3.13 Cell populations in the spleen of WT, HET and KO Ig mice. a) B cell development in the spleen indicated by the cell surface expressions of IgM^a and IgD^a. b) Absolute cell counts of cell populations indicated in the spleen. c) Cell counts of follicular and marginal zone (MZ) B cells in the spleen. d) Median values of HyHEL9 and IgM^a staining of immature and mature B cells in the spleen. Error bars showing mean and standard error of mean (SEM); data points represent individual animals. p values are shown if $p \leq 0.05$.

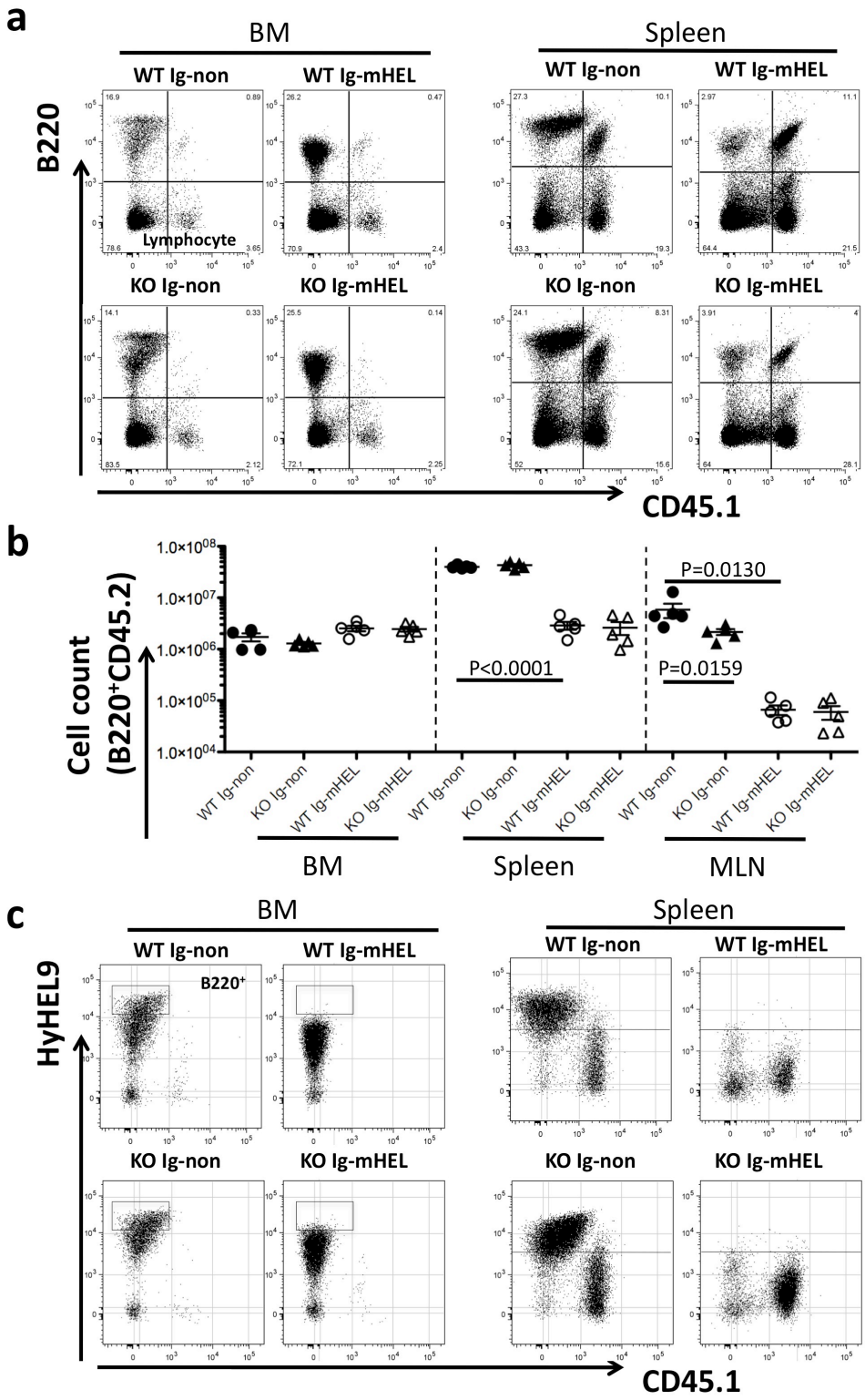

Figure 3.14 Overview of B cell populations in Ig-mHEL mice. The phenotype of B cells in Ig-mHEL and Ig (Ig-non) mice produced by a single-donor chimera. a) Flow cytometry plots showing the occupations of CD45.2 ($CD45.1^{neg}$) donor cells and $CD45.1^{+}$ residue recipient cells in the bone marrow and spleen. b) Cell counts of the CD45.2 donor B cells in the bone marrow, spleen and mesenteric lymph nodes. Error bars showing mean and standard error of mean (SEM); data points represent individual animals. c) Flow cytometry plots demonstrating the HEL-binding of CD45.2 donor B cells. p values are shown if $p \leq 0.05$.

reduced in the spleen and the lymph nodes. Instead the majority of the B cells in these organs were CD45.1 positive and originated from radio-resistant recipient cells (Figure 3.14a). No difference was found between WT and KO CD45.2 donors in the reconstitution of these subsets. As expected, the surviving CD45.2 donor B cells showed little or no HEL binding (Figure 3.14c). The $B220^{+}CD45.1^{neg}$/$B220^{+}$CD45.2 $HyHEL9^{hi}$ population seen in Ig single transgenics was absent in the double transgenics. In the spleen, the HyHEL9 staining in double transgenics again lacked the $HyHEL9^{hi}CD45.1^{neg}$ population. The $B220^{+}CD45.1^{+}$ cells did not express the high-affinity Ig receptor but did express mHEL itself. The HyHEL9 staining of the CD45.2 B cells was comparable but lower than CD45.1 B cells in the double transgenics, which shows a very high level of tolerance.

In the bone marrow, Ig-mHEL mice showed a typical developmental block; demonstrated by the CD43/B220 plots (Figure 3.15a), with the absence of the $CD43^{neg}B220^{hi}$ mature B cell population. Enumeration of the pre/pro, immature and mature cell populations showed little difference between WT and KO CD45.2 cells (Figure 3.15b). The developmental arrest seen in the response to membrane antigen was also reflected in the IgM^{a} and IgD^{a} expression. The Ig-mHEL cells showed scarcely detectable levels of surface IgM^{a} due to receptor endocytosis in response to antigen encounter (Figure 3.15c) and the median values of HyHEL9 were similarly reduced in the bone marrow (Figure 3.15d, Table 3.2). It is worth noting here that, in contrust to the finding in the last section, the median values of IgM^{a} on spleen B cells of KO Ig mice were higher than those on the WT equivalents.

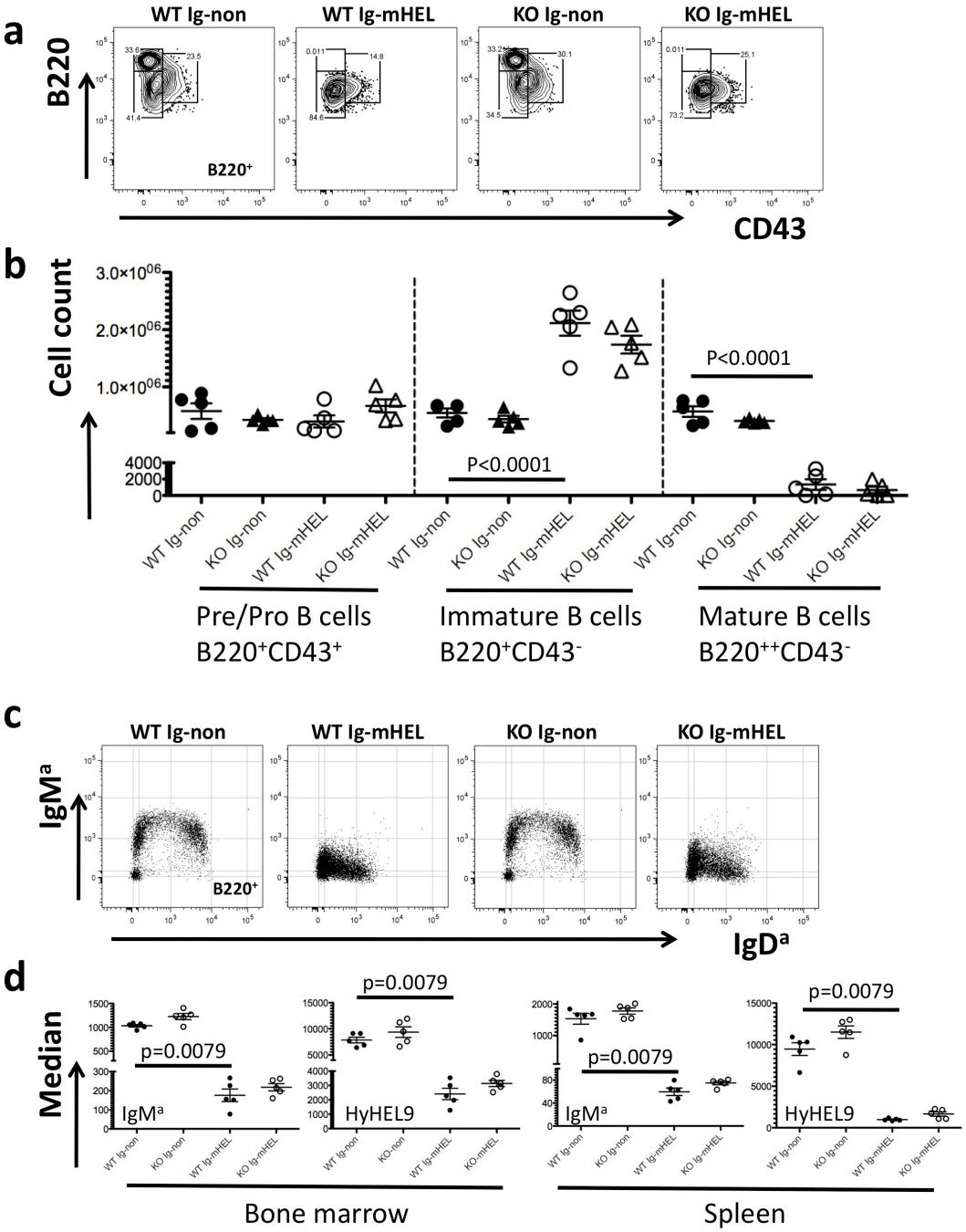

Figure 3.15 Negative selection in the bone marrow of Ig-mHEL mice. a) Flow cytometry plots demonstrating the developmental blocks of Ig-mHEL mice. B cell development was followed by B220 and CD43. b) Cell counts of B cell sub-populations indicated .c) Flow cytometry plots to show the down-regulations of IgM^a and IgD^a in Ig-mHEL B cells. d) Median values of IgM^a and HyHEL9 of B cells. Error bars showing mean and standard error of mean (SEM); data points represent individual animals. p values are shown if $p \leq 0.05$.

Median		WT Ig-non	KO Ig-non	WT Ig-mHEL	KO Ig-mHEL
BM	IgM^a	1034.00±27.17	1227.00±63.75	175.80±32.88	218.00±18.98
	Hy9	7854.00±560.90	9379.00±1017.00	2416.00±394.30	3139.00±211.50
Spl	IgM^a	1533.00±172.70	1776.00±100.40	59.54±6.55	74.86±3.02
	Hy9	9471.00±759.00	11510.00±749.90	986.00±66.17	1667.00±255.00

Table 3.2 Median values of IgM^a and HyHEL9 antibody staining of B cells in flow cytometry analysis. Each entry is mean ± SEM of 5 samples. BM, bone marrow; Spl, spleen; Hy9, HyHEL9

3.5.3. Selection of B cells reactive towards soluble self-antigen

Tolerance towards low avidity but abundant soluble antigen results in varying degrees of B cell anergy, which is a state of functional inactivation[279]. To examine this, WT and KO Ig-sHEL mice were generated by breeding and were examined to investigate the response to the lower avidity antigen.

The self-reactive B cells were not depleted in Ig-sHEL mice and present in similar numbers in WT and KO mice (Figure 3.16a). The numbers of mature/recirculating B220^{hi}CD43^{neg} population in the bone marrow were reduced in Ig-sHEL mice (Figure 3.16b and c). This reflects the decrease in mature B cells that survive to return to the bone marrow. Reduced HEL-binding mirrored the modulation of IgM^a on the mature anergic cells (Figure 3.17a and b). In the spleen, mature B cells (CD21$^+$) showed binding of HEL (Figure 3.17c). There was no significant difference between WT and KO mice in any of these parameters (Figures 3.16 and 3.17).

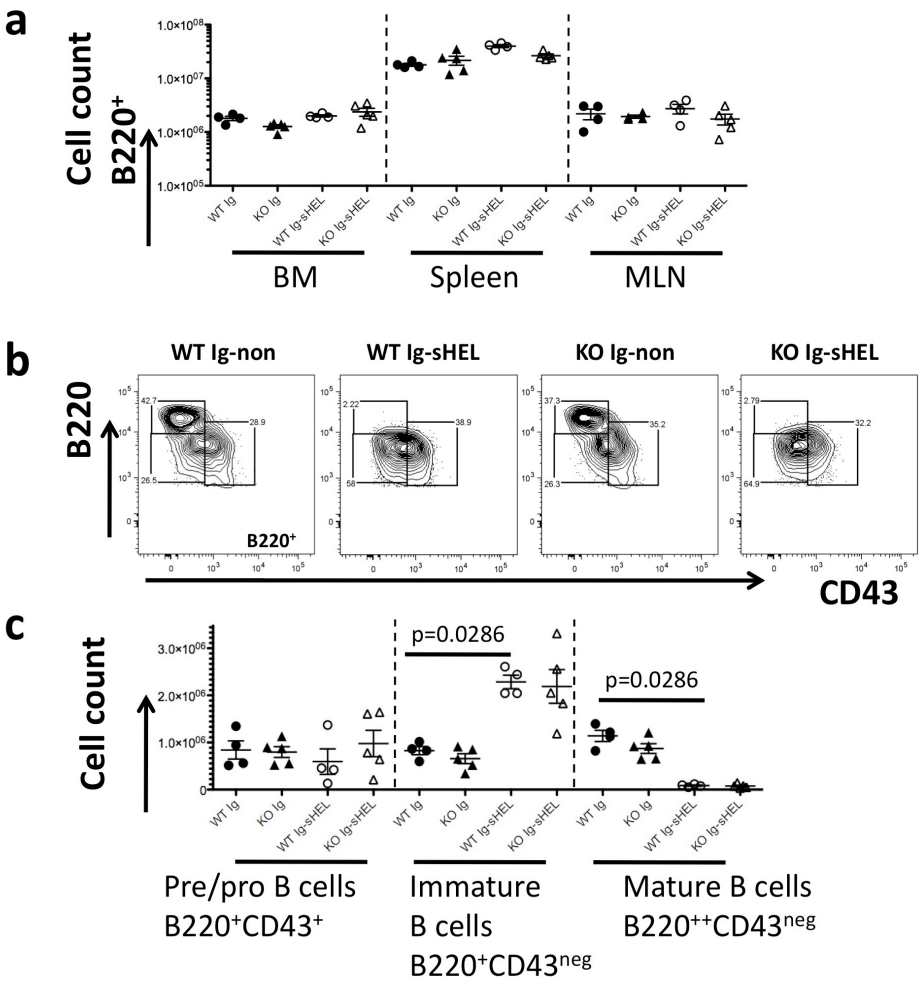

Figure 3.16 The induction of anergy in Ig-sHEL mice. The phenotype of B cells in Ig-sHEL and Ig (Ig-non) mice. a) B cell counts in the bone marrow, spleen and mesenteric lymph nodes. b) Flow cytometry plots showing surface expressions of B220 and CD43 in the bone marrow B cells. c) Cell counts of pre/pro, immature and mature B cells in the bone marrow, gated as in b. Error bars showing mean and standard error of mean (SEM); data points represent individual animals. p values are shown if $p \leq 0.05$.

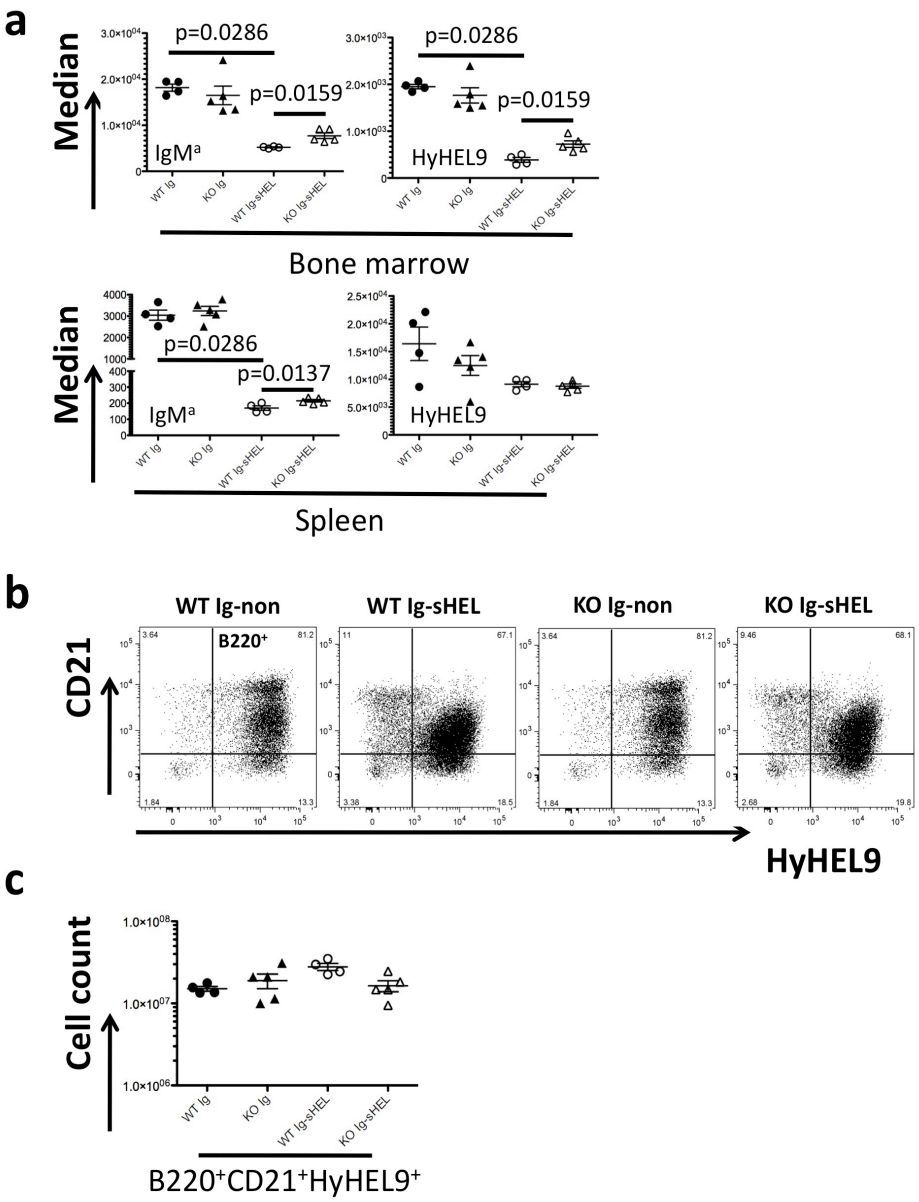

Figure 3.17 The phenotype of B cells in Ig-sHEL mice. a) Median values of IgM^a and HyHEL9 staining of HEL-binding B cells (B220$^+$HyHEL9$^+$) in the bone marrow and the spleen. b) Tolerance in the spleen shown by CD21 and HyHEL9 staining. c) Quantification of the number of mature HEL-binding B cells. Error bars showing mean and standard error of mean (SEM); data points represent individual animals. p values are shown if $p \leq 0.05$.

3.5.4. Positive selection of B1 B cells reactive towards intracellular self-antigen

In contrast to extracellular antigen, an intracellular form of mHEL that is tethered in the endoplasmic reticulum by virtue of a cytoplasmic di-lysine motif (inHEL) induces positive selection of self-reactive B1 B cells[280].

Bone marrow B cells of Ig-inHEL mice developed normally. The presence of some cleaved extracellular soluble antigen was sufficient to induce down-regulation of B220 and IgM^a (Figure 3.18a and b), which were similar in WT and KO Ig-inHEL mice. The number of the $B220^{++}CD43^{neg}$ mature/recirculating B cells in the bone marrow was again reduced. The size of the $IgM^{alo}IgD^{a+}$ population was used to indicate the level of anergy and was found similar between WT and KO species.

The positive selection of B1 B cells ($B220^{lo}IgM^{ahi}$) was deficient in KO Ig-inHEL mice. KO Ig-inHEL mice produced fewer B1 B cells, both in fraction and in actual cell numbers, with statistically significant differeces compared with WT Ig-inHEL (Figure 3.19a and b). KO Ig mice also produced smaller B1 B cell populations. Yet the difference between WT and KO Ig mice was not statistically significant.

As discussed previously, B1 B cells are major producers of peripheral IgM antibodies. Intracellular HEL also induce a 10-50 fold increase in plasma cells[280]. WT Ig-inHEL mice indeed showed elevated levels of serum IgM^a compared with WT Ig mice (Figure 3.19c, Table 3.3). However, KO Ig-inHEL mice showed IgM^a titres similar to that of Ig mice. Strikingly, the KO Ig single transgenic mice showed lower IgM^a titres than WT Ig mice. This also suggests reduced constitutive BCR signalling, similar to the increased cell surface IgM expression. It is difficult to separate the effects of lower basal

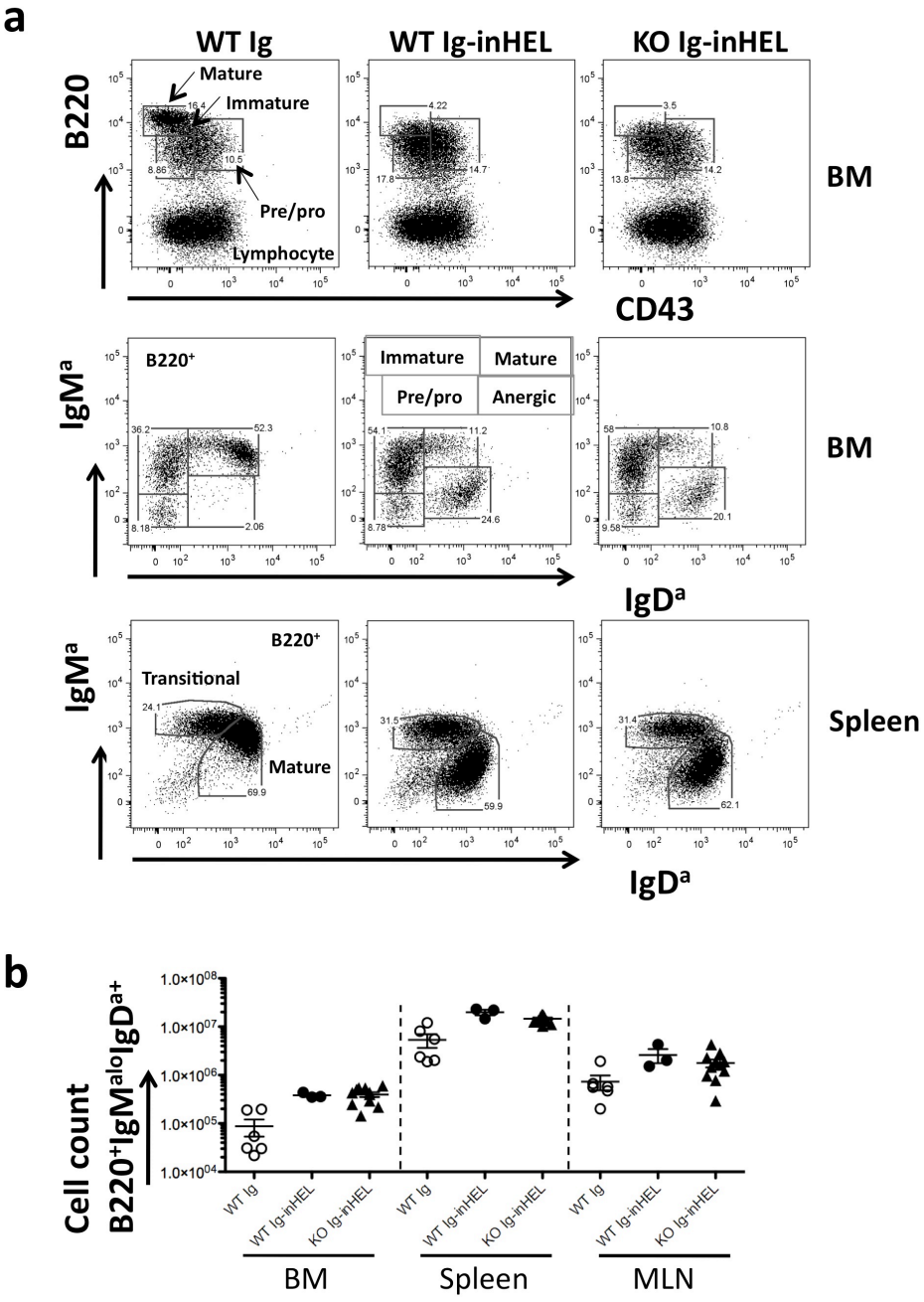

Figure 3.18 Conventional B cells in Ig-inHEL mice. a) Upper row: CD43 and B220 staining of bone marrow cells; Middle and lower rows, IgM^a and IgD^a expression in the bone marrow and spleen. b) Number of IgM^a down-regulated mature B cells of the three organs indicated. Error bars showing mean and standard error of mean (SEM); data points represent individual animals. p values are shown if $p \leq 0.05$.

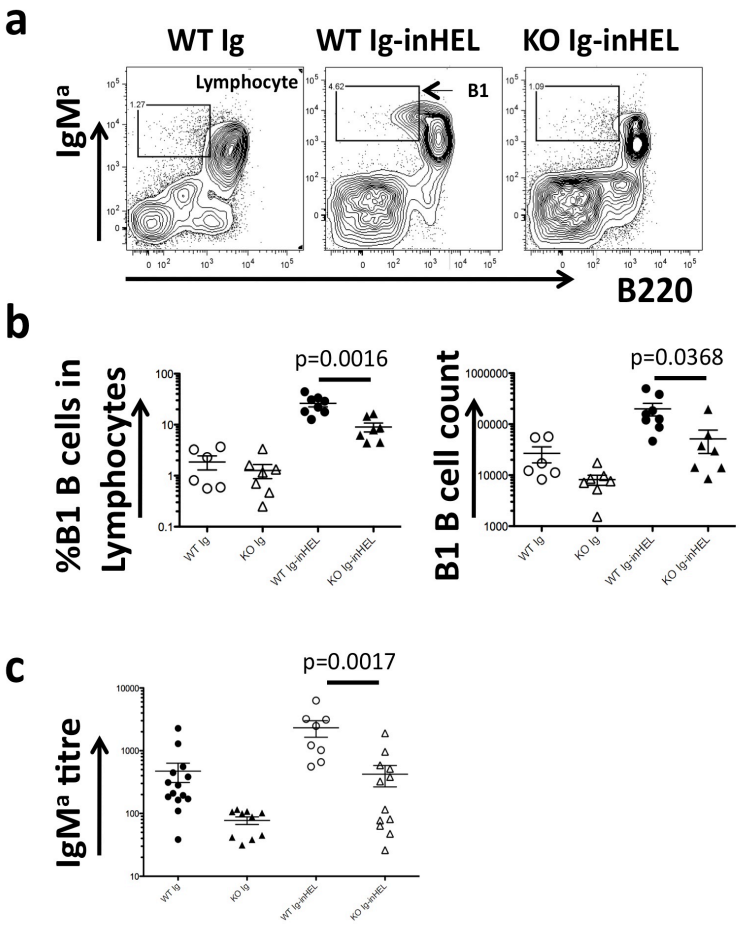

Figure 3.19 Positive selection of B1 B cells in Ig-inHEL mice a). Flow cytometry plots showing the gating for $IgM^{ahi}B220^{neg}$ B1 B cells. b) Percentage of B1 B cells in the lymphocyte population in the peritoneum of mice indicated. c) IgM^{a} titres in the sera of mice indicated. Error bars showing mean and standard error of mean (SEM); data points represent individual animals. p values are shown if $p \leq 0.05$.

IgM^a in KO Ig mice and defected B1 B cell selection in the reduction of IgM^a titre in KO Ig-inHEL mice.

	WT Ig-inHEL	KO Ig-inHEL	WT Ig	KO Ig
n	8	12	14	10
mean±SEM	2317.9x10^6 ±682.6	422.7x10^6 ±157.3	471.9x10^6 ±160.8	77.5x10^6 ±10.7
t test	p=0.0044		p=0.0518	

Table 3.3. Data of serum IgM^a titer in Ig or Ig-inHEL mice; n, number of samples.

In conclusion, the lack of Icb-1 resulted in few differences in Ig B cell populations. Compared with non-transgenic KO mice, I did not observe consistently enlarged marginal zone B cell populations. The increased cell surface IgM^a expression was inconsistent in the spleen mature B cells, but was clearly visible in BM mature B cells. They also showed reduced levels of serum IgM^a, additional evidence for defected constitutional BCR signalling. KO B cells showed normal negative selections and tolerance. However, lower positive selection into the B1 B cell subset in the Ig-inHEL model were observed in KO mice.

Chapter Four The responses of Icb-1$^{-/-}$ B cells to foreign antigens

4.1. Introduction

To address the possibility that Icb-1 deficiency might affect the B cell response to foreign antigens WT and KO mice were challenged with sheep red-blood cells (SRBCs), which are known to produce a robust germinal centre reaction. The SRBC challenge was also performed on chimeric mice to observe the difference between WT and KO B cells in competition. The mice were further challenged with a hapten-carrying antigen, 4-hydroxy-3-nitrophenylacetyl chicken gamma globulin (NP-CGG). To examine the T cell-independent response, I challenged the mice with NP-Ficoll.

To better analyse the B cell response to antigen and pathogen recognition molecules, I then looked at early B cell activation by anti-μ (anti-IgM, F'(ab)$_2$) and LPS (TLR4 ligand) *in vitro*. Ig B cells were stimulated with soluble HEL (sHEL) and with fibroblast cells expressing membrane-bound HEL molecules (mHEL) with different affinities, with or without membrane-bound ICAM. I also looked into antigen presentation to T cells and IL-2 production. Finally, the proliferation of WT and KO splenocytes was monitored in response to a variety of stimuli.

4.2. *In vivo stimulation*

4.2.1. SRBCs

Challenge with SRBCs gives robust germinal centre responses and was used to first screen for defects in KO B cells. All the mice challenged with

intraperitoneal SRBCs developed elevated total lymphocyte and B cell ($B220^+$) numbers compared with naïve controls, indicative of the robust polyclonal immune response and associated B cell proliferation (Figure 4.1a, Table 4.1). The number of total B cells was similar in challenged WT and KO mice.

Counts ($x10^5$)	WT	HET	KO	NS
Lymphocyte	2131.0±90.33	1880.0±104.80	2115.0±92.24	1259.0±65.48
$B220^+$	1285±66.00	1250±73.55	1386±74.13	816.8±39.15
GC B cells	18.2±1.68	7.2±0.90	5.8±1.62	0.9±0.31
$IgG1^+$ B cells	10.3±0.96	4.8±1.17	3.2±0.49	0.8±0.08
Titre (mg/mL)				
IgG1	4.45±0.45	2.63±1.00	1.33±0.23	0.37±0.05

Table 4.1 Cell counts after SRBC challenge of the populations indicated and serum titre of IgG1 antibody. Each entry is the mean±SEM of 8 samples in cases of WT and KO; 4 samples in cases of HET and NS. GC, germinal centre; NS, non-stimulated.

However, KO mice showed significantly reduced GC ($B220^+GL7^+CD95^+$, Figure 4.1b) and class-switched $IgG1^+$ ($B220^+IgG1^+$) B cells compared to age-matched WT mice (Figure 4.1b and c, Table 4.1), indicative of an impaired response. The reduced response of KO mice was also evident in the reduction in serum titre of IgG1 (Figure 4.1c, Table 4.1). Interestingly, the cell counts and serum titres of heterozygous mice were intermediate between those of WT and KO, indicating a quantitative and dose-dependent effect on the immune response.

To test if the impairment in germinal centre response was B cell intrinsic, I challenged mixed chimeric mice reconstituted with a mixture of 1:1 CD45.2 (WT or KO donors) and CD45.1 (WT donor and recipients) adult bone marrow cells (Figure 4.1d). The level of reconstitution with WT and KO donor cells was similar in the bone marrow and follicular B cells, reaching

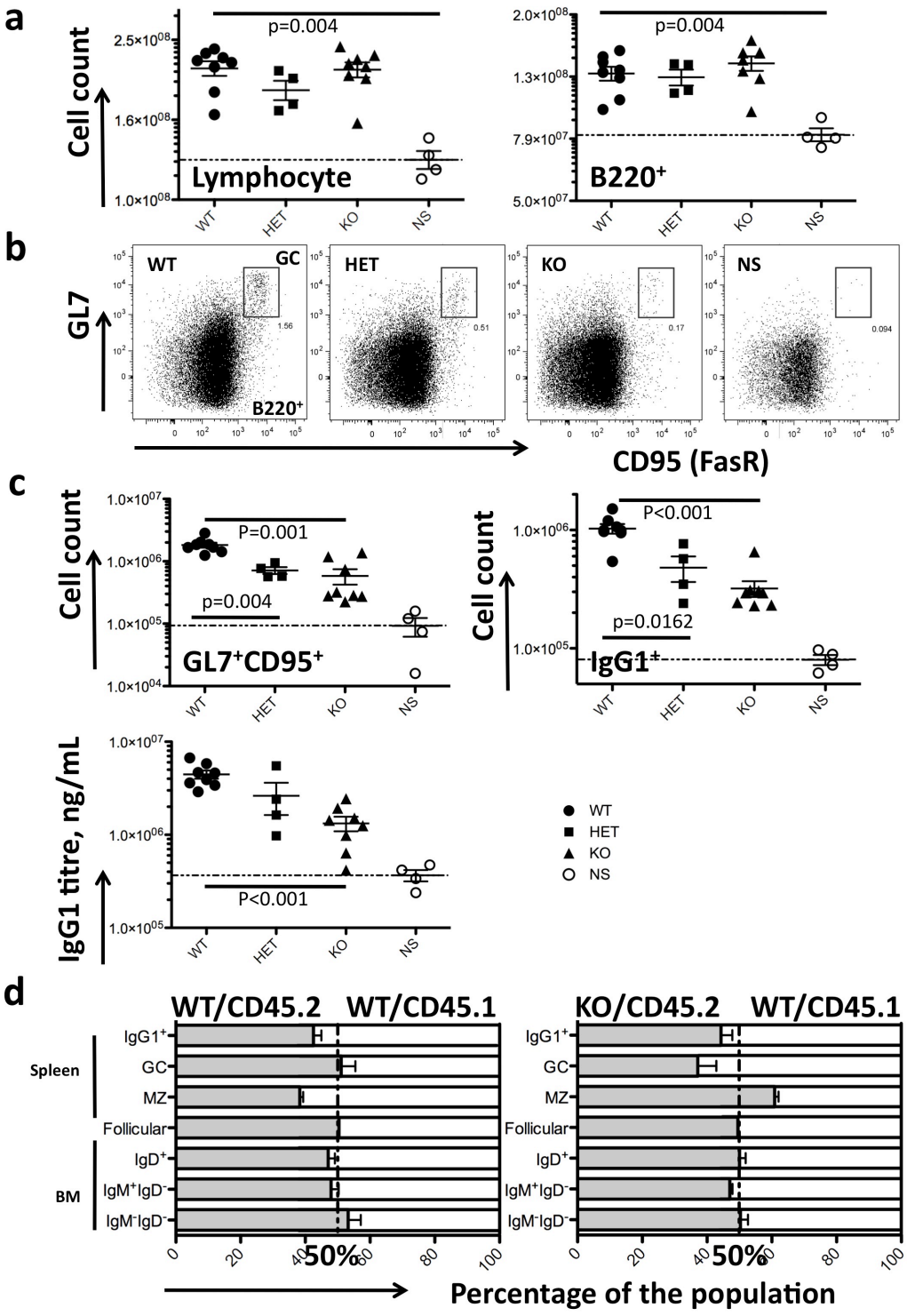

Figure 4.1 The Germinal Centre Response to Immunisation with SRBCs. Analysis was 8 days (a-c) and 9 days (d) after immunization. a) Number of spleen lymphocytes and B cells. b) Flow cytometry plots of GC B cells ($CD95^+$ $GL7^+$), gated on $B220^+$ splenocytes. c) Number of GC B cells, class switched ($IgG1^+$) B cells and serum titre of IgG1 antibody. d) Figure showing the percentages of reconstituted CD45.2 (grey, left) and CD45.1 (white, right) B cells in the populations indicated: left side shows control mice reconstituted with WT CD45.2 and WT CD45.1 donor bone marrow cells; right side, mice reconstituted from KO and WT donor cells. Each group contained 6 samples. Data are presented as mean and standard error of mean (SEM); values in each column represent individual mice. p values are shown if $p \leq 0.05$.

approximately 50% in the reconstituted mice. In contrast, CD45.2 WT MZ B cells reconstituted on average 38.3%±1.05% (mean±SEM), while those of KO reconstituted to an average of 60.9%±1.23%. These observations provided further confirmation of those found in non-stimulated mixed-chimera mice shown in Chapter 3.

CD45.2 WT donor cells consisted of approximately 50% of overall GC B cells (mean±SEM, 51.07%±4.41%), whereas the fraction of KO donor cells was considerably less than 50%, with mean and SEM of 37.1%±5.73%. This reduction is therefore similar to that found in SRBC-challenged non-chimeric mice. Although both lower than 50%, the KO and WT CD45.2 cells counted for about the same fraction of the IgG1$^+$ B cell populations (mean±SEM 42.54%±2.45% and 44.31%±3.51%, respectively). This may imply that the effects of Icb-1 deficiency in response to SRBCs could be partly rescued in an environment that is not entirely Icb-1-free, hence with normal macrophage and dendritic cell functions.

4.2.2. NP-CGG

I challenged mice with a less complex antigen NP-CGG in order to confirm the defects found in KO B cells using SRBCs. As might be expected in a more focused response, the challenged mice showed no overall change in lymphocyte or B cell numbers compared to unstimulated mice (Figure 4.2a). However, GC and IgG1$^+$ B cells were increased (Figure 4.2b, Table 4.2), indicating responses to the antigen. KO and interestingly HET mice showed lower GC and IgG1$^+$ B cell compared with WT mice on days 7 and 14 after stimulation. The differences were smaller than those found in SRBC challenge, perhaps a reflection of the less robust response.

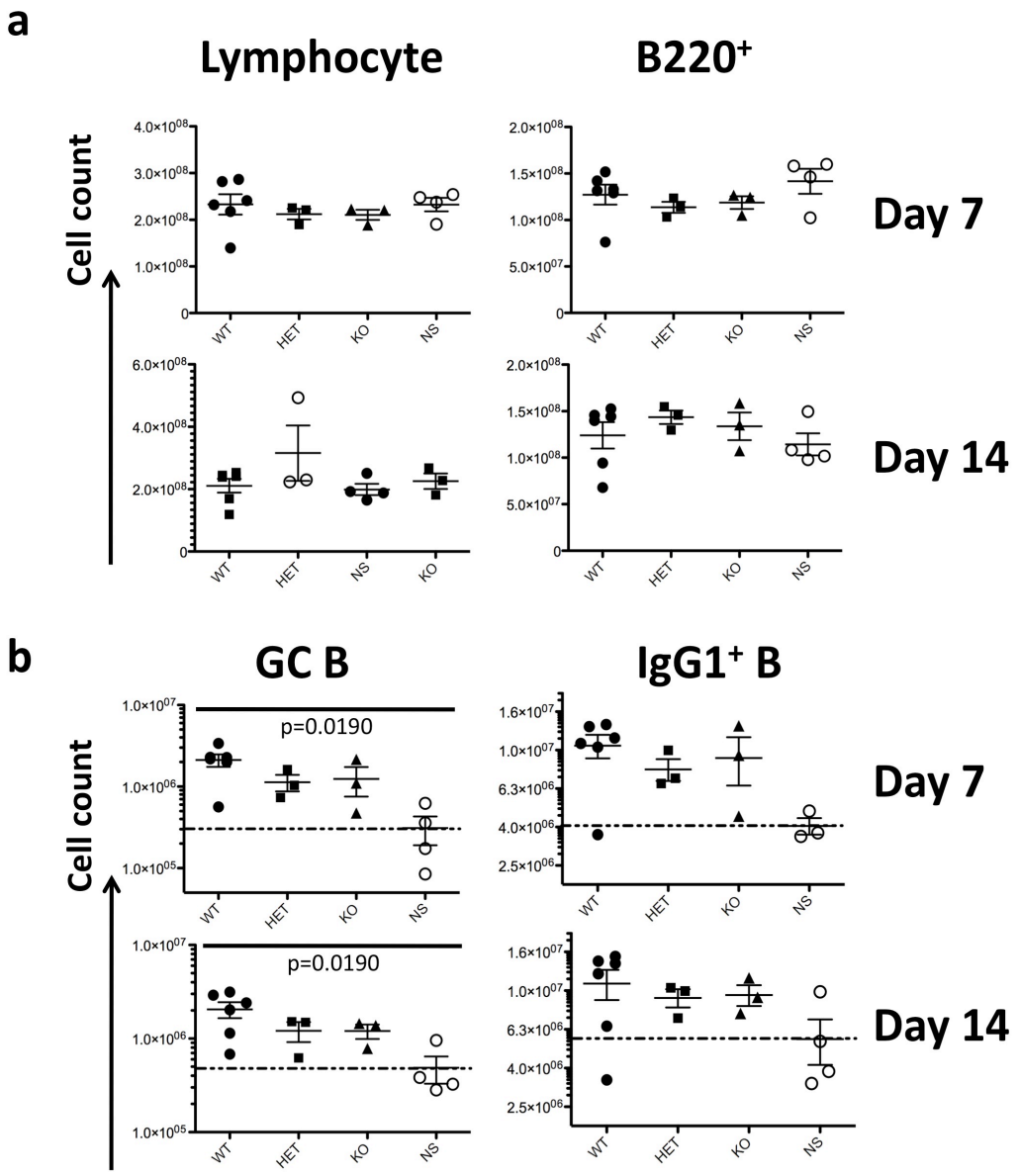

Figure 4.2 Immunisation with NP-CGG. a) Number of splenic lymphocytes and B cells. b) Number of GC B cells and class switched ($IgG1^+$) B cells. Data are presented as mean and standard error of mean (SEM); values in each column represent individual mice. p values are shown if $p \leq 0.05$.

Cell counts (x10^5)		WT	HET	KO	NS
Day 7	GC	21.2±3.69	11.3±2.60	12.4±4.90	3.1±1.19
	IgG1$^+$	105.4±14.79	79.4±10.27	91.1±25.61	40.3±3.99
Day 14	GC	20.5±3.99	12.1±2.94	12.0±2.11	4.9±1.58
	IgG1$^+$	108.8±19.35	91.7±9.87	95.0±11.65	56.2±14.87

Table 4.2 Cell counts (x10^5) after NP-CGG challenge, of time points and B cell populations indicated. Each entry is mean±SEM.

4.2.3. NP-Ficoll

Mice were challenged with a T cell-independent antigen, NP-Ficoll and were bled on days 7, 14, 21 and 28 post immunisation. Antigens of the IgM and IgG_3 isotypes specific for NP were measured in anti-NP ELISA. For both isotypes, KO mice produced about twice as much antibody as WT mice, at the time points measured (Figure 4.3 a and b. n=9 for WT; n=10 for KO). However, the differences were not statistically significant. This may be a result of the enlarged marginal zone B cell population in KO mice, as presented in previous sections. It is difficult in correlate quantitatively the number of MZ B cells and the amount of antibody produced. Therefore, it could not be concluded whether KO B cells respond to T-I antigens normally.

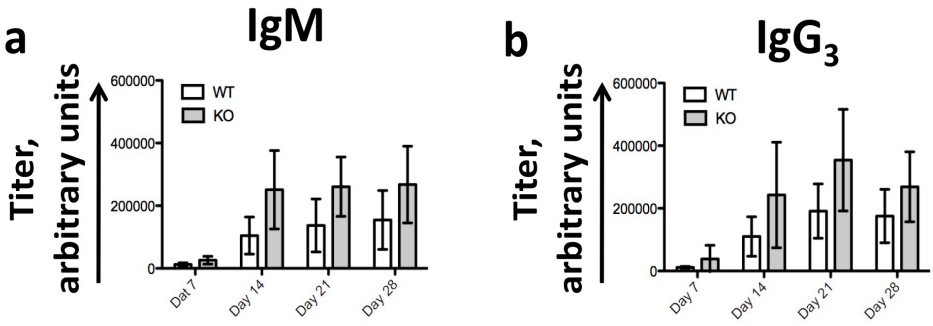

Figure 4.3 Antibody titres of a, IgM and b, IgG_3, specific to NP, of mice challenged with NP-Ficoll. None of the differences between WT and KO had p values smaller than 0.05 and are not shown.

To summarise, Icb-$1^{-/-}$ mice mounted a weaker germinal centre response to SRBCs and NP-CGG. In the SRBC challenge, KO mice produced significantly fewer GC and class-switched B cells. The serum titre of IgG1 was also significantly lower in KO mice. HET mice demonstrated an intermediate phenotype between WT and KO mice in the SRBC challenge, and were similar to KO mice in the NP-CGG challenge. The loss of GC B cells was due to a cell intrinsic defect, as demonstrated in challenged mixed-chimeric mice. The KO mice showed a trend towards the production of more antibodies in response to T cell-independent antigen, NP-Ficoll, rather than less. KO mice have more marginal zone B cells, which is likely to contribute to this result.

Cell intrinsic defects in the germinal centre response could result from changes in antigen engagement and collection, cell signalling, presentation to T cells, survival or proliferation. Several of these possibilities were addressed in subsequent experiments.

4.3. *In vitro* stimulation

4.3.1. Soluble antigens

Early responses to antigen crucially affect the B cells' fate in the germinal centre. To examine this, WT and KO splenocytes were stimulated *in vitro* with different dilutions of either high avidity anti-μ ($F'(ab)_2$ region), TLR4 ligand LPS or, in the case of Ig mice, with sHEL.

I evaluated the early B cell response by recording the percentage of the $B220^+$ population expressing activation markers CD69 and CD86 ($CD69^+D86^+$) 16-hour post stimulation (Figure 4.4a). Importantly, WT and KO B cells showed no difference in their response to stimulation with anti-μ ($F'(ab)_2$ region) or LPS at any concentration used (Figure 4.4b, c). However, the KO Ig B cells showed a higher activation threshold in their response to sHEL (Figure 4.4d). This result was consistently found in five repeat experiments. Lower percentages of KO B cells were activated than WT or HET Ig B cells at the lower end of sHEL concentration range. When sHEL concentration 100 ng/mL or greater, the fractions of KO B cells activated were similar to those of WT B cells. The greatest difference between KO and WT was at sHEL concentration of around 10 ng/mL, just below the threshold for the induction of B cell anergy *in vivo* [280].

In addition, KO B cells showed reduced overall surface expression of both CD69 and CD86 after sHEL stimulation (Figure 4.4e and f). Remarkably, the impairment remained clearly visible at the upper end of the sHEL concentration range, with KO B cells reaching a lower plateau. Levels of MHC II were found to be similar for WT and KO activated B cells over the sHEL dilution range (not shown).

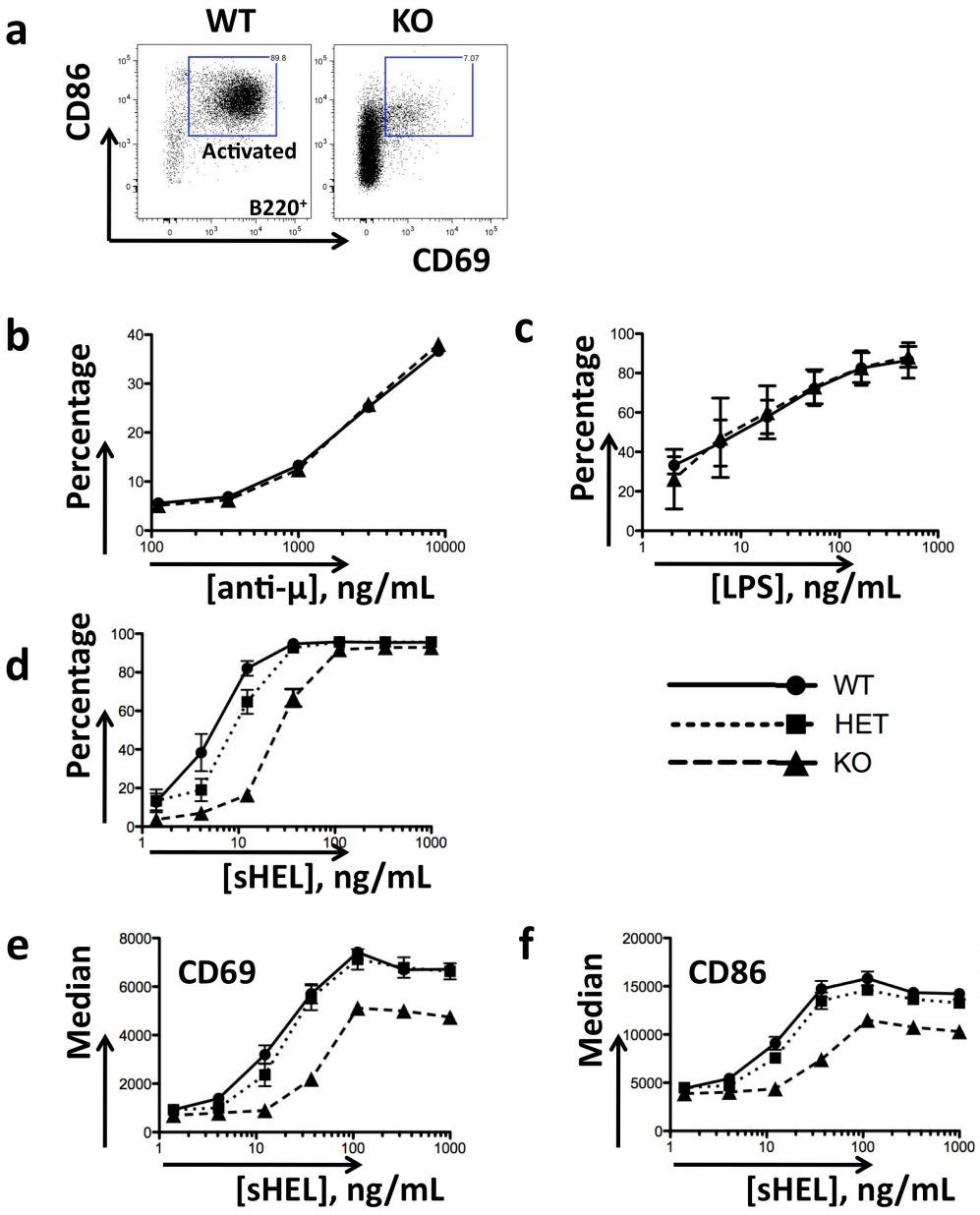

Figure 4.4 *In vitro* stimulation by soluble antigens. a). Representative flow cytometry plots showing CD86 and CD69 expressions on $B220^+$ lymphocytes stimulated for 16 hours with 12.3 ng/ml sHEL. b-d). Percentage of $CD69^+CD86^+$ cells in the $B220^+$ population after stimulation with varying concentrations of anti-μ (anti-IgM, F'$(ab)_2$), LPS or sHEL. For anti-μ (anti-IgM, F'$(ab)_2$) and LPS, n=4 for all groups. For sHEL, n=4 for WT, n=7 for HET and n=8 for KO. e-f). Median of CD69 and CD86 expression on activated B cells at different concentrations of sHEL in the same experiment as in d. Data are presented as mean and standard error of mean (SEM).

4.3.2. Membrane-bound antigens

To obtain a system more representative of B cell responding to antigens presented by antigen presenting cells, I stimulated Ig splenocytes by HEL-expressing cell lines.

Dr Delphine Baup in my research group produced NIH3T3 cell line clones expressing membrane-bound forms of HEL, HEL^{2x} and HEL^{3x}, with or without intracellular adhesion molecule ICAM. The affinities (K_a) of the BCRs of Ig mice (derived from the monoclonal hybridoma HyHEL10) towards HEL, HEL^{2x} and HEL^{3x} molecules are $2x10^{10}$ M^{-1}, $8x10^{7}$ M^{-1} and $1.5x10^{6}$ M^{-1}, respectively[274]. The density of mHEL on the clones was measured using flow cytometry, stained with the HyHEL9 antibody. To represent low HEL density in sHEL stimulation (Section 4.3.1), clones expressing the lowest detectable levels of HEL were selected as illustrated (Figure 4.5a, HEL^{2x} and HEL^{3x} clones were similar and are not shown). To control for variations in the conditions, mixtures of allotype marked WT and KO splenocytes were co-stimulated in these experiments.

The B cell response was assessed according to the influence of three variables: antigen affinity, antigen avidity and integrin binding. In almost every case, KO B cells showed a lower level of activation compared with WT (Figure 4.5 b-d). This difference was more noticeable with lower affinity antigens HEL^{2x} and HEL^{3x}. The HEL expression was shown as fold changes compared with WT clone and is shown above each column. The percentages of activated B cells grossly correlated with the antigen densities. Similar to sHEL stimulation, higher antigen density induced more activated B cells, and smaller difference between WT and KO B cells. The introduction of ICAM improved cell-cell adhesion and as a result, activated more B cells compared with clones expressing similar levels of mHEL but no ICAM. There

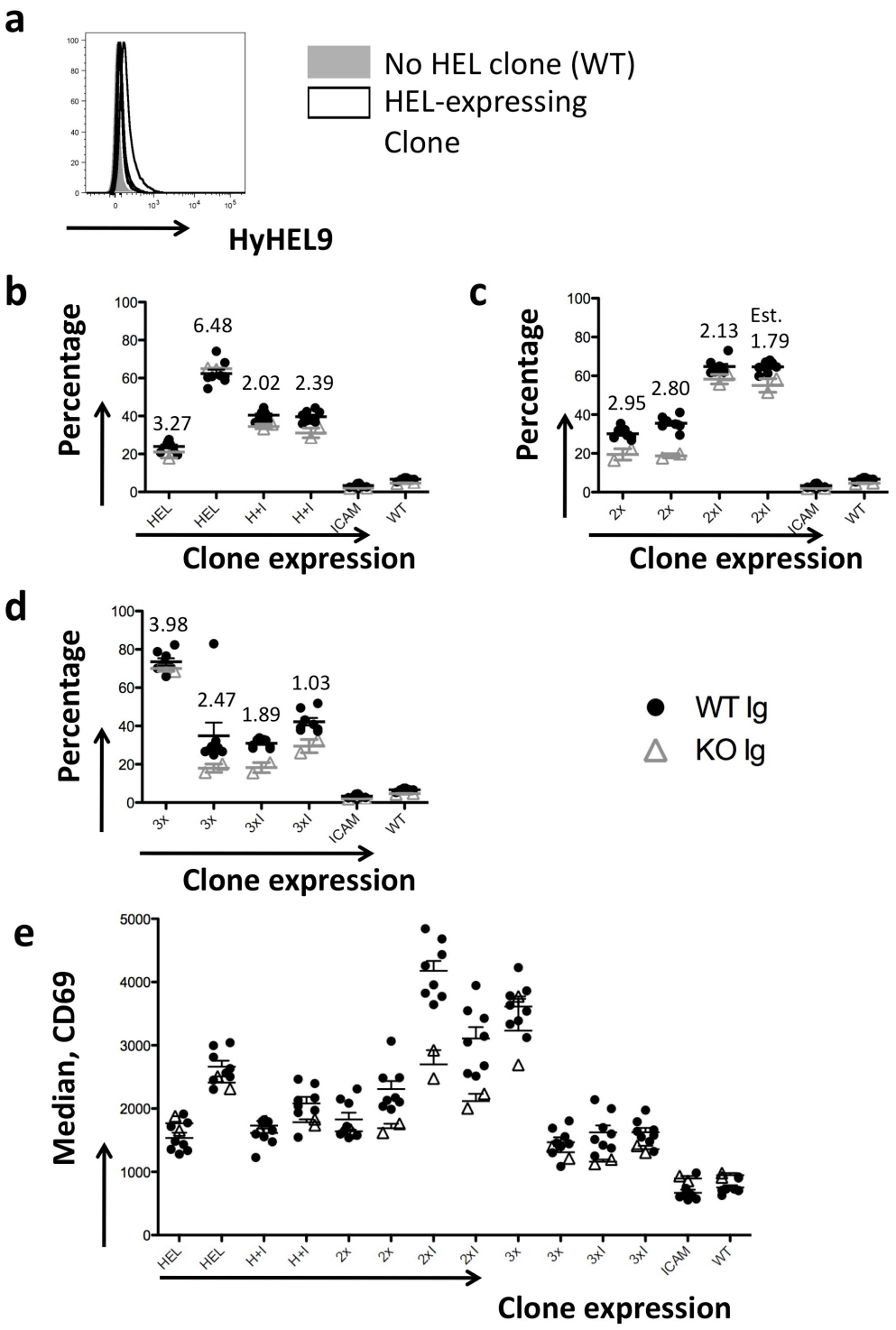

Figure 4.5 *In vitro* stimulation by membrane-bound HEL. a). The expression levels of HEL on the surface of NIH3T3 cell line clones, showing HEL-expression clones. b-d). Percentage of activated B cells ($CD69^+$) in $B220^+$ population, stimulated with cell lines expressing HEL, HEL^{2x} (2x) and HEL^{3x} (3x) respectively. Two cell line clones were used for each type of HEL molecule and two more co-expressed with ICAM (H+I, 2xI and 3xI respectively). Controls expressed only ICAM or no additional molecule (WT clone). The numbers above each colume indicate the fold change of HEL expression of each clone compared with WT. e). Median of CD69 of $CD69^+$ B cells. Data are presented as mean and standard error of mean (SEM); values in each column represent individual mice. Est, estimated

is no indication that the expression of ICAM narrowed the gap between WT and KO B cells.

Little difference was found between WT and KO activated B cells in the median of CD69 (Figure 4.5e). The exceptions were with one HEL^{2x} and two HEL^{2x}+ICAM clones. This may be an indication that the affinity of HEL^{2x} differentiates WT and KO B cells. The increase of cell-cell adhesion with ICAM in these situations may favour WT B cells more than KO B cells.

4.3.3. IL-2 production

The normal expression of surface MHC II in KO B cells suggests that KO B cells may present antigen to T cells normally, even if their stimulation is impaired; and it is well known that these functions are separated in anergic B cells, which show no defect in antigen presentation despite the block in BCR signalling. To assess this, I used an $I\text{-}E^{k}$ restricted anti-HEL CD4 T hybridoma 2G7.1 (a gift from Prof M. Neuberger) as a reporter in stimulation experiments by measuring the amount of IL-2 in the culturing supernatant.

2G7.1 T cells are restricted to the $H\text{-}2E^{k}$ MHC class II haplotype, so I crossed WT and KO Ig mice expressing $H\text{-}2^{b}$ to the closely related B10.BR strain and generated Ig^{kb} mice, which can present to 2G7.1 cells and trigger IL-2 production. Splenic Ig^{kb} B cells were purified by negative selection and mixed with saturating numbers of 2G7.1 T cells (1.2 times the number of B cells) for stimulation with sHEL or mHEL. The cells were analysed by flow cytometry and T cell derived IL-2 was measured in the supernatant.

B cells stimulated with sHEL in the presence of 2G7.1 cells showed a pattern of reduced CD69 upregulation in KO B Ig B cells similar to that seen in the

absence of the responsive T cell line (Figure 4.6a); but no defect in expression of T cell interacting class II (pan) or CD86 was observed (Figure 4.6a). Indeed I-A expression was enhanced in KO B cells when stimulated with high concentrations of sHEL. Preliminary data from two experiments indicated little or no reduction in IL2 production in KO mice.

2G7.1 IL-2 production induced by Ig B cells in the presence of mHEL NIH3T3 cells expressing the lowest levels of mHEL was below the level of detection (data not shown), So subsequently, only clones expressing high or medium levels of mHEL were used. The level of mHEL expression on the clones was demonstrated by flow cytometry (Figure 4.6b). At these levels of antigen density all Ig^{kb} B cells were activated and showed similar upregulation of CD69, CD86 and IL-2 production. The median of MHC II was found to be higher in KO B cells stimulated with all cell line clones, which is similar to the higher level of MHCII observed with high sHEL concentrations. The significance and robustness of this response is difficult to interpret. Speculatively, greater antigen presentation via the MHC Class II pathway might be the consequence of reduced signalling via other activation pathways or higher levels of resting IgM on the mature KO B cells.

4.3.4. Proliferation

Defects in early B cell responses to foreign antigens could lead to reduced or delayed proliferation in KO B cells. To examine this, I cultured splenocytes with various stimuli *in vitro*.

Splenocytes were incubated with a combination of ionomycin and Phorbol 12,13-dibutyrate, (PDBu, 1000-12 ng/mL and 2000-24 ng/mL, respectively) to

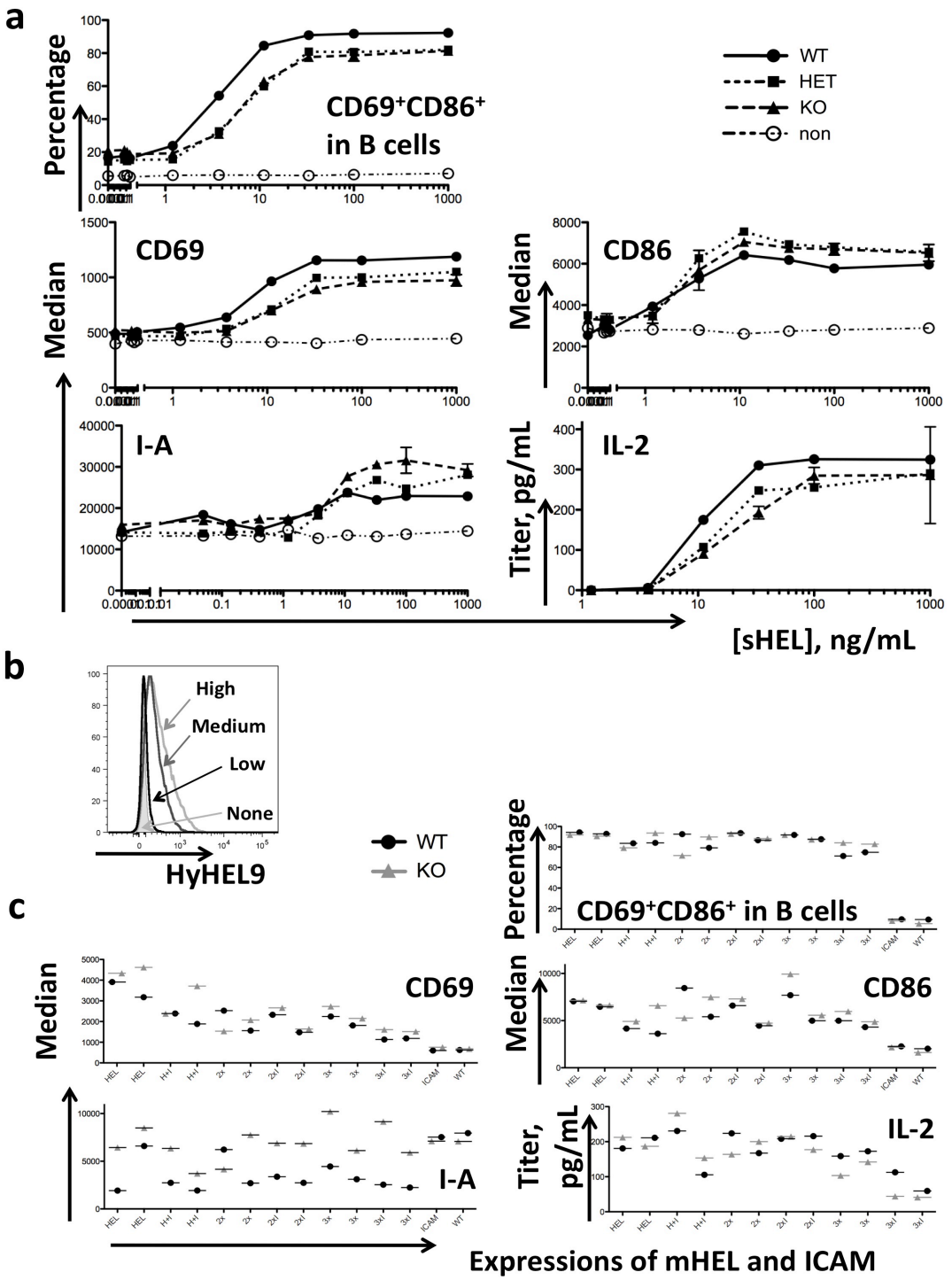

Figure 4.6 Activation, T cell help and IL-2 production. a) sHEL stimulation: top: percentage of $CD69^{+}CD86^{+}$ cells in the B cell populations; middle row: median of CD69 and CD86 antibody staining in flow cytometry analysis; bottom left: median of I-A antibody staining for MHC II molecules; bottom right: titre of IL-2 in the supernatant produced by T cells. b) Flow cytometry plot showing the expression of HEL (shown by HyHEL9 staining) on the surface of NIH3T3 cell clones. The clones were classified as 'high', 'medium' or 'low' according to HEL expression. c) Similar to a, but after mHEL stimulation. Data points represent a single WT or HET sample, mean and SEM of two KO samples.

drive proliferation by mobilised Ca^{2+} and PKC activation without surface receptor engagement. CD45.1 WT splenocytes were mixed in a 1:1 ratio with CD45.2 KO splenocytes and proliferation was monitored by the dilution of CFSE. No differences were detected between WT and KO cells at 48 or 72 hrs (Figure 4.7a, upper row). Stimulation with LPS at a mitogenic dose (20 μg/mL-27 ng/mL) also showed no difference between WT and KO in this assay (Figure 4.7a, lower row).

Differences in early activation were observed at low sHEL concentrations. However, antigen-receptor stimulation of mature B cells at these levels is pro-apoptotic rather than mitogenic in the absence of co-stimulation (data not shown). After varying the range of concentrations (not shown), combinations of low levels of LPS and sHEL (as indicated in Figure 4.7b) in the culture media were used to induce proliferation of Ig B cells. Although the sHEL concentrations were within the same range that failed to activate CD69 in KO B cells, there was no clear difference in B cell proliferation to sHEL plus LPS after four days of stimulation (Figure 4.7b).

To summarise, KO Ig B cells were shown to have a higher activation threshold than WT Ig equivalents in their response to low abundance soluble antigen; but the response to an abundant and high avidity antigen-receptor signal was normal. At low levels of sHEL, activated KO Ig B cells might also be less effective at inducing IL-2 production. Membrane bound HEL induced less activation of KO Ig B cells and the differences diminished with higher antigen avidity and higher antigen affinity. The presence of ICAM increased the percentages of activated B cells of both types. Interestingly, KO Ig B cells showed higher MHC II expression after stimulation with high antigen

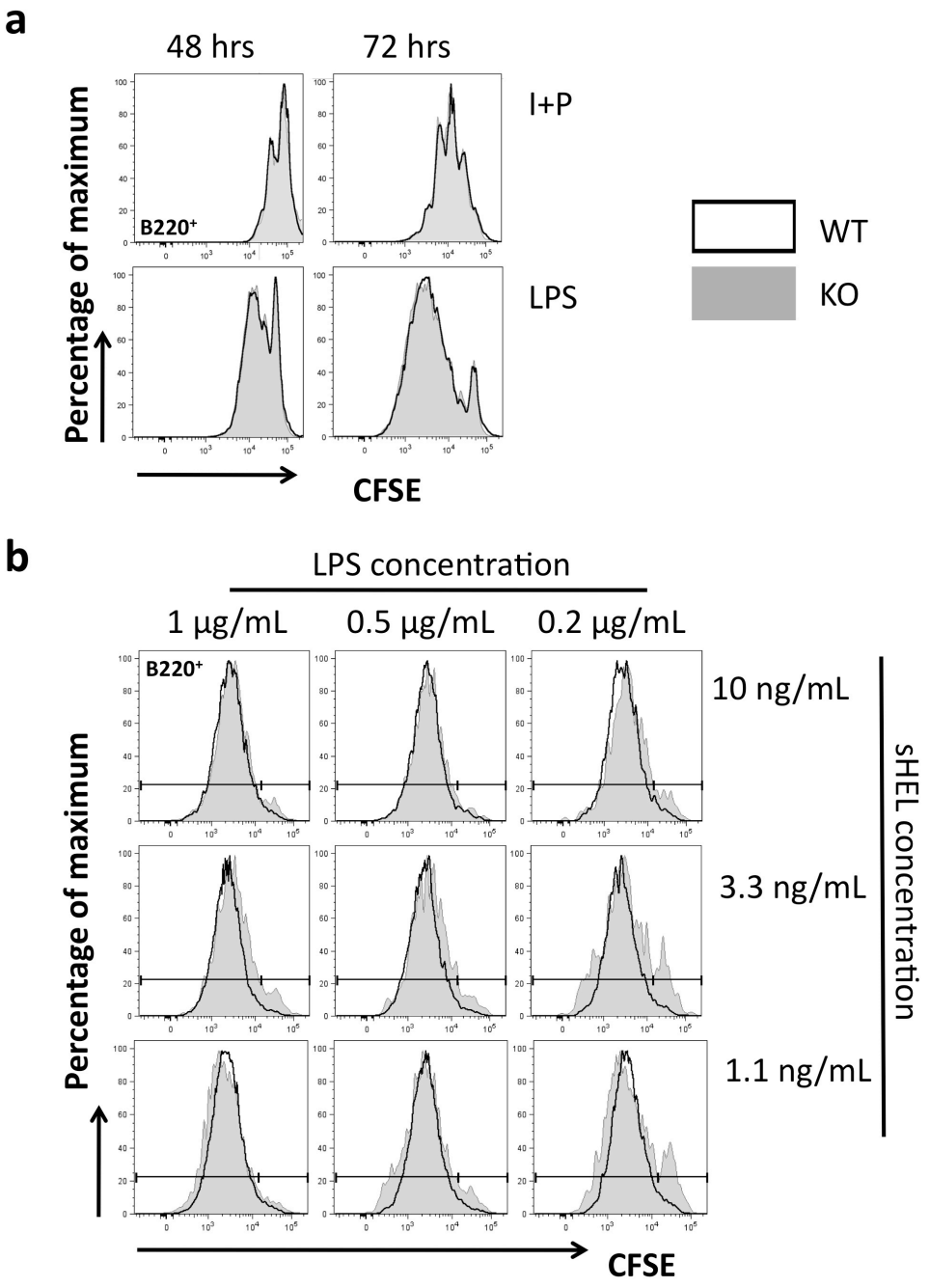

Figure 4.7 Proliferation of splenocytes. a). Flow cytometry data showing the dilution of CFSE as an indication of cell division, after stimulation with ionomycin and PDBu (I+P) or with LPS. b). Cells were incubated with a mixture of LPS and soluble HEL at different concentrations as indicated. The flow cytometry examination was carried out 4 days after the start of stimulation.

avidity, and the significance of this result requires further investigation. No difference was detected between WT and KO B cells in proliferation or survival under the conditions applied.

The initiation of the GC response at least partially depends on the BCR activation threshold, which appears to be raised in Icb-1 KO mice. The survival of GC B cells also depends on an ability to compete for antigen on FDC and present peptide to follicular helper T cells, which may also be defective[83]. These defects are not detectable in the response to high avidity and abundant antigens, which are less likely to be the target of positive selection in the immune response. The reduced responsiveness of Icb-1$^{-/-}$ B cells under these conditions may be the reason for the GC defects. The findings also indicate that Icb-1 is likely to be involved in fine-tuning antigen responses.

Chapter Five B cell receptor signalling in Icb-1$^{-/-}$ B cells

5.1. Introduction

Analysis of the Icb-1-deficient mice provides several strands of information suggesting a subtle defect in B cell signalling, namely reduced constitutive IgM modulation in naïve B cells, increased numbers of MZ B cells and reduced positive selection of auto-reactive B1 B cells. GC B cells are reduced but I detected no impairment of proliferative capacity or survival, nor did I notice any defects in MHC II presentation. Strikingly, B cell activation, as measured by CD69 upregulation, to a soluble, low abundance, low avidity antigen is impaired; but the response to high avidity signals or co-stimulation via TLR4 is normal. Taken together these facts suggest that Icb-1 may be involved in fine-tuning the BCR response to antigen. I examined the BCR-induced signalling in terms of the phosphorylation of key signalling proteins and Ca^{2+} flux.

5.2. Phosphorylation of signalling molecules down-stream of BCR

To begin to dissect the signalling pathways downstream of the BCR I measured BCR-dependent activation of Syk, BLNK, as well as downstream pathways, p38 MAPK, Akt and Erk1/2. Antigen-receptor dependent upregulation of CD69 has previously been shown to be related to Erk1/2 phosphorylation[178], making this a primary target of the analysis.

Phospho-flow cytometry was used to follow the activation of pathways following BCR stimulation. No difference was seen in Syk, BLNK, p38, pAKT or pErk1/2 between WT and KO B cells stimulated with anti-μ (anti-IgM, F'$(ab)_2$), data not shown). However, I then stimulated the splenic B cells of

WT and KO Ig mice with sHEL at a range of concentrations similar to that used in previous experiments and started to see significant differences in the response to the soluble antigen (Figure 5.1). No difference was found between WT and KO Ig B cells phosphorylation of Syk or its target BLNK, across the wide range of antigen concentrations, suggesting that the signalling cascade immediately following BCR activation was intact. However, KO Ig B cells did show a marked reduction in the phosphorylation of Erk1/2 at all non-zero sHEL concentrations used (Figure 5.1). The absence of a difference in the phosphorylation of p38 MAPK supports the notion that the defect in Erk1/2 signalling is specific. Phosphorylation at the two sites of Akt was more minimally reduced: uniformly across the full range of sHEL at Threonine 308 and at intermediate levels of sHEL on Serine 473.

I then used western blot to confirm the findings in the flow cytometric analysis and expanding the examination. Spleen samples from WT and KO spleen cells were enriched for B cells (>95%) by negative selection. The cells were then stimulated with 1 μg/mL sHEL for 0-10 min (Figure 5.2a). Except for the phosphorylation of Erk1/2 after stimulation with sHEL, little difference was found between WT and KO B cells. (Figure 5.2b).

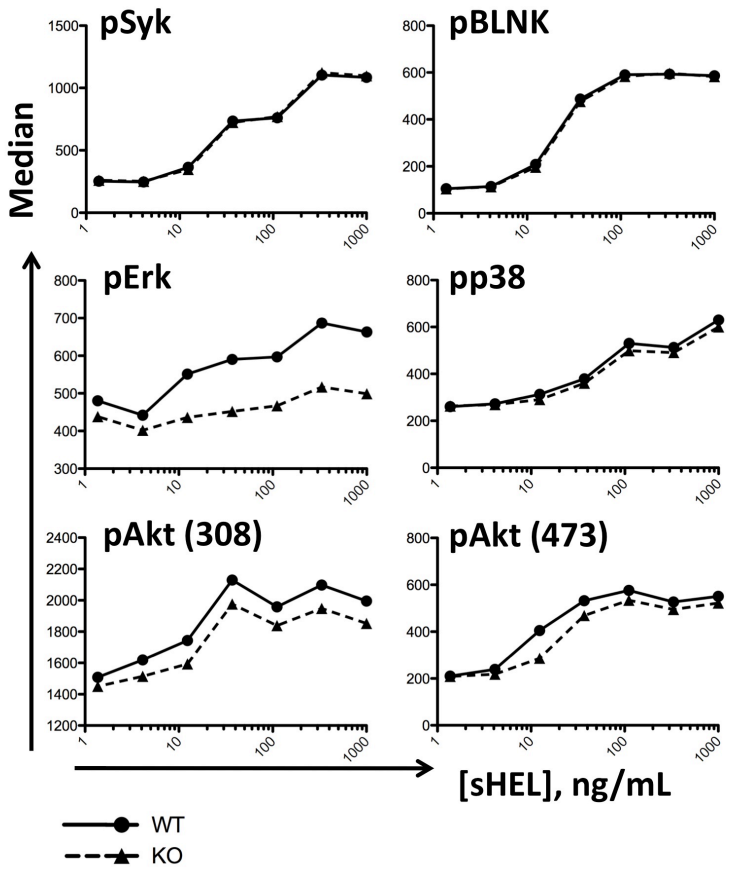

Figure 5.1 Flow cytometry analysis of B cell signalling in the absence of Icb-1. Splenic cells were stimulated with sHEL for 5 minutes. The median of antibody staining was shown as the measure of phosphorylation. Each data point represents one sample. The x-axis shows the concentration of sHEL used to stimulate the B cells.

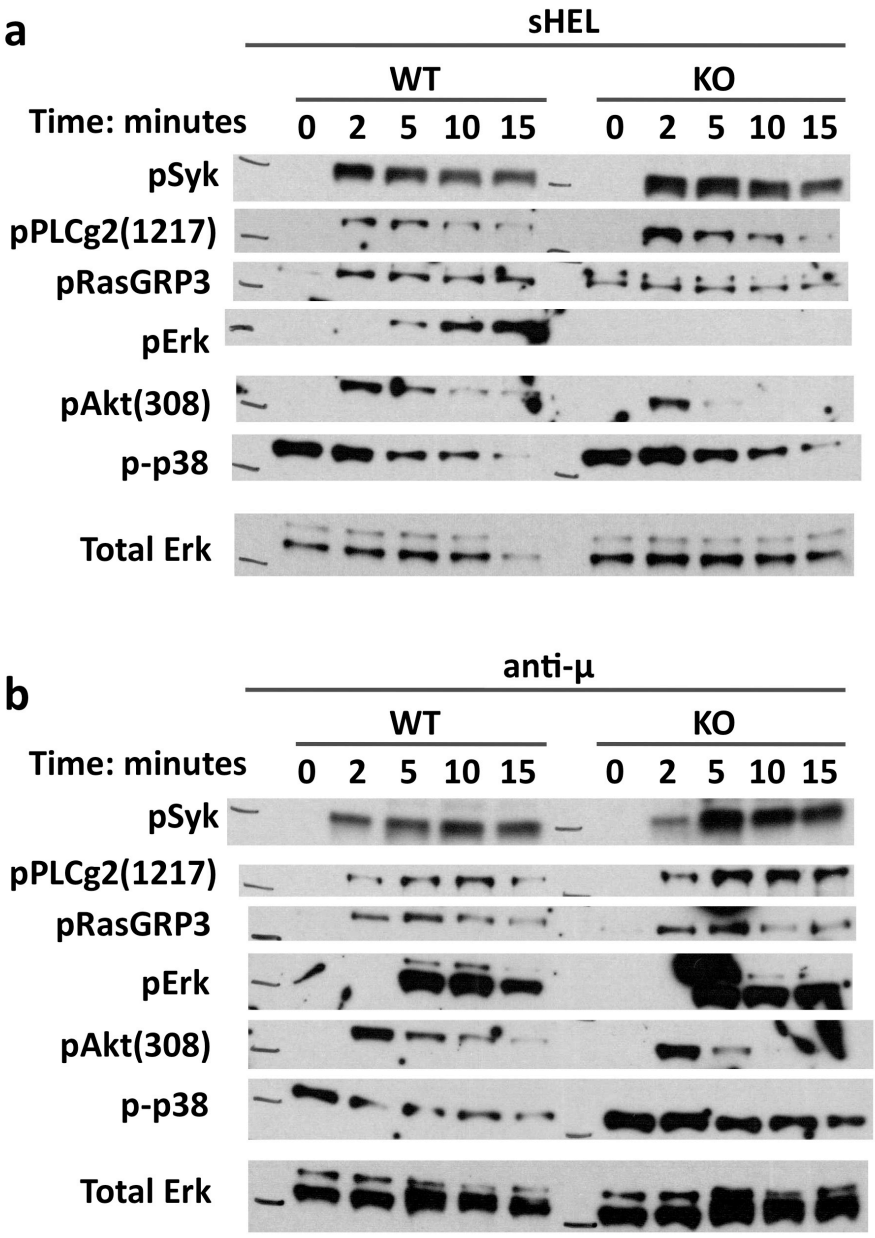

Figure 5.2 Analysis of Protein phosphorylation by western blot. The phosphorylation of signalling molecules indicated, after BCR stimulation. WT and KO B cell enriched spleen samples were stimulated for the duration indicated. a) Stimulation with sHEL on Ig B cells. b) Stimulation of anti-μ (anti-IgM, F'$(ab)_2$) on Ig B cells. The phosphorylated proteins studied are indicated.

5.3. Ca^{2+} flux in $Icb1^{-/-}$ B cells

To further my investigation, I examined the Ca^{2+} flux in KO B cells after BCR stimulation. Ca^{2+} flux influences pathways including Ras-Raf-MAPK (Erk1/2), NF-κB (Ικκα/β) and NFAT and is down stream of activated Syk, BLNK, PI3K and PLCγ2. After findings differences in the phosphorylation of some signalling molecules, it was of keen interest to know if Ca^{2+} flux was normal in KO B cells.

To achieve equal conditions in this experiment I stimulated mixed samples of labelled WT and KO splenocytes. After stimulation with sHEL at 1μg/mL, KO Ig B cells showed clearly reduced Ca^{2+} flux compared with WT Ig B cells (Figure 5.3a). Yet again, no difference in Ca^{2+} flux was found for cells stimulated with anti-μ (anti-IgM, $F'(ab)_2$). WT and KO Ig B cells were identical in controls using ionomycin or buffer. I then measured the height of the peak and the time when the peak appeared whilst varying sHEL concentration (Figure 5.3b). At higher sHEL concentrations, the peaks were higher and appeared sooner. Although the kinetics of the flux was similar for WT and KO B cells, the KO Ig B cells showed a measurable reduction in the median of Ca^{2+} flux over a wide range of concentrations of sHEL (Figure 5.3b)

To summarise, KO Ig B cells signal normally immediately after BCR stimulation, but show an impaired Ca^{2+} flux and Erk1/2 phosphorylation to soluble antigen. Small differences were found in the two types of Akt phosphorylation. From preliminary results, PLCγ2 and Ικκα/β phosphorylation may also be reduced in KO Ig B cells, which if confirmed, would place Icb-1 activity upstream of PLCγ2. The defect in pErk1/2 could be due to effects on Sos, RasGRP3 or via Ca^{2+}-dependent activation of PCKβ. Confirming the

results so far and distinguishing between the downstream possibilities and nature of the quantitative signal will be the next priority.

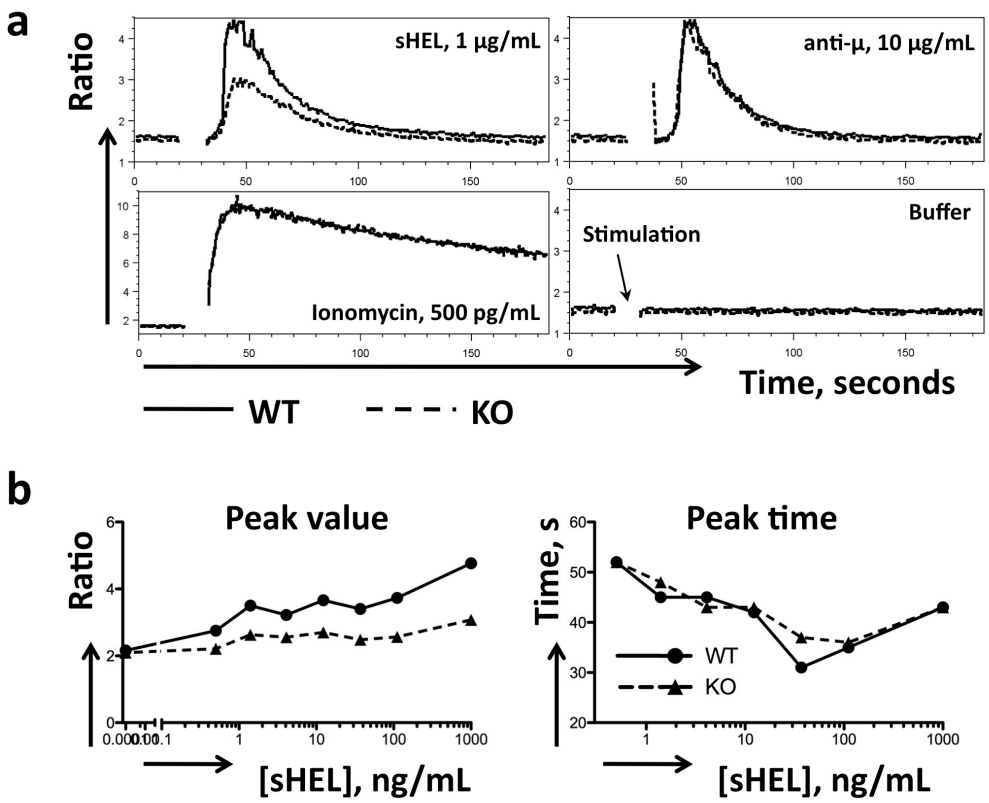

Figure 5.3 Flow cytometry analysis of Ca^{2+} flux following BCR stimulation. WT and KO spleen cells were labeled separately, mixed and stimulated together. In each experiment, a baseline was first established, then stimulus added and Ca^{2+} flux monitored. The vertical axis shows the ratio of positive and negative signals. a) Figures showing the profile of Ca^{2+} flux under different stimulations. b) Analysis of sHEL stimulation, by peak value (height) and peak time, with different sHEL concentrations.

Chapter Six Discussion and further work

6.1. Summary of observations

This thesis presents the study of protein Icb-1 (Themis2), mainly based on the comparison of Icb-1 knockout mice with wild-type controls, focusing on B cell development, selection and immune responses. Subtle changes in immunity and the selection of the B cell repertoire are associated with defects in B cell signalling that are likely to fine-tune the B cell response. These abnormalities are only detectable in response to antigen of low affinity and/or avidity. The defect in Icb-1 may provide clues to explain the more profound defect in T cell development that is seen in the thymus of Themis1$^{-/-}$ mice.

Icb-1$^{-/-}$ B cell repertoire was shown to be largely normal in adult bone marrow, spleen, mesenteric lymph nodes and peritoneal cavities. Icb-1$^{-/-}$ mice showed normal cell numbers and proportions of almost all B cell subpopulations studied, except for an enlarged marginal zone B cell population. The mature Icb-1$^{-/-}$ B cells were different from WT B cells in that they express higher levels of surface IgM. These findings were confirmed in five independent experiments and equivalent results were also seen in mice crossed to Themis1$^{-/-}$ mice. The results were also true for Icb-1$^{-/-}$ B cells in competition with WT B cells, in mixed adult bone marrow chimeras, confirming that these effects of Icb-1 are B cell intrinsic.

The largely normal B cell development in Icb-1$^{-/-}$ mice is in obvious contrast to the T cell developmental block caused by the lack of Themis1. I considered a number of possible artefacts that could account for this. Firstly, my data demonstrate the complete lack of Icb-1 protein in the spleen B cells of Icb-1$^{-/-}$ mice. Secondly, sequencing results of the Icb-1$^{-/-}$ mice, which were

first produced in the 129 strain, showed a high degree of backcrossing to B6 background. 129-originated variants were confined in a small region of under 11 million bases around the location of Icb-1 gene (in Chromosome 4, which contains a total of 155.6 million bases). To the best of our current knowledge, I could not link any other variants in this region directly to significant alteration in B cell development, immunity or signalling in adult mice. Although an Icb-1 WT congenic region from this region would be required to exclude this possibility, the chance of a relevant linked mutation is low. Hence, I believe the comparison between Icb-$1^{-/-}$ mice and B6 controls (including siblings) were reasonable and meaningful. The mice used in the experiments were age and sex matched. Littermates were used whenever possible and no difference were noticed in experiments using siblings or non-related controls. These facts give me confidence that the phenotypes I have seen are the results of removing Icb-1.

Another possibility for the lack of phenotype in naïve Icb-$1^{-/-}$ mice would be the redundancy arising from low-level co-expression of Themis1. The functions of Themis1 and Icb-1 was demonstrated to be interchangeable in T cells[5]. Low and possibly undetectable expression of Themis1 in Icb-$1^{-/-}$ B cells could have compensated for the lack of Icb-1. However, as demonstrated by the characterisation of Themis1/Icb-1 double knockout mice, the lack of the two proteins resulted in phenotypes that were identical to the respective single knockout mice with no added effects. The exception was that the double knockout mice showed elevated mature B cell numbers in the spleen. However, this was not found in competitive adult bone marrow chimera mice. These results confirmed the exclusive expressions of Themis1 and Icb-1, as well as their independent functions.

Modifications in B cell selection could also cover up development defects and result in alterations in characteristics of the repertoire other than composition. To examine this, I characterised Icb-1$^{-/-}$ mice with Ig transgene specific for HEL. The changes to the Ig B cells can be tracked through development. Selection of Ig B cells was studied in Ig mice crossed to strains expressing membrane HEL, soluble HEL or intracellular HEL (the HEL molecure is tethered in the endoplasmic reticulum by virtue of a cytoplasmic di-lysine motif) as systematic self-antigens.

Icb-1$^{-/-}$ Ig mice showed few differences from WT Ig mice, and on this background the increase in marginal zone B cells was inconsistent. There has been evidence that Ig transgenic mice have altered spleen B cell compositions, favouring a larger MZ B cell population[38]. One possibility is that other specificities in a mixed repertoire are selected into this location in the absence of Icb-1. This is lost in the uniform B cell repertoire in the Ig mice. The surface IgM^{a} expression remained higher in mature Icb-1$^{-/-}$ Ig B cells in the bone marrow, though it was inconsistent in the spleen – possibly due to the change in the repertoire. The serum titre of IgM^{a} in Icb-1$^{-/-}$ mice, which is due to a low-level plasma cell differentiation even in the absence of antigen, was also lower than that in WT Ig mice. IgM modulation and spontaneous plasma cell differentiation have both been linked to the level of constitutive BCR signalling in naïve follicular B cells.

In Ig-HEL double transgenic mice, the clonal depletion induced by mHEL and the anergy induced by sHEL were found to be normal in Icb-1$^{-/-}$ mice. However, the positive selection of B1 B cells induced by inHEL was defective without Icb-1. Moreover, comparison of serum anti-HEL IgM^{a} antibody titres from WT and Icb-1$^{-/-}$ double transgenic mice showed lower antibody titres in the latter. The positive selection of B1 cells by the intracellular self-antigen is normally accompanied by a 10 to 50-fold increase in anti-HEL secreting

plasma cells[280]. This could result from both the failure to generate B1 cells and reduced differentiation into plasma cells. It is notable that the fold reduction in plasma cell generation is equivalent from WT to Icb-1$^{-/-}$ Ig-inHEL double transgenic mice and from WT to Icb-1$^{-/-}$ Ig single transgenic mice.

KO mice showed impaired responses to T cell dependent foreign antigens. After being challenged with either SRBCs or NP-CGG, Icb-1$^{-/-}$ mice showed significantly reduced numbers of germinal centre and class-switched B cells. The serum level of IgG1 was also significantly lower in Icb-1$^{-/-}$ mice following SRBC challenge. Icb-1$^{-/-}$ germinal centre B cells were also reduced in mixed adult bone marrow chimeras, though class switching was intact. This hints at the involvement of Icb-1 in the B cell specific selection events of the germinal centre, rather than T/B cell collaboration, or subsequent class switching.

In responding to the T cell-independent antigen NP-Ficoll, KO mice produced approximately twice the amounts of IgM and IgG_3 antibodies as WT controls, up to 28 days post immunisation. The kinetics of the antigen production was identical in both groups. This may be a result of increased MZ B cells in KO mice. However, the response of individual B cells could not be concluded from these data.

Multiple reasons could have led to the effects on positive selection in the pre-immune and immune repertoires, but it is tempting to suggest that defects in BCR-induced cell signalling are the cause in this case. In five independent stimulations each by either sHEL or mHEL, Icb-1$^{-/-}$ Ig B cells showed higher activation threshold than WT Ig B cells, as indicated by CD69 and CD86 upregulation. The impairment of total CD69 upregulation was visible even at high concentrations of sHEL. The difference between WT and KO B cells was reduced with antigens of higher affinity (using membrane bound antigen), greater abundance (using membrane and soluble antigen) or higher avidity

(using membrane antigen or soluble HEL, versus anti-IgM, F'(ab)$_2$). No difference was found between WT and Icb-1$^{-/-}$ cells stimulated with soluble, bivalent antibody against IgM F'(ab)$_2$, which can cross link BCRs and induce potent signalling. No difference was found after stimulation of TLR4 with LPS. These suggest that the impairment is specific for BCR-induced signalling, and is more apparent when the signalling is weak. The conditions under which Icb-1$^{-/-}$ Ig B showed reduced activation are physiologically relevant to those at the beginning of germinal centre formation, when immune cells compete for antigens and are yet to develop high-affinity cell receptors.

Further evidence of specificity in the response comes from the findings that antigen presentation to T cells, as well as B cell proliferation were normal in Icb-1$^{-/-}$ Ig B cells stimulated with sHEL. Icb-1$^{-/-}$ Ig B cells upregulated CD86 normally when responding T cells were present and expressed normal or higher levels of surface MHC II molecules. On two occasions, little or no difference was found in IL-2 production induced by Icb-1$^{-/-}$ Ig B cells. Triggered by ionomycin and PDBu, LPS or combinations of LPS and sHEL, Icb-1$^{-/-}$ Ig B cells showed no difference in proliferation or survival. These findings suggest that an intrinsic defect in B cell antigen presentation to T cells or defected proliferation/survival are not likely to be the underlying cause of the germinal centre defects.

The findings in B cell development and phenotype, selection and the immune responses suggest that the deletion of Icb-1 is likely to cause a defect in BCR-induced signalling. In confirmation of this, Ca^{2+} mobilization and Erk1/2 phosphorylation were reduced in Icb-1$^{-/-}$ Ig B cells activated with sHEL, while phosphorylation of upstream Syk and BLNK were normal. The reduction affected the magnitude rather than the kinetics of the two responses, and was specific since the phosphorylation of p38, another MAPK, was found to be normal. BCR-induced phosphorylation of Akt was marginally reduced at

two sites in Icb-1$^{-/-}$ Ig B cells. This might implicate subtle defects in CD19-dependent signalling, which also tunes the signalling threshold and affect Ca^{2+} flux. The reduced phosphorylation of Erk has been confirmed by Western Blots. However, the changes in the phosphorylation of other key signalling molecules are subtle and no difference between WT and KO B cells has been noticed using this method. Ca^{2+} flux has wide implications in cellular response, including cell activation and survival. Erk1/2 phosphorylation in particular has been linked to CD69 upregulation[178].

In relation to these findings, it would be interesting to consider the possible effect of the removal of Icb-1 on macrophages and dendritic cells. Peirce *et. al.* have demonstrated in a macrophage cell line that Icb-1 is involved in TLR signalling and the production of TNF[11]. The expression of Icb-1 in macrophages and dendritic cells are the same, if not higher than that in B cells. If the signalling and functions of these two cell types are reduced in KO mice, this could play an important part in the initiation of the germinal centre processes. The fact that KO B cells show defects in class-switching after stimulation with SRBCs in naturally grown mice, but these effects are not significantly different in adult mixed bone marrow chimeras, might be evidence in support of this hypothesis. The *in vitro* stimulations used purified B cells, therefore the results from these experiments are not affected by the changes in any other cell types, nor would effects on macrophage and dendritic cells affect the B cell development in the pre-immune repertoire. Whether or not they play a role in the selection of MZ and B1 B cells awaits further investigation.

6.2. Analysis and hypothesis

6.2.1. Themis1 and Icb-1

Despite the similarity of the proteins and interchangeable function (at least in T cells[5]), Icb-1$^{-/-}$ mice and Themis1$^{-/-}$ mice are clearly very different. As is well documented, Themis1$^{-/-}$ mice show T cell developmental block, variously hypothesized as being due to alterations in positive or negative selection, or both. In contrast, Icb-1$^{-/-}$ mice show largely unaffected B cell development and selection, save for a slightly larger marginal zone B cell population and reduced B1 B cell positive selection induced by intracellular self-antigen. But Icb-1$^{-/-}$ mice do show impaired selection of germinal centre B cells, which I hypothesize is due to defected BCR-induced signalling and selection of germinal centre B cells.

Although many observations support the idea that Themis1 has a role in cell signalling, including TCR-induced phosphorylation of the protein and its association with Vav1 and key adaptor protein Grb2, there has been little and inconsistent evidence for signalling defects in Themis1$^{-/-}$ T cells following TCR cross-linking. In the initial studies, Gu *et. al.* were the only group to show subtle reduction and possible delay in Ca^{2+} influx and Erk1/2 phosphorylation[3]. Unlike in Icb-1$^{-/-}$ mice, where B cell populations are little affected, changes in Themis1$^{-/-}$ thymus composition might result in misleading findings. Lesourne *et. al.* recently reported reduction in Erk1/2, p38 and Vav1 phosphorylation, in purified CD4 SP thymocytes[5]. However, they could not detect any signalling defects in DP Themis1$^{-/-}$ T cells, even though this population has the highest Themis1 expression level in WT mice. There is clearly more room for discoveries.

As demonstrated by Daniels *et. al.*, T cell positive selection is delicately controlled by antigen potency, and is delivered by different Ras/Erk1/2

signalling characteristics, especially strength, duration and localization[240]. The level of these effects is difficult to detect, in contrast to the strong signals that normally induce negative selection. CD69 upregulation, which was used to demonstrate a normal response to different agonists or partial agonists in Themis1 deficient DP T cells, is unable to detect more subtle changes in signalling. The Icb-1 dependent defects in B cells were only evident when BCR signalling was weak, either as a result of antigen valency/avidity, abundance or affinity. Studies on Themis1 have so far not intensively investigated the differential signalling strength or duration. Under the strong conditions used, other pathways may override the effects of the absence of Themis1.

It is also tempting to speculate on the relative importance of Icb-1 and Themis1 in B and T cells respectively, based on the mRNA levels of the two proteins, shown by real-time reverse-transcript PCR. Using the same standard, Themis1 mRNA level in T cells is roughly ten times that of Icb-1 in B cells. In addition, while Icb-1 expression gradually increased from pre/pro to follicular B cells, Themis1 expression peaks in DP T cells and is reduced in SP T cells. This could relate to the requirement of each protein in early (Themis1) and late (Icb-1) selection events; or relate to the fact that T cell selection is itself more robust[65]. Other examples of homologue pairs of proteins having different effects do exist, such as LAT and NTAL[281,282]. Of course, different developmental expression of other Themis1/Icb-1 interacting proteins in B and T cells could also explain the difference in absolute levels between the two cell types. At this stage, no firm conclusion can therefore be made.

6.2.2. Icb-1 in BCR-induced signalling

It is now accepted that the dominant Erk1/2 activation pathway occurs via PLCγ2 leading to DAG-dependent recruitment and PKC activation of first RasGRP and then its target Ras. In B cells, the Grb2-Sos dependent pathway is secondary, but perhaps amplifies and/or sustains total Erk1/2 signalling, as Sos activity is positively regulated by binding its product Ras-GTP (also generated by RasGRP). Finally, a proapoptotic Erk1/2 signalling pathway is also described, in which PKCδ is activated by the Ca^{2+} flux[223]. PKC-δ independently phosphorylates and activates RasGRP. The calcium-dependent pathway generates a strong signal, which may be associated with negative selection. Therefore the Erk1/2 signalling pathways combine to generate signals of different strength, location and duration. Hypothetically, this provides the mechanism for integrating and fine-tuning positive and negative selection.

The function of Icb-1 within these pathways is unclear, but it may be rellated to Ca^{2+} flux in the cytoplasm. High sHEL concentration can induce some Erk1/2 phosphorylation in Icb-$1^{-/-}$ Ig B cells. Partial effects like this may suggest that the Grb2-Sos amplification pathway is defective, supported by fact that Icb-1 itself associates with Grb2. However, it is not known if Icb-1 is required to activate the canonical PLCγ2/DAG/RasGRP pathway when signal strength is low. This might also occur by inhibiting DAG kinases. More detailed analysis of these pathways is required.

Involvement of Icb-1 in PLCγ2 signalling could explain the effect of Icb-1 deficiency on the B cell Ca^{2+} flux. The Ca^{2+} flux is independent of Sos and is negatively regulated by Grb2, as described previously[270]. Since Themis1 and Icb-1 have both been shown to constitutively associate with Grb2, it is

possible that association with Icb-1 constrains Grb2's negative regulatory effects on Ca^{2+} flux. In this scenario Icb-1 might recruit Grb2 to Sos and limit the amount of Grb2 at sites associated with inhibition of Ca^{2+} flux. However, so far there is no evidence of a direct association of either Icb-1 or Themis1 with Sos or Shc, nor any evidence suggesting that the negative regulation of Grb2 on BCR-induced signalling is reduced in Icb-$1^{-/-}$ B cells [270].

On the other hand, both Icb-1 and Themis1 have been shown to bind Vav, which contributes to Ca^{2+} mobilization by unknown mechanisms. Themis1 was also shown to affect Vav1 phosphorylation in single positive T cells following TCR cross-linking[5]. Vav activation downstream of CD19 could be assisted by Grb2. The binding of Icb-1 and Themis1 to Vav and Grb2 could provide a plausible mechanism that could modifies the Ca^{2+} flux. Stimulation of Icb-$1^{-/-}$ B cells showed no defect in Syk or BLNK signalling, showing intact early events in BCR stimulation. Hence the possible Icb-1-Vav function is confined to later signalling events but not involved in Rac activation.

A third possibility involves PI3K. BCR-dependent PLCγ2 phosphorylation is probably reduced in Icb-$1^{-/-}$ B cells, following normal Syk and BLNK signalling. This is likely to be the direct cause of Ca^{2+} reduction and may be due to defective PI3K activation, downstream of CD19 assisting the function of Btk. Akt activation was found to be slightly reduced in activated Icb-$1^{-/-}$ B cells, which also points to defective CD19 downstream signalling. There is no T cell equivalent in CD19 function, which may explain the normal Ca^{2+} flux in Themis$1^{-/-}$ T cells. This and other possibilities will need to be investigated in future experiments.

The subtle nature of the signalling defect in Icb-$1^{-/-}$ B cells suggests that Icb-1 is required for fine-tuning B cell response. Together with other observations on antigen affinity and/or potency, this suggests that the role of Icb-1 is more

import at low BCR activation. It is possibly involved in mechanisms to enhance the signalling in these circumstances. This would be analogous to the low intensity signals seen in positive selection in the thymus.

Ca^{2+}-dependent Erk1/2 phosphorylation was suggested to facilitate negative selection in immature B cells. Yet I did not observe any reduction in negative selection in the Icb-$1^{-/-}$ Ig-HEL mouse models. Erk1/2 signalling may not be necessary for the induction of anergy by sHEL – though it is required for its maintenance. I have shown that B cell signalling is normal in response to abundant high avidity BCR ligands mimicking mHEL, which causes deletion/receptor editing.

B cell positive selection correlates with signal strength in several animal models. B1 cells are increased in the absence of negative regulatory signalling CD22, Lyn and SHP1 or the presence of transgenic CD19[275,283]. This may explain the involvement of Icb-1 in positive selection, though details of the normal mechanism are still unclear. MZ B cell selection is favoured when BCR signalling is relatively weak, especially when Ca^{2+} flux is disturbed[45]. This may explain the larger marginal zone B cell population when Icb-1 is absent and Ca^{2+} flux defective. The defective activation possibly means that Icb-$1^{-/-}$ B cell are put at a disadvantage during germinal centre selection. This is likely to be the cause of the reduced B cell immune response seen in the Icb-$1^{-/-}$ mice.

6.3. Summary and future work

Overall, current evidence suggests that the function of Icb-1 lies in enhancing BCR signalling. The mechanism involves the Ca^{2+} and Erk1/2 pathways and is more influencing when BCR activation is weak. The defects were apparent and robust in *in vivo* and *in vitro* stimulations. However, few and small effects were seen in B cell development and selection. Hence the role of Icb-1 seems likely to lie in fine-tuning BCR signalling and cell responses. Although Themis 1 and Icb-1 are likely have a similar function, on the basis of interchangeability in T cells, their role in their respective cell types is apparently different: Themis1 is essential in T cell selection, while Icb-1 is more important in B cell immunity.

Adaptor proteins are particularly important in modifying antigen receptor signals, in magnitude, duration and subcellular localization[167]. They lead to the differentiation among specialized pathways and eventually result in a wide range of cellular responses. Themis1 and Icb-1 lack obvious active sites and contain multiple common interaction domains. So they may be adaptor proteins. The differences seen in Themis1$^{-/-}$ and Icb-1$^{-/-}$ mice possibly reflect on the difference between T and B cells in signalling and immunity. While the function of the proteins remains unexplained, it is easy to attribute the lack of phenotype to redundant proteins and/or pathways. The subtly of their function and its uncertain purpose, mean one has to look harder into the fine details of the biology.

Immediate experiments need to involve studies that will clarify the role of Icb-1 in BCR-induced signalling. The focus should include (i) defining its role in the three pathways leading to Erk1/2 activation; (ii) assessing PLCγ2/PI3K activation (iii) ascertaining if Icb-1 deficiency alters the location of Ras/Erk1/2 activation by confocal microscopy; and (iv) assessing the implications of its

associations with Grb2 and Vav. The final test of function will be complementation and rescue of the Themis1-deficient phenotypes in the thymus. Further investigations should also include the comparison of macrophage and dendritic cell populations between WT and KO mice. The phenotypes of the KO mice discovered so far also indicates the role of the protein in infectious and autoimmune diseases. Mouse models of these should be used in further studies.

Appendix

A.1

Genomic sequence 500bp upstream of the *icb-1* gene, taken from Ensembl

>ENSMUSG00000037731|ENSMUST00000045154
AATTATCTGGGAACCTCTGTTGAGAAATGCCTCCATCAGACTGCTTGTAGG
CAAGCCTGTAGTGCATTTTCTCCACTTATGATTGGTGTGGGTGGGCCCAGC
CCATAGGGTGTAGGTAGTGCCAACCCTGGGCAGGTGGTCCTGAGTTGTGT
AAGAAAGCAAACTGAGCAAACCAGTAAGCTGTGTTTCTTTATGGCTTGTAC
CAGTCCCAGTCCCTTTATCTCTCTCTATCTGTCCGGAGTTTCTGTTCTGACT
AACCTCTGTGATCCCAGAGTTGTAAGATAATAAACCCTTCCCTCCCCAAGT
TGCTTTTGGTCATGGTGTTTTATCACATTAGAAACCTTAAGAAAAGATTCAAT
TTTAGAGATGAAGAGACAGGTCAGGGGAAATAAAGTCCCCATTCAAGAGT
TCGGGGCGCTTCAGAGAACCCTGTAGGGCTCCCGACCTGAGGGGCGTG
GCCTCGGTGGGCGTGGCTTCCGG ACTGTCCTCTGCAAGCTGCC

A.2

Lists of potential transcription factors analysed by TRAP or TFSEARCH, from the sequence listed in Section A.1

TRAP		TFSEARCH	
Entry	P-value	Entry	Score
CEBPB_02	0.00554	AP-1	88.9
GLI_Q2	0.00735	AP-1	88.9
GLI3_01	0.00969	c-Ets-	93.1
NKX26_01	0.0145	C/EBPb	86.2
P53_02	0.0153	C/EBPb	86.2
GATA1_04	0.016	C/EBPb	86.8
CMYC_02	0.0174	C/EBPb	89.6
GR_01	0.0183	C/EBPb	89.6

P53_DECAMER_Q2	0.0203	CdxA	85.9
DBP_Q6	0.0209	CdxA	86.4
GLI3_Q5_01	0.0244	CdxA	86.4
MEF2_01	0.0252	CdxA	86.4
GKLF_02	0.0254	CdxA	86.4
GATA3_02	0.0254	CdxA	87.1
LPOLYA_B	0.0255	CdxA	87.2
FLI1_Q6	0.0258	CdxA	88.5
MYOD_Q6	0.0262	CdxA	96.2
EBOX_Q6_01	0.0272	E47	90.4
CMYC_01	0.0273	Elk-1	88.3
NKX32_02	0.0295	GATA-1	85.3
CDX2_01	0.0296	GATA-1	85.7
T3R_Q6	0.0303	GATA-1	87.3
PAX2_02	0.0348	GATA-1	88.4
PBX1_03	0.0353	GATA-1	89.7
GATA1_06	0.0367	GATA-1	91.6
E12_Q6	0.0381	GATA-2	86.2
MMEF2_Q6	0.0396	GATA-2	87.4
MECP2_02	0.0397	GATA-3	90
CEBP_Q2_01	0.0414	GATA-3	91.9
E2A_Q6	0.0416	GATA-X	85.3
ZIC1_01	0.042	GATA-X	87.6
E2A_Q2	0.0422	Ik-2	89.5
PBX1_02	0.0426	Lyf-1	88.3
ISRE_01	0.0433	Lyf-1	88.3
CACD_01	0.0443	MyoD	88.4
CDX1_01	0.0454	MZF1	88.7
GATA2_02	0.0489	MZF1	88.7
CETS168_Q6	0.0498	MZF1	93.9
		MZF1	93.9
		Nkx-2.	88.4
		Pbx-1	92.2
		Sp1	89
		Sp1	89
		SRY	86.4
		SRY	89.1
		SRY	90
		SRY	92.7

A.3

Table showing the genes containing the SNPs in the KO mice, compared with WT C57BL/6 mice, together with reasons to consider the SNPs not significant in altering the results presented in this thesis. The reasons were based on current knowledge of these genes and proteins, listed in Section A1.2. In addition, possible primary investigations to establish causation are listed here:

Protein name	Reason to dismiss	Possible primary investigation
Csf3r	Low PolyPhen score indicating insignificant effect on protein activity; The function fo the protein is not directly related to B cell biology; No B cell defect was found in the bone marrow of KO mice, where the protein is expressed	Examine the development of granulocytes in the bone marrow
Thrap3	No informaiton of the protein's function (only by similarity)	Examine Pol II activity, eg, trancription level changes in KO and WT cells
Gm12942	No evidence at the protein level; No informaiton of the protein's function	NA
4930465 A12Rik	Existance was predicted; Low PolyPhen score indicating insignificant effect on protein activity	NA
Phc2	PolyPhen score zero, indicating little effect on protein activity; Mice lacking this protein die prematurally, which is not observed in Icb-1 KO mice	Examine the skeleton formation of KO embryos
Adc	Expression in non-lymphid organs	Examine ornithine decarboxylase activity
Tmem54	No evidence at the protein level; No informaiton on the protein's function	NA
S100pbp	No evidence at the protein level; Little information on the protein's function	Confirm nuclear location and co-localization with S100P
C77080	Existence was predicted	NA
Sync	PolyPhen score zero, indicating little effect on protein activity	NA
Fam167b	No information on the protein’s function; PolyPhen score zero, indicating insignificant effect on protein activity	NA
Dcdc2b	Existence was predicted	NA
Iqcc	No evidence at the protein level; No information on the protein's function	NA
Ccdc28b	Expression in non-lymphid organs; PolyPhen score zero, indicating insignificant effect on protein activity; No information on protein’s function	NA
Tmem39b	The function of the protein not studied, predicted protein family not studied	NA
Col16a1	No expression detected in lymphoid organs	Examine KO cell morphology and response to integrin

Pef1	No information on the protein's function (only by similarity)	Examine the Ca2+-induced apoptosis of KO cells
Rab42-ps	No information of the protein's function (only by similarity); Low PolyPhen score indicating insignificant effect on protein activity	Difficult due to the redundancies among the small GTPase superfamily proteins
Trnau1ap	PolyPhen score zero, indicating little effect on protein activity	Examine the production and the rate of production of proteins containing selenocysteine in KO cells
Phactr4	Mice with disrupted Phactr4 gene were born with severe birth defects, which were not seen in Icb-1 KO mice.	Check phosphorylation of PPI and Rb in embryo Neural Tube

A.4

Table showing the exonic and nonsynonymous variants found in Icb1$^{-/-}$ mice compared with the C57BL/6J sequence. Also listed: substitution of amino acid, PolyPhen score (HumDiv) and current knowledge of the gene and the protein.

Protein name, Gene ID	Site	Hum Div	Evidence level	Expression	Gene Ontology	Other related information
Csf3r, NM_007782	S379N	0.212	Protein	Bone marrow	Cell adhesion, Neutrophil chemotaxis, Cytokine receptor activity,	Receptor for granulocyte colony-stimulating factor (CSF3), and other possible functions
Thrap3, NM_146153	S162L	N/A	Protein	Nucleus	Transcription coactivation (by similarity)	Mus musculus thyroid hormone receptor associated protein 3.
Gm12942, NM_001099319	G149S	0.991	Transcript			Also called Zmym6nb
Phc2, NM_018774	T293P	0	Protein	Nucleus	Multicellular organismal development Spermatogenesis DNA binding zinc ion	Polyhomeotic-like protein 2, Early development regulatory protein. Mice lacking functional Phc2 show visible defects in early development.

					binding	
Adc, NM_172875	Y317H	0.09	Transcript	Brain and testis, mitochondria	Ornithine metabolic process (decarboxylase activator), Polyamine biosynthetic process, Positive regulation of catalytic activity	Acts as an antizyme inhibitor and prevents antizyme-dependent degradation of ornithine decarboxylase. Does not appear to possess arginine decarboxylase or ornithine decarboxylase activity.
Tmem54, NM_133881	S174N	0.924	Transcript		Integral to membrane	Transmembrane protein 54. Belongs to the TMEM54 family.
Tmem54, NM_025452	P205L	0.001				
S100pbp, NM_029036	D269G	1	Transcript			Predicted by similarity: Colocalizes with S100P in the nucleus.
	I83T	0				
Sync, NM_023485	L79Q	0	Protein	Skeletal muscle, heart, lung and testis.	Protein binding	Interacts with DES and DTNA. Up-regulated in dystrophic muscle (at protein level). Belongs to the intermediate filament family.
Fam167b, NM_182783	K14E	0	Transcript			Belongs to the FAM167 (SEC) family. Was originally (Ref.3) thought to originate from human.
Iqcc, NM_198026	R412C	0.71	Transcript			IQ-domain containing protein c
	N358S	0.004				
	Q338L	0.009				
	G294R	0.997				
	D117G	0.051				
Ccdc28b, NM_025455	P17Q	0	Transcript	Retina, pericardium and limb epitheliu m		Coiled-coil domain-containing protein 28B.
Tmem39b, NM_199305	H337R	0.745	Protein			By potential, multi-pass membrane protein. Part of the TMEM39 family.

Col16a1, NM_028266	R140Q	N/A	Transcript	High expression in the heart and the kidney, weak in the lungs. Also detected in the ciliary muscle of the eye, on the serosa layer lining the muscularis externa of intestinal tissue, and in the perimysium membrane lining both the cardiac muscle bundle and the smooth muscle tissue of the small intestine. Strongly stained in particulate or granular structures. Expression level varies at different developmental stages	Cellular response to amino acid stimulus Cell adhesion	Involved in mediating cell attachment and inducing integrin-mediated cellular reactions, such as cell spreading and alterations in cell morphology.
	V373A					
	T515K					
	A646V					
	M655T					
	M655I					
	H766R					
	R820Q					
Pef1, NM_026441	G28S	N/A	Transcript		Calcium ion binding	By similarity, heterodimerizes with PDCD6. Dissociates from PDCD6 in presence of Ca^{2+}.
Rab42-ps, NM_001081651	A53T	0.004	Transcript			By sequence similarity: Belongs to the small GTPase superfamily. Rab family. GTP-binding
Trnau1ap, NM_027	V135M	0.01	Protein		Selenocysteine incorporatio	Involved in the early steps of selenocysteine biosynthesis and tRNA (Sec) charging to the

925					n, Protein binding	later steps resulting in the cotranslational incorporation of selenocysteine into selenoproteins. Stabilizes the SECISBP2, EEFSEC and tRNA (Sec) complex. May be involved in the methylation of tRNA (Sec). Enhances efficiency of selenoproteins synthesis. Found in a complex with tRNA (Sec) By similarity. Interacts with SEPSECS By similarity. Component of the tRNA (Sec) complex composed at least of EEFSEC, SECISBP2, SEPHS1, SEPSECS, TRNAU1AP and tRNA (Sec). Associates with mRNP and/or polysomes.
Phactr4, NM_175306	I511V	0.455	Protein		Rho protein signal transduction Actin cytoskeleton organization, Negative regulation of Integrin-mediated signaling pathway Protein phosphatase inhibitor activity Protein phosphatase type 1 activator activity	Regulator of protein phosphatase 1 (PP1) required for neural tube and optic fissure closure, and enteric neural crest cell (ENCCs) migration during development. Acts as an activator of PP1 by interacting with PPP1CA and preventing phosphorylation of PPP1CA at 'Thr-320'. During neural tube closure, localizes to the ventral neural tube and activates PP1, leading to down-regulate cell proliferation within cranial neural tissue and the neural retina. Also acts as a regulator of migration of enteric neural crest cells (ENCCs) by activating PP1, leading to dephosphorylation and subsequent activation of cofilin (COF1 or COF2) and repression of the integrin signaling through the RHO/ROCK pathway

					Regulation of cell cycle Closure of optic fissure, Enteric nervous system developmen t,	
	V28 0L	0				

Reference

1. Johnson, A. L. ***et al.*** Themis is a member of a new metazoan gene family and is required for the completion of thymocyte positive selection. ***Nature Publishing Group*** **10**, 831–839 (2009).
2. Lesourne, R. ***et al.*** Themis, a T cell-specific protein important for late thymocyte development. ***Nature Publishing Group*** **10**, 840–847 (2009).
3. Fu, G. ***et al.*** Themis controls thymocyte selection through regulation of T cell antigen receptor–mediated signaling. ***Nature Publishing Group*** **10**, 848–856 (2009).
4. Kakugawa, K. ***et al.*** A Novel Gene Essential for the Development of Single Positive Thymocytes. ***Mol. Cell. Biol.*** **29**, 5128–5135 (2009).
5. Lesourne, R. ***et al.*** Interchangeability of Themis1 and Themis2 in Thymocyte Development Reveals Two Related Proteins with Conserved Molecular Function. (2012).
6. Treeck, O., Strunck, E. & Vollmer, G. A novel labsment membrane-induced gene identified in the human endometrial adenocarcinoma cell line HEC1B. ***Federatio of European Biochemical Societies*** **425**, 426–430 (1998).
7. Treeck, O. ***et al.*** Detection of increased ***icb-1*** transcript levels in maturing HL-60 cells: a novel marker for granulocytic and monocytic in vitro differentiation. 1–5 (2002).
8. Treeck, O., Kindzorra, I., Pauser, K., Treeck, L. & Ortmann, O. Expression of icb-1 gene is interferon-gamma inducible in breast and ovarian cancer cell lines and affects the IFNγ-response of SK-OV-3 ovarian cancer cells. ***Cytokine*** **32**, 137–142 (2005).
9. Bollmann, J., Ortmann, O. & Treeck, O. Expression of differentiation-associated gene icb-1 is estrogen-responsive in ovarian and breast cancer cell lines. ***The Journal of Steroid Biochemistry and Molecular Biology*** **109**, 16–21 (2008).
10. Treeck, O. ***et al.*** Network analysis of icb-1 gene function in human breast cancer cells - Treeck - Journal of Cellular Biochemistry - Wiley Online Library. ***J. Cell. Biochem.*** (2012).doi:10.1002/jcb.24175
11. Peirce, M. J. ***et al.*** Themis2/ICB1 Is a Signaling Scaffold That Selectively Regulates Macrophage Toll-Like Receptor Signaling and Cytokine Production. ***PLoS ONE*** **5**, e11465 (2010).
12. Sanger Institute Mouse Resources Portal Search Results for 'BC013712'. ***sanger.ac.uk*** at <http://www.sanger.ac.uk/mouseportal/search?query=BC013712>
13. International Knockout Mouse Consortium (IKMC) Search results for: BC013712. ***knockoutmouse.org*** at <http://www.knockoutmouse.org/search_results?criteria=BC013712>
14. Martin, F. & Kearney, J. F. B-cell subsets and the mature preimmune repertoire. Marginal zone and B1 B cells as part of a "natural immune memory". ***Immunol. Rev.*** **175**, 70–79 (2000).
15. Martin, F., Oliver, A. M. & Kearney, J. F. Marginal zone and B1 B cells unite in the early response against T-independent blood-borne particulate antigens. ***Immunity*** **14**, 617–629 (2001).
16. Sykes, M. Immune tolerance: mechanisms and application in clinical transplantation. ***Journal of Internal Medicine*** **262**, 288–310 (2007).

17. Hayakawa, K., Hardy, R. R. & Stall, A. M. Immunoglobulin-bearing B cells reconstitute and maintain the murine Ly-1 B cell lineage. *Eur. J. Immunol.* **16**, 1313–1316 (1986).
18. Cinamon, G., Zachariah, M. A., Lam, O. M., Foss, F. W. & Cyster, J. G. Follicular shuttling of marginal zone B cells facilitates antigen transport. *Nat Immunol* **9**, 54–62 (2008).
19. Hayakawa, K. *et al.* Positive selection of anti-thy-1 autoreactive B-1 cells and natural serum autoantibody production independent from bone marrow B cell development. *Journal of Experimental Medicine* **197**, 87–99 (2003).
20. Wen, L. *et al.* Evidence of marginal-zone B cell- positive selection in spleen. *Immunity* **23**, 297–308 (2005).
21. Mandel, E. M. & Grosschedl, R. Transcription control of early B cell differentiation. *Current Opinion in Immunology* **22**, 161–167 (2010).
22. Nagasawa, T. Microenvironmental niches in the bone marrow required for B-cell development. *Nat Rev Immunol* **6**, 107–116 (2006).
23. Freeden-Jeffry, Von, U. *et al.* Lymphopenia in interleukin (IL)-7 gene-deleted mice identifies IL-7 as a nonredundant cytokine. *Journal of Experimental Medicine* **181**, 1519–1526 (1995).
24. Carvalho, T. L., Mota-Santos, T., Cumano, A., Demengeot, J. & Vieira, P. Arrested B lymphopoiesis and persistence of activated B cells in adult interleukin 7 -/- mice. *Journal of Experimental Medicine* **194**, 1141–1150 (2001).
25. Busslinger, M. *Transcriptional control of early B cell development*. *Annual Review of Immunology* **22**, 55–79 (2004).
26. Igarashi, H., Gregory, S. C., Yokota, T., Sakaguchi, N. & Kincade, P. W. Transcription from the RAG1 locus marks the earliest lymphocyte progenitors in bone marrow. *Immunity* **17**, 117–130 (2002).
27. Kluiver, J., Kroesen, B.-J., Poppema, S. & van den Berg, A. The role of microRNAs in normal hematopoiesis and hematopoietic malignancies. *Leukemia* **20**, 1931–1936 (2006).
28. Monticelli, S. *et al.* MicroRNA profiling of the murine hematopoietic system. *Genome Biol.* **6**, (2005).
29. Hirose, J. *et al.* A developing picture of lymphopoiesis in bone marrow. *Immunol. Rev.* **189**, 28–40 (2002).
30. Welner, R. S. *et al.* Interferon-producing killer dendritic cells (IKDCs) arise via a unique differentiation pathway from primitive c-kitHiCD62L+ lymphoid progenitors. *Blood* **109**, 4825–4831 (2007).
31. Rumfelt, L. L., Zhou, Y., Rowley, B. M., Shinton, S. A. & Hardy, R. R. Lineage specification and plasticity in CD19- early B cell precursors. *Journal of Experimental Medicine* **203**, 675–687 (2006).
32. Clark, M. R., Cooper, A. B., Wang, L. D. & Aifantis, I. The pre-B cell receptor in B cell development: recent advances, persistent questions and conserved mechanisms. *Current Topics in Microbiology and Immunology* **290**, 87–103 (2005).
33. Nishimoto, N. *et al.* Normal pre-B cells express a receptor complex of μ heavy chains and surrogate light-chain proteins. *Proc. Natl. Acad. Sci. U.S.A.* **88**, 6284–6288 (1991).
34. Tussiwand, R., Bosco, N., Ceredig, R. & Rolink, A. G. Tolerance checkpoints in B-cell development: Johnny B good. *Eur. J. Immunol.* **39**, 2317–2324 (2009).

35. Hardy, R. R., Carmack, C. E., Shinton, S. A., Kemp, J. D. & Hayakawa, K. Resolution and characterization of pro-B and pre-pro-B cell stages in normal mouse bone marrow. *Journal of Experimental Medicine* **173**, 1213–1225 (1991).
36. Rolink, A., Grawunder, U., Winkler, T. H., Karasuyama, H. & Melchers, F. IL-2 receptor α chain (CD25,TAC) expression defines a crucial stage in pre-B cell development. *Int. Immunol.* **6**, 1257–1264 (1994).
37. Allman, D. *et al.* Resolution of three nonproliferate immature splenic B cell subsets reveals multiple selection points during peripheral B cell maturation. *Journal of Immunology* **167**, 6834–6840 (2001).
38. Cariappa, A. A. *et al.* The recirculating B cell pool contains two functionally distinct, long-lived, posttransitional, follicular B cell populations. *J. Immunol.* **179**, 2270–2281 (2007).
39. Pillai, S. & Cariappa, A. The follicular versus marginal zone B lymphocyte cell fate decision. *Nat Rev Immunol* **9**, 767–777 (2009).
40. Bannish, G., Fuentes-Pananá, E. M., Cambier, J. C., Pear, W. S. & Monroe, J. G. Ligand-independent Signaling Functions for the B Lymphocyte Antigen Receptor and Their Role in Positive Selection during B Lymphopoiesis. *Journal of Experimental Medicine* **194**, 1583–1596 (2001).
41. Mackay, F., Schneider, P., Rennert, P. & Browning, J. *BAFF and APRIL: A tutorial on B cell survival*. *Annual Review of Immunology* **21**, 231–264 (2003).
42. Smith, S. H. & Cancro, M. P. Cutting edge: B cell receptor signals regulate BLyS receptor levels in mature B cells and their immediate progenitors. *Journal of Immunology* **170**, 5820–5823 (2003).
43. Hsu, B. L., Harless, S. M., Lindsley, R. C., Hilbert, D. M. & Cancro, M. P. Cutting edge: BLyS enables survival of transitional and mature B cells through distinct mediators. *Journal of Immunology* **168**, 5993–5996 (2002).
44. Cariappa, A. & Pillai, S. Antigen-dependent B-cell development. *Current Opinion in Immunology* **14**, 241–249 (2002).
45. Cariappa, A. *et al.* The Follicular versus Marginal Zone B Lymphocyte Cell Fate Decision Is Regulated by Aiolos, Btk, and CD21. *Immunity* **14**, 603–615 (2001).
46. Pappu, R. Requirement for B Cell Linker Protein (BLNK) in B Cell Development. *Science* **286**, 1949–1954 (1999).
47. Xu, S. B cell development and activation defects resulting in xid-like immunodeficiency in BLNK/SLP-65-deficient mice. *Int. Immunol.* **12**, 397–404 (2000).
48. Rickert, R. C., Rajewsky, K. & Roes, J. Impairment of T-cell-dependent B-cell responses and B-1 cell development in CD19-deficient mice. *Nature* **376**, 352–355 (1995).
49. Sato, S. *et al.* CD22 Is Both a Positive and Negative Regulator of B Lymphocyte Antigen Receptor Signal Transduction: Altered Signaling in CD22-Deficient Mice. *Immunity* **5**, 551–562 (1996).
50. Ujike, A. *et al.* Impaired dendritic cell maturation and increased TH2 responses in PIR-B−/− mice. *Nat Immunol* **3**, 542–548 (2002).
51. Croker, B. A. The Rac2 guanosine triphosphatase regulates B-lymphocyte antigen-receptor responses and chemotaxis and is required for establishment of B-1a and marginal-zone B lymphocytes. *J. Immunol.* **168**, 3376–3386 (2002).
52. Guinamard, R., Okigaki, M., Schlessinger, J. & Ravetch, J. V.

Absence of marginal-zone B cells in Pyk-2-deficient mice defines their role in the humoral response. *Nature Immunol.* **1**, 31–36 (2000).
53. Niiro, H. & Clark, E. A. Regulation of B-cell fate by antigen-receptor signals. *Nat Rev Immunol* **2**, 945–956 (2002).
54. Saito, T. *et al.* Notch2 is preferentially expressed in mature B cells and indispensable for marginal zone B lineage development. *Immunity* **18**, 675–685 (2003).
55. Tanigaki, K. *et al.* Notch-RBP-J signaling is involved in cell fate determination of marginal zone B cells. *Nat Immunol* **3**, 443–450 (2002).
56. Schiemann, B. *et al.* An Essential Role for BAFF in the Normal Development of B Cells Through a BCMA-Independent Pathway. *Science* **293**, 2111–2114 (2001).
57. Ferry, H., Jones, M., Vaux, D. J., Roberts, I. S. D. & Cornall, R. J. The Cellular Location of Self-antigen Determines the Positive and Negative Selection of Autoreactive B Cells. *Journal of Experimental Medicine* **198**, 1415–1425 (2003).
58. Wardemann, H. *et al.* Predominant autoantibody production by early human B cell precursors. *Science* **301**, 1374–1377 (2003).
59. Melamed, D., Benschop, R. J., Cambier, J. C. & Nemazee, D. Developmental regulation of B lymphocyte immune tolerance compartmentalizes clonal selection from receptor selection. *Cell* **92**, 173–182 (1998).
60. Shlomchik, M. J. Sites and Stages of Autoreactive B Cell Activation and Regulation. *Immunity* **28**, 18–28 (2008).
61. Halverson, R., Torres, R. M. & Pelanda, R. Receptor editing is the main mechanism of B cell tolerance toward membrane antigens. *Nat Immunol* **5**, 645–650 (2004).
62. Casellas, R. *et al.* Contribution of receptor editing to the antibody repertoire. *Science* **291**, 1541–1544 (2001).
63. Liu, S. *et al.* Receptor editing can lead to allelic inclusion and development of B cells that retain antibodies reacting with high avidity autoantigens. *Journal of Immunology* **175**, 5067–5076 (2005).
64. Wardemann, H. & Nussenzweig, M. C. B-Cell Self-Tolerance in Humans. *Advances in Immunology* **95**, 83–110 (2007).
65. Boehmer, von, H. & Melchers, F. Checkpoints in lymphocyte development and autoimmune disease. *Nature Publishing Group* **11**, 14–20 (2010).
66. Cambier, J. C., Gauld, S. B., Merrell, K. T. & Vilen, B. J. B-cell anergy: from transgenic models to naturally occurring anergic B cells? *Nat Rev Immunol* **7**, 633–643 (2007).
67. Yarkoni, Y., Getahun, A. & Cambier, J. C. Molecular underpinning of B-cell anergy. *Immunol. Rev.* **237**, 249–263 (2010).
68. Merrell, K. T. *et al.* Identification of Anergic B Cells within a Wild-Type Repertoire. *Immunity* **25**, 953–962 (2006).
69. Nemazee, D. A. & Burki, K. Clonal deletion of B lymphocytes in a transgenic mouse bearing anti-MHC class I antibody genes. *Nature* **337**, 562–566 (1989).
70. Hartley, S. B. *et al.* Elimination from peripheral lymphoid tissues of self-reactive B lymphocytes recognizing membrane-bound antigens. *Nature* **353**, 765–769 (1991).

71. Hardy, R. R. B-1 B cell development. *Journal of Immunology* **177**, 2749–2754 (2006).
72. Jellusova, J., Wellmann, U., Amann, K., Winkler, T. H. & Nitschke, L. CD22 x Siglec-G double-deficient mice have massively increased B1 cell numbers and develop systemic autoimmunity. *The Journal of Immunology* **184**, 3618–3627 (2010).
73. Zhao, D.-M., Thornton, A. M., DiPaolo, R. J. & Shevach, E. M. Activated CD4 +CD25 + T cells selectively kill B lymphocytes. *Blood* **107**, 3925–3932 (2006).
74. Ludwig-Portugall, I., Hamilton-Williams, E. E., Gottschalk, C. & Kurts, C. Cutting edge: CD25+ regulatory T cells prevent expansion and induce apoptosis of B cells specific for tissue autoantigens. *The Journal of Immunology* **181**, 4447–4451 (2008).
75. Ricklin, D., Hajishengallis, G., Yang, K. & Lambris, J. D. Complement: a key system for immune surveillance and homeostasis. *Nature Publishing Group* **11**, 785–797 (2010).
76. Carter, R. H. & Fearon, D. T. CD19: Lowering the threshold for antigen receptor stimulation of B lymphocytes. *Science* **256**, 105–107 (1992).
77. Dempsey, P. W., Allison, M. E., Akkaraju, S., Goodnow, C. C. & Fearon, D. T. C3d of complement as a molecular adjuvant: bridging innate and acquired immunity. *Science* **271**, 348–350 (1996).
78. Carroll, M. The complement system in B cell regulation. *Mol. Immunol.* **41**, 141–146 (2004).
79. Eisen, H. N. & Siskind, G. W. Variations in affinities of antibodies during the immune response. *Biochemistry* **3**, 996–1008 (1964).
80. Benson, M. J., Erickson, L. D., Gleeson, M. W. & Noelle, R. J. Affinity of antigen encounter and other early B-cell signals determine B-cell fate. *Current Opinion in Immunology* **19**, 275–280 (2007).
81. Paus, D. *et al.* Antigen recognition strength regulates the choice between extrafollicular plasma cell and germinal center B cell differentiation. *Journal of Experimental Medicine* **203**, 1081–1091 (2006).
82. Cyster, J. G. Chemokines, sphingosine-1-phosphate, and cell migration in secondary lymphoid organs. *Annu. Rev. Immunol.* **23**, 127–159 (2005).
83. Victora, G. D. *et al.* Germinal center dynamics revealed by multiphoton microscopy with a photactivatable fluorescent reporter. *Cell* **143**, 503–505 (2010).
84. Okada, T. *et al.* Antigen-engaged B cells undergo chemotaxis toward the T zone and form motile conjugates with helper T cells. *PLoS Biology* **3**, 1047–1061 (2005).
85. Cyster, J. G. & Goodnow, C. C. Antigen-induced exclusion from follicles and anergy are separate and complementary processes that influence peripheral B cell fate. *Immunity* **3**, 691–701 (1995).
86. Ekland, E. H., Förster, R., Lipp, M. & Cyster, J. G. Requirements for follicular exclusion and competitive elimination of autoantigen-binding B cells. *J. Immunol.* **172**, 4700–4708 (2004).
87. Coffey, F., Alabyev, B. & Manser, T. Initial Clonal Expansion of Germinal Center B Cells Takes Place at the Perimeter of Follicles. *Immunity* **30**, 599–609 (2009).
88. Kelly, L. M., Xu, Y. & Cyster, J. G. EBI2 mediates B cell segregation between the outer and centre follicle. *Nature* **460**, 1122–1126 (2009).

89. Gatto, D., Paus, D., Basten, A., Mackay, C. R. & Brink, R. Guidance of B Cells by the Orphan G Protein-Coupled Receptor EBI2 Shapes Humoral Immune Responses. *Immunity* **31**, 259–269 (2009).
90. Shaffer, A. L. *et al.* Blimp-1 orchestrates plasma cell differentiation by extinguishing the mature B cell gene expression program. *Immunity* **17**, 51–62 (2002).
91. Shapiro-Shelef, M. & Calame, K. Regulation of plasma-cell development. *Nat Rev Immunol* **5**, 230–242 (2005).
92. Sciammas, R. *et al.* Graded Expression of Interferon Regulatory Factor-4 Coordinates Isotype Switching with Plasma Cell Differentiation. *Immunity* **25**, 225–236 (2006).
93. Saito, M. *et al.* A signaling pathway mediating downregulation of BCL6 in germinal center B cells is blocked by BCL6 gene alterations in B cell lymphoma. *Cancer Cell* **12**, 280–292 (2007).
94. Chan, T. D. *et al.* Antigen Affinity Controls Rapid T-Dependent Antibody Production by Driving the Expansion Rather than the Differentiation or Extrafollicular Migration of Early Plasmablasts. *J. Immunol.* **183**, 3139–3149 (2009).
95. Anderson, S. M. *et al.* Taking advantage: high-affinity B cells in the germinal center have lower death rates, but similar rates of division, compared to low-affinity cells. *The Journal of Immunology* **183**, 7314–7325 (2009).
96. Weigert, M. G., Cesari, I. M., Yonkovich, S. J. & Cohn, M. Variability in the lambda light chain sequences of mouse antibody. *Nature* **228**, 1045–1047 (1970).
97. Berek, C., Berger, A. & Apel, M. Maturation of the immune response in germinal centers. *Cell* **67**, 1121–1129 (1991).
98. Jacob, J., Kelsoe, G., Rajewsky, K. & Weiss, U. Intraclonal generation of antibody mutants in germinal centres. *Nature* **354**, 389–392 (1991).
99. Koni, P. A. & Flavell, R. A. Lymph node germinal centers form in the absence of follicular dendritic cell networks. *J. Exp. Med.* **189**, 855–864 (1999).
100. Wang, Y. *et al.* Antigen persistence is required for somatic mutation and affinity maturation of immunoglobulin. *Eur. J. Immunol.* **30**, 2226–2234 (2000).
101. Blink, E. J. *et al.* Early appearance of germinal center-derived memory B cells and plasma cells in blood after primary immunization. *Journal of Experimental Medicine* **201**, 545–554 (2005).
102. McHeyzer-Williams, L. J., Malapati, S. & McHeyzer-Williams, M. G. Checkpoints in memory B-cell evolution. *Immunol. Rev.* **211**, 255–268 (2006).
103. Nieuwenhuis, P. & Opstelten, D. Functional anatomy of germinal centers. *Am. J. Anat.* **170**, 421–435 (1984).
104. Millikin, P. D. Anatomy of germinal centers in human lymphoid tissue. *Archives of pathology* **82**, 499–505 (1966).
105. Kosco-Vilbois, M. H. Are follicular dendritic cells really good for nothing? *Nat Rev Immunol* **3**, 764–769 (2003).
106. MacLennan, I. C. M. Germinal centers. *Annu. Rev. Immunol.* **12**, 117–139 (1994).
107. Schwickert, T. A. *et al.* In vivo imaging of germinal centres reveals a dynamic open structure. *Nature* **446**, 83–87 (2007).
108. Hauser, A. E. *et al.* Definition of germinal-center B cell migration in

vivo reveals predominant intrazonal circulation patterns. *Immunity* **26**, 655–667 (2007).
109. Naito, Y. ***et al.*** Germinal center marker GL7 probes activation-dependent repression of N-glycolylneuraminic acid, a sialic acid species involved in the negative modulation of B-cell activation. ***Mol. Cell. Biol.*** **27**, 3008–3022 (2007).
110. Green, J. A. ***et al.*** The sphingosine 1-phosphate receptor $S1P_2$ maintains the homeostasis of germinal center B cells and promotes niche confinement. ***Nat Immunol*** **12**, 672–680 (2011).
111. Basso, K. & Dalla-Favera, R. BCL6: master regulator of the germinal center reaction and key oncogene in B cell lymphomagenesis. *Advances in Immunology* **105**, 193–210 (2010).
112. Basso, K. ***et al.*** Integrated biochemical and computational approach identifies BCL6 direct target genes controlling multiple pathways in normal germinal center B cells. ***Blood*** **115**, 975–984 (2010).
113. Allen, C. D. C., Okada, T., Tang, H. L. & Cyster, J. G. Imaging of germinal center selection events during affinity maturation. ***Science*** **315**, 528–531 (2007).
114. Kremmidiotis, G. & Zola, H. Changes in CD44 expression during B cell differentiation in the human tonsil. ***Cellular Immunology*** **161**, 147–157 (1995).
115. Feuillard, J., Taylor, D., Casamayor-Palleja, M., Johnson, G. D. & MacLennan, I. C. Isolation and characteristics of tonsil centroblasts with reference to Ig class switching. ***Int. Immunol.*** **7**, 121–130 (1995).
116. Klein, U. ***et al.*** Transcriptional analysis of the B cell germinal center reaction. ***Proc. Natl. Acad. Sci. U.S.A.*** **100**, 2639–2644 (2003).
117. Nakayama, Y. ***et al.*** A limited number of genes are involved in the differentiation of germinal center B cells. ***J. Cell. Biochem.*** **99**, 1308–1325 (2006).
118. Allen, C. D. C. ***et al.*** Germinal center dark and light zone organization is mediated by CXCR4 and CXCR5. ***Nat Immunol*** **5**, 943–952 (2004).
119. Kocks, C. R. K. Stepwise intraclonal maturation of antibody affinity through somatic hypermutation. ***Proc. Natl. Acad. Sci. U.S.A.*** **85**, 8206–8210 (1988).
120. Brown, M., Stenzel-Poore, M., Stevens, S., Kondoleon, S. K., Ng, J., Bachinger, H. P. & Rittenberg, M.B. Immunologic memory to phosphocholine keyhole limpet hemocyanin: Recurrent mutations in the λ1 light chain increase affinity for antigen. ***Journal of Immunology*** **148**, 339–346 (1992).
121. Mandel, T. E., Phipps, R. P., Abbot, A. P. & Tew, J. G. Long-term antigen retention by dendritic cells in the popliteal lymph node of immunized mice. ***Immunology*** **43**, 353–362 (1981).
122. Szakal, A. K., Gieringer, R. L., Kosco, M. H. & Tew, J. G. Isolated follicular dendritic cells: cytochemical antigen localization, Nomarski, SEM, and TEM morphology. ***J. Immunol.*** **134**, 1349–1359 (1985).
123. Victoratos, P. ***et al.*** FDC-Specific Functions of p55TNFR and IKK2 in the Development of FDC Networks and of Antibody Responses. ***Immunity*** **24**, 65–77 (2006).
124. Wu, Y. ***et al.*** IL-6 produced by immune complex-activated follicular dendritic cells promotes germinal center reactions, IgG responses and somatic hypermutation. ***Int. Immunol.*** **21**, 745–756 (2009).
125. Suzuki, K. ***et al.*** The sensing of environmental stimuli by follicular

dendritic cells promotes immunoglobulin A generation in the gut. *Immunity* **33**, 71–83 (2010).
126. Pasparakis, M., Alexopoulou, L., Episkopou, V. & Kollias, G. Immune and inflammatory responses in TNF alpha-deficient mice: a critical requirement for TNF alpha in the formation of primary B cell follicles, follicular dendritic cell networks and germinal centers, and in the maturation of the humoral immune response. *J. Exp. Med.* **184**, 1397–1411 (1996).
127. Le Hir, M. *et al.* Differentiation of follicular dendritic cells and full antibody responses require tumor necrosis factor receptor-1 signaling. *J. Exp. Med.* **183**, 2367–2372 (1996).
128. Gunn, M. D. *et al.* A B-cell-homing chemokine made in lymphoid follicles activates Burkitt's lymphoma receptor-1. *Nature* **391**, 799–803 (1998).
129. Szakal, A. K., Kosco, M. H. & Tew, J. G. A novel in vivo follicular dendritic cell-dependent iccosome-mediated mechanism for delivery of antigen to antigen-processing cells. *J. Immunol.* **140**, 341–353 (1988).
130. Scheidegger, M. H. & Kosco-Vilbois, D. Follicular dendritic cells: Antigen retention, B cell activation, and cytokine production. *Current Topics in Microbiology and Immunology* **201**, 69–82 (1995).
131. Crotty, S. Follicular Helper CD4 T cells (T FH). *Annu. Rev. Immunol.* **29**, 621–663 (2011).
132. Rolf, J. *et al.* Phosphoinositide 3-kinase activity in T cells regulates the magnitude of the germinal center reaction. *Journal of Immunology* **185**, 4042–4052 (2010).
133. Vinuesa, C. G., Tangye, S. G., Moser, B. & Mackay, C. R. Follicular B helper T cells in antibody responses and autoimmunity. *Nat Rev Immunol* **5**, 853–865 (2005).
134. Kim, C. H. *et al.* Subspecialization of CXCR5+ T cells: B helper activity is focused in a germinal center-localized subset of CXCR5+ T cells. *J. Exp. Med.* **193**, 1373–1381 (2001).
135. Hsu, H.-C. *et al.* Interleukin 17-producing T helper cells and interleukin 17 orchestrate autoreactive germinal center development in autoimmune BXD2 mice. *Nature Publishing Group* **9**, 166–175 (2008).
136. Alexander, C.-M. *et al.* T regulatory cells participate in the control of germinal centre reactions. *Immunology* **133**, 452–468 (2011).
137. Hanayama, R. *et al.* Autoimmune disease and impaired uptake of apoptotic cells in MFG-E8-deficient mice. *Science* **304**, 1147–1150 (2004).
138. Liu, Y. J. *et al.* Mechanism of antigen-driven selection in germinal centres. *Nature* **342**, 929–931 (1989).
139. Allen, C. D. C., Okada, T. & Cyster, J. G. Germinal-center organization and cellular dynamics. *Immunity* **27**, 190–202 (2007).
140. Meyer-Hermann, M. E., Maini, P. K. & Iber, D. An analysis of B cell selection mechanisms in germinal centers. *Mathematical Medicine and Biology* **23**, 255–277 (2006).
141. Depoil, D. *et al.* Immunological synapses are versatile structures enabling selective T cell polarization. *Immunity* **22**, 185–194 (2005).
142. Reinhardt, R. L., Liang, H.-E. & Locksley, R. M. Cytokine-secreting

follicular T cells shape the antibody repertoire. *Nat Immunol* **10**, 385–393 (2009).
143. Draghi, N. A. & Denzin, L. K. H2-O, a MHC class II-like protein, sets a threshold for B-cell entry into germinal centers. *PNAS* **107**, 16607–16612 (2010).
144. Fang, Y., Xu, C., Fu, Y.-X., Holers, V. M. & Molina, H. Expression of complement receptors 1 and 2 on follicular dendritic cells is necessary for the generation of a strong antigen-specific IgG response. *J. Immunol.* **160**, 5273–5279 (1998).
145. Huntington, N. D. *et al.* CD45 links the B cell receptor with cell survival and is required for the persistence of germinal centers. *Nat Immunol* **7**, 190–198 (2006).
146. Glazier, K. S. *et al.* Germinal center B cells regulate their capability to present antigen by modulation of HLA-DO. *J. Exp. Med.* **195**, 1063–1069 (2002).
147. Chalouni, C., Banchereau, J., Vogt, A. B., Pascual, V. & Davoust, J. Human germinal center B cells differ from naive and memory B cells by their aggregated MHC class II-rich compartments lacking HLA-DO. *Int. Immunol.* **15**, 457–466 (2003).
148. Yoshino, T. *et al.* Inverse expression of bcl-2 protein and Fas antigen in lymphoblasts in peripheral lymph nodes and activated peripheral blood T and B lymphocytes. *Blood* **83**, 1856–1861 (1994).
149. Haynes, N. M. *et al.* Role of CXCR5 and CCR7 in follicular Th cell positioning and appearance of a programmed cell death gene-1high germinal center-associated subpopulation. *The Journal of Immunology* **179**, 5099–5108 (2007).
150. Marinova, E., Han, S. & Zheng, B. Germinal center helper T cells are dual functional regulatory cells with suppressive activity to conventional CD4+ T cells. *J. Immunol.* **178**, 5010–5017 (2007).
151. Barber, D. L. *et al.* Restoring function in exhausted CD8 T cells during chronic viral infection. *Nature* **439**, 682–687 (2006).
152. Day, C. L. *et al.* PD-1 expression on HIV-specific T cells is associated with T-cell exhaustion and disease progression. *Nature* **443**, 350–354 (2006).
153. Fleire, S. J. *et al.* B cell ligand discrimination through a spreading and contraction response. *Science* **312**, 738–741 (2006).
154. Carter, R. H. & Myers, R. Germinal center structure and function: lessons from CD19. *Seminars in Immunology* **20**, 43–48 (2008).
155. Healy, J. I. & Goodnow, C. C. Positive versus negative signaling by lymphocyte antigen receptors. *Annu. Rev. Immunol.* **16**, 645–670 (1998).
156. Hardy, R. R. & Hayakawa, K. B cell development pathways. *Annu. Rev. Immunol.* **19**, 595–621 (2001).
157. Cheng, A. M. *et al.* Syk tyrosine kinase required for mouse viability and B-cell development. *Nature* **378**, 303–306 (1995).
158. Turner, M. *et al.* Perinatal lethality and blocked B-cell development in mice lacking the tyrosine kinase Syk. *Nature* **378**, 298–302 (1995).
159. Lam, K.-P., Kühn, R. & Rajewsky, K. In vivo ablation of surface immunoglobulin on mature B cells by inducible gene targeting results in rapid cell death. *Cell* **90**, 1073–1083 (1997).
160. Srinivasan, L. *et al.* PI3 kinase signals BCR-dependent mature B cell

survival. *Cell* **139**, 573–586 (2009).
161. Tolar, P., Sohn, H. W. & Pierce, S. K. The initiation of antigen-induced B cell antigen receptor signaling viewed in living cells by fluorescence resonance energy transfer. *Nat Immunol* **6**, 1168–1176 (2005).
162. Pierce, S. K. & Liu, W. The tipping points in the initiation of B cell signalling: how small changes make big differences. *Nat Rev Immunol* **10**, 767–777 (2010).
163. Batista, F. D., Iber, D. & Neuberger, M. S. B cells acquire antigen from target cells after synapse formation. *Nature* **411**, 489–494 (2001).
164. Kurosaki, T. & Hikida, M. Tyrosine kinases and their substrates in B lymphocytes. *Immunol. Rev.* **228**, 132–148 (2009).
165. Kurosaki, T. *et al.* Syk activation by the Src-family tyrosine kinase in the B cell receptor signaling. *J. Exp. Med.* **179**, 1725–1729 (1994).
166. Ishiai, M., Sugawara, H., Kurosaki, M. & Kurosaki, T. Cutting edge: association of phospholipase C-gamma 2 Src homology 2 domains with BLNK is critical for B cell antigen receptor signaling. *J. Immunol.* **163**, 1746–1749 (1999).
167. Kurosaki, T. Regulation of B-cell signal transduction by adaptor proteins. *Nat Rev Immunol* **2**, 354–363 (2002).
168. King, L. B. & Freedman, B. D. B-lymphocyte calcium influx. *Immunol. Rev.* **231**, 265–277 (2009).
169. Crabtree, G. R. & Olson, E. N. NFAT signaling: choreographing the social lives of cells. *Cell* **109 Suppl**, S67–S79 (2002).
170. Macian, F. NFAT proteins: key regulators of T-cell development and function. *Nat Rev Immunol* **5**, 472–484 (2005).
171. Ogawa, Y., Takai, Y., Kawahara, Y., Kimura, S. & Nishizuka, Y. A new possible regulatory system for protein phosphorylation in human peripheral lymphocytes. I. Characterization of a calcium-activated, phospholipid-dependent protein kinase. *J. Immunol.* **127**, 1369–1374 (1981).
172. Saijo, K. *et al.* Protein Kinase C beta Controls Nuclear Factor kappaB Activation in B Cells Through Selective Regulation of the IkappaB Kinase alpha. *Journal of Experimental Medicine* **195**, 1647–1652 (2002).
173. Thome, M. CARMA1, BCL-10 and MALT1 in lymphocyte development and activation. *Nat Rev Immunol* **4**, 348–359 (2004).
174. Grossmann, M. *et al.* The anti-apoptotic activities of Rel and RelA required during B-cell maturation involve the regulation of Bcl-2 expression. *EMBO Journal* **19**, 6351–6360 (2000).
175. Grumont, R. J., Rourke, I. J. & Gerondakis, S. Rel-dependent induction of A1 transcription is required to protect B cells from antigen receptor ligation-induced apoptosis. *Genes and Development* **13**, 400–411 (1999).
176. Gerondakis, S., Grossmann, M., Nakamura, Y., Pohl, T. & Grumont, R. Genetic approaches in mice to understand Rel/NF-kappaB and IkappaB function: transgenics and knockouts. *Oncogene* **18**, 6888–6895 (1999).
177. Yasuda, T. & Kurosaki, T. Regulation of lymphocyte fate by Ras/ERK signals. *Cell Cycle* **7**, 3634–3640 (2008).
178. Richards, J. D., Davé, S. H., Chou, C. H., Mamchak, A. A. & DeFranco, A. L. Inhibition of the MEK/ERK signaling pathway blocks a

subset of B cell responses to antigen. *J. Immunol.* **166**, 3855–3864 (2001).
179. Ishiura, N. *et al.* Differential phosphorylation of functional tyrosines in CD19 modulates B-lymphocyte activation. *Eur. J. Immunol.* **40**, 1192–1204 (2010).
180. Tybulewicz, V. L. J. & Henderson, R. B. Rho family GTPases and their regulators in lymphocytes. *Nat Rev Immunol* **9**, 630–644 (2009).
181. Weber, M. *et al.* Phospholipase C-γ2 and Vav cooperate within signaling microclusters to propagate B cell spreading in response to membrane-bound antigen. *Journal of Experimental Medicine* **205**, 853–868 (2008).
182. Arana, E. *et al.* Activation of the small GTPase Rac2 via the B cell receptor regulates B cell adhesion and immunological-synapse formation. *Immunity* **28**, 88–99 (2008).
183. Doody, G. M. Signal transduction through Vav-2 participates in humoral immune responses and B-cell maturation. *Nature Immunol.* **2**, 542–547 (2001).
184. Tedford, K. *et al.* Compensation between Vav-1 and Vav-2 in B cell development and antigen receptor signaling. *Nat Immunol* **2**, 548–555 (2001).
185. Vigorito, E., Gambardella, L., Colucci, F., McAdam, S. & Turner, M. Vav proteins regulate peripheral B-cell survival. *Blood* **106**, 2391–2398 (2005).
186. Fujikawa, K. *et al.* Vav1/2/3-null mice define an essential role for Vav family proteins in lymphocyte development and activation but a differential requirement in MAPK signaling in T and B cells. *Journal of Experimental Medicine* **198**, 1595–1608 (2003).
187. Lemmon, M. A., Ferguson, K. M. & Schlessinger, J. PH domains: diverse sequences with a common fold recruit signaling molecules to the cell surface. *Cell* **85**, 621–624 (1996).
188. Okada, T., Maeda, A., Iwamatsu, A., Gotoh, K. & Kurosaki, T. BCAP: The tyrosine kinase substrate that connects B cell receptor to phosphoinositide 3-kinase activation. *Immunity* **13**, 817–827 (2000).
189. Aiba, Y., Kameyama, M., Yamazaki, T., Tedder, T. F. & Kurosaki, T. Regulation of B-cell development by BCAP and CD19 through their binding to phosphoinositide 3-kinase. *Blood* **111**, 1497–1503 (2008).
190. Calamito, M. *et al.* Akt1 and Akt2 promote peripheral B-cell maturation and survival. *Blood* **115**, 4043–4050 (2010).
191. Gold, M. R. *et al.* The B cell antigen receptor activates the Akt (protein kinase B)/glycogen synthase kinase-3 signaling pathway via phosphatidylinositol 3-kinase. *J. Immunol.* **163**, 1894–1905 (1999).
192. Birkenkamp, K. U. & Coffer, P. J. FOXO transcription factors as regulators of immune homeostasis: molecules to die for? *J. Immunol.* **171**, 1623–1629 (2003).
193. Dijkers, P. F., Medema, R. H., Lammers, J. W., Koenderman, L. & Coffer, P. J. Expression of the pro-apoptotic Bcl-2 family member Bim is regulated by the forkhead transcription factor FKHR-L1. *Curr. Biol.* **10**, 1201–1204 (2000).
194. Dijkers, P. F. *et al.* Forkhead transcription factor FKHR-L1 modulates cytokine-dependent transcriptional regulation of p27(KIP1). *Mol. Cell. Biol.* **20**, 9138–9148 (2000).
195. Chen, J., Yusuf, I., Andersen, H.-M. & Fruman, D. A. FOXO

transcription factors cooperate with delta EF1 to activate growth suppressive genes in B lymphocytes. *J. Immunol.* **176**, 2711–2721 (2006).
196. Hinman, R. M., Bushanam, J. N., Nichols, W. A. & Satterthwaite, A. B. B cell receptor signaling down-regulates forkhead box transcription factor class O 1 mRNA expression via phosphatidylinositol 3-kinase and Bruton's tyrosine kinase. *J. Immunol.* **178**, 740–747 (2007).
197. Niiro, H., Maeda, A., Kurosaki, T. & Clark, E. A. The B Lymphocyte Adaptor Molecule of 32 kD (Bam32) Regulates B Cell Antigen Receptor Signaling and Cell Survival. *Journal of Experimental Medicine* **195**, 143–149 (2002).
198. Marshall, A. J. *et al.* A Novel B Lymphocyte-Associated Adaptor Protein, Bam32, Regulates Antigen Receptor Signaling Downstream of Phosphatidylinositol 3-Kinase. *Journal of Experimental Medicine* **191**, 1319–1332 (2000).
199. Chacko, G. W. *et al.* Negative signaling in B lymphocytes induces tyrosine phosphorylation of the 145-kDa inositol polyphosphate 5-phosphatase, SHIP. *J. Immunol.* **157**, 2234–2238 (1996).
200. Maeda, A. *et al.* Paired immunoglobulin-like receptor B (PIR-B) inhibits BCR-induced activation of Syk and Btk by SHP-1. *Oncogene* **18**, 2291–2297 (1999).
201. Stork, B. *et al.* Subcellular localization of Grb2 by the adaptor protein Dok-3 restricts the intensity of Ca 2+ signaling in B cells. *EMBO Journal* **26**, 1140–1149 (2007).
202. Berridge, M. J., Bootman, M. D. & Roderick, H. L. Calcium signalling: Dynamics, homeostasis and remodelling. *Nat. Rev. Mol. Cell Biol.* **4**, 517–529 (2003).
203. Parekh, A. B. & Putney, J. W., Jr Store-operated calcium channels. *Physiological Reviews* **85**, 757–810 (2005).
204. Putney, J. W., Jr A model for receptor-regulated calcium entry. *Cell Calcium* **7**, 1–12 (1986).
205. Lewis, R. S. *Calcium signaling mechanisms in T lymphocytes*. *Annual Review of Immunology* **19**, 497–521 (2001).
206. Roos, J. *et al.* STIM1, an essential and conserved component of store-operated Ca 2+ channel function. *Journal of Cell Biology* **169**, 435–445 (2005).
207. Liou, J. *et al.* STIM is a Ca2+ sensor essential for Ca2+-store-depletion-triggered Ca2+ influx. *Current Biology* **15**, 1235–1241 (2005).
208. Baba, Y. & Kurosaki, T. Physiological function and molecular basis of STIM1-mediated calcium entry in immune cells. *Immunol. Rev.* **231**, 174–188 (2009).
209. Hogan, P. G., Lewis, R. S. & Rao, A. Molecular basis of calcium signaling in lymphocytes: STIM and ORAI. *Annu. Rev. Immunol.* **28**, 491–533 (2010).
210. Fujimoto, M., Poe, J. C., Hasegawa, M. & Tedder, T. F. CD19 Amplification of B Lymphocyte Ca2+ Responses: A role for Lyn sequestration in extinguishing negative regulation. *Journal of Biological Chemistry* **276**, 44820–44827 (2001).
211. Chen, J. *et al.* CD22 attenuates calcium signaling by potentiating plasma membrane calcium-ATPase activity. *Nat Immunol* **5**, 651–657

(2004).
212. Horikawa, K. ***et al.*** Enhancement and suppression of signaling by the conserved tail of IgG memory-type B cell antigen receptors. ***Journal of Experimental Medicine*** **204**, 759–769 (2007).
213. Engels, N. ***et al.*** Recruitment of the cytoplasmic adaptor Grb2 to surface IgG and IgE provides antigen receptor-intrinsic costimulation to class-switched B cells. ***Nat Immunol*** **10**, 1018–1025 (2009).
214. Feske, S. Calcium signalling in lymphocyte activation and disease. ***Nat Rev Immunol*** **7**, 690–702 (2007).
215. Shultz, L. D., Rajan, T. V. & Greiner, D. L. Severe defects in immunity and hematopoiesis caused by SHP-1 protein- tyrosine-phosphatase deficiency. ***Trends in Biotechnology*** **15**, 302–307 (1997).
216. Nitschke, L. The role of CD22 and other inhibitory co-receptors in B-cell activation. ***Current Opinion in Immunology*** **17**, 290–297 (2005).
217. Bolland, S. & Ravetch, J. V. Spontaneous autoimmune disease in FcγRIIB-deficient mice results from strain-specific epistasis. ***Immunity*** **13**, 277–285 (2000).
218. Enyedy, E. J., Mitchell, J. P., Nambiar, M. P. & Tsokos, G. C. Defective FcγRIIb1 signaling contributes to enhanced calcium response in B cells from patients with systemic lupus erythematosus. ***Clinical Immunology*** **101**, 130–135 (2001).
219. Yu, P. ***et al.*** Autoimmunity and inflammation due to a gain-of-function mutation in phospholipase Cγ2 that specifically increases external Ca 2+ entry. ***Immunity*** **22**, 451–465 (2005).
220. Picard, C. ***et al.*** STIM1 mutation associated with a syndrome of immunodeficiency and autoimmunity. ***New England Journal of Medicine*** **360**, 1971–1980 (2009).
221. Feske, S., Picard, C. & Fischer, A. Immunodeficiency due to mutations in ORAI1 and STIM1. ***Clinical Immunology*** **135**, 169–182 (2010).
222. Matsumoto, M. ***et al.*** The calcium sensors STIM1 and STIM2 control B cell regulatory function through interleukin-10 production. ***Immunity*** **34**, 703–714 (2011).
223. Limnander, A. ***et al.*** STIM1, PKC-δ and RasGRP set a threshold for proapoptotic Erk signaling during B cell development. ***Nature Publishing Group*** **12**, 425–433 (2011).
224. Lazarus, A. H., Kawauchi, K., Rapoport, M. J. & Delovitch, T. L. Antigen-induced B lymphocyte activation involves the p21ras and ras.GAP signaling pathway. ***J. Exp. Med.*** **178**, 1765–1769 (1993).
225. Harwood, A. E. & Cambier, J. C. B cell antigen receptor cross-linking triggers rapid protein kinase C independent activation of p21ras1. ***J. Immunol.*** **151**, 4513–4522 (1993).
226. Bell, S. E. ***et al.*** PLCgamma2 regulates Bcl-2 levels and is required for survival rather than differentiation of marginal zone and follicular B cells. ***Eur. J. Immunol.*** **34**, 2237–2247 (2004).
227. Saxton, T. M., Van Oostveen, I., Bowtell, D., Aebersold, R. & Gold, M. R. B cell antigen receptor cross-linking induces phosphorylation of the p21(ras) oncoprotein activators SHC and mSOS1 as well as assembly of complexes containing SHC, GRB-2, mSOS1, and a 145-kDa tyrosine-phosphorylated protein. ***Journal of Immunology*** **153**, 623–636 (1994).
228. D'Ambrosio, D., Hippen, K. L. & Cambier, J. C. Distinct mechanisms

mediate SHC association with the activated and resting B cell antigen receptor. *Eur. J. Immunol.* **26**, 1960–1965 (1996).
229. Margarit, S. M. *et al.* Structural evidence for feedback activation by Ras.GTP of the Ras-specific nucleotide exchange factor SOS. *Cell* **112**, 685–695 (2003).
230. Roose, J. P., Mollenauer, M., Ho, M., Kurosaki, T. & Weiss, A. Unusual interplay of two types of Ras activators, RasGRP and SOS, establishes sensitive and robust Ras activation in lymphocytes. *Mol. Cell. Biol.* **27**, 2732–2745 (2007).
231. Boykevisch, S. *et al.* Regulation of ras signaling dynamics by Sos-mediated positive feedback. *Curr. Biol.* **16**, 2173–2179 (2006).
232. Aiba, Y. *et al.* Activation of RasGRP3 by phosphorylation of Thr-133 is required for B cell receptor-mediated Ras activation. *Proc. Natl. Acad. Sci. U.S.A.* **101**, 16612–16617 (2004).
233. Zheng, Y. *et al.* Phosphorylation of RasGRP3 on threonine 133 provides a mechanistic link between PKC and Ras signaling systems in B cells. *Blood* **105**, 3648–3654 (2005).
234. Benschop, R. J., Brandl, E., Chan, A. C. & Cambier, J. C. Unique signaling properties of B cell antigen receptor in mature and immature B cells: implications for tolerance and activation. *J. Immunol.* **167**, 4172–4179 (2001).
235. Gross, A. J., Lyandres, J. R., Panigrahi, A. K., Prak, E. T. L. & DeFranco, A. L. Developmental acquisition of the Lyn-CD22-SHP-1 inhibitory pathway promotes B cell tolerance. *The Journal of Immunology* **182**, 5382–5392 (2009).
236. Hoek, K. L. *et al.* Transitional B cell fate is associated with developmental stage-specific regulation of diacylglycerol and calcium signaling upon B cell receptor engagement. *J. Immunol.* **177**, 5405–5413 (2006).
237. King, L. B., Norvell, A. & Monroe, J. G. Antigen-receptor-induced signal-transduction imbalances associated with the negative selection of immature B cells. *J. Immunol.* **162**, 2655–2662 (1999).
238. Guilbault, B. & Kay, R. J. RasGRP1 sensitizes an immature B cell line to antigen receptor-induced apoptosis. *J Biol Chem* **279**, 19523–19530 (2004).
239. Stang, S. L. *et al.* A proapoptotic signaling pathway involving RasGRP, Erk, and Bim in B cells. *Exp. Hematol.* **37**, 122–134 (2009).
240. Daniels, M. A. *et al.* Thymic selection threshold defined by compartmentalization of Ras/MAPK signalling. *Nature* **444**, 724–729 (2006).
241. Mor, A. & Philips, M. R. Compartmentalized Ras/MAPK signaling. *Annu. Rev. Immunol.* **24**, 771–800 (2006).
242. Choy, E. *et al.* Endomembrane trafficking of ras: the CAAX motif targets proteins to the ER and Golgi. *Cell* **98**, 69–80 (1999).
243. Rocks, O. *et al.* An acylation cycle regulates localization and activity of palmitoylated Ras isoforms. *Science* **307**, 1746–1752 (2005).
244. Philips, M. R. Sef: a MEK/ERK catcher on the Golgi. *Mol. Cell* **15**, 168–169 (2004).
245. Bivona, T. G. *et al.* Phospholipase Cgamma activates Ras on the Golgi apparatus by means of RasGRP1. *Nature* **424**, 694–698 (2003).
246. Chiu, V. K. *et al.* Ras signalling on the endoplasmic reticulum and the

Golgi. *Nat. Cell Biol.* **4**, 343–350 (2002).
247. Singer, A., Adoro, S. & Park, J.-H. Lineage fate and intense debate: myths, models and mechanisms of CD4- versus CD8-lineage choice. *Nat Rev Immunol* **8**, 788–801 (2008).
248. Lowenstein, E. J. *et al.* The SH2 and SH3 domain-containing protein GRB2 links receptor tyrosine kinases to ras signaling. *Cell* **70**, 431–442 (1992).
249. Matuoka, K., Shibata, M., Yamakawa, A. & Takenawa, T. Cloning of ASH, a ubiquitous protein composed of one Src homology region (SH) 2 and two SH3 domains, from human and rat cDNA libraries. *Proc. Natl. Acad. Sci. U.S.A.* **89**, 9015–9019 (1992).
250. Feng, G.-S. *et al.* Grap is a novel SH3-SH2-SH3 adaptor protein that couples tyrosine kinases to the Ras pathway. *Journal of Biological Chemistry* **271**, 12129–12132 (1996).
251. Liu, S. K. & McGlade, C. J. Gads is a novel SH2 and SH3 domain-containing adaptor protein that binds to tyrosine-phosphorylated Shc. *Oncogene* **17**, 3073–3082 (1998).
252. Law, C.-L. *et al.* GrpL, a Grb2-related adaptor protein, interacts with SLP-76 to regulate nuclear factor of activated T cell activation. *Journal of Experimental Medicine* **189**, 1243–1253 (1999).
253. Bourette, R. P. *et al.* Mona, a novel hematopoietic-specific adaptor interacting with the macrophage colony-stimulating factor receptor, is implicated in monocyte/macrophage development. *EMBO Journal* **17**, 7273–7281 (1998).
254. Ellis, J. H. *et al.* GRID: A novel GrB-2-related adapter protein that interacts with the activated T cell costimulatory receptor CD28. *Journal of Immunology* **164**, 5805–5814 (2000).
255. Asada, H. *et al.* Grf40, a novel Grb2 family member, is involved in T cell signaling through interaction with SLP-76 and LAT. *Journal of Experimental Medicine* **189**, 1383–1390 (1999).
256. Qiu, M. *et al.* Molecular cloning and expression of human Grap-2, a novel leukocyte-specific SH2- and SH3-containing adaptor-like protein that binds to Gab-1. *Biochem. Biophys. Res. Commun.* **253**, 443–447 (1998).
257. Maignan, S. *et al.* Crystal structure of the mammalian Grb2 adaptor. *Science* **268**, 291–293 (1995).
258. Yuzawa, S. *et al.* Solution structure of Grb2 reveals extensive flexibility necessary for target recognition. *J. Mol. Biol.* **306**, 527–537 (2001).
259. Kessels, H. W. H. G., Ward, A. C. & Schumacher, T. N. M. Specificity and affinity motifs for Grb2 SH2-ligand interactions. *Proc. Natl. Acad. Sci. U.S.A.* **99**, 8524–8529 (2002).
260. Sparks, A. B. *et al.* Distinct ligand preferences of Src homology 3 domains from Src, Yes, Abl, Cortactin, p53bp2, PLCγ, Crk, and Grb2. *Proc. Natl. Acad. Sci. U.S.A.* **93**, 1540–1544 (1996).
261. Harkiolaki, M. *et al.* Distinct Binding Modes of Two Epitopes in Gab2 that Interact with the SH3C Domain of Grb2. *Structure/Folding and Design* **17**, 809–822 (2009).
262. Isnardi, I. *et al.* Two distinct tyrosine-based motifs enable the inhibitory receptor FčRIIB to cooperatively recruit the inositol phosphatases SHIP1/2 and the adapters Grb2/Grap. *Journal of Biological Chemistry* **279**, 51931–51938 (2004).

263. Otipoby, K. L., Draves, K. E. & Clark, E. A. CD22 Regulates B Cell Receptor-mediated Signals via Two Domains That Independently Recruit Grb2 and SHP-1. *Journal of Biological Chemistry* **276**, 44315–44322 (2001).
264. Lemay, S., Davidson, D., Latour, S. & Veillette, A. Dok-3, a novel adapter molecule involved in the negative regulation of immunoreceptor signaling. *Mol. Cell. Biol.* **20**, 2743–2754 (2000).
265. Brooks, S. R., Kirkham, P. M., Freeberg, L. & Carter, R. H. Binding of cytoplasmic proteins to the CD19 intracellular domain is high affinity, competitive, and multimeric. *Journal of Immunology* **172**, 7556–7564 (2004).
266. Johmura, S. *et al.* Regulation of Vav localization in membrane rafts by adaptor molecules Grb2 and BLNK. *Immunity* **18**, 777–787 (2003).
267. Stork, B. *et al.* Grb2 and the non-T cell activation linker ntal constitute a Ca 2+-regulating signal circuit in B lymphocytes. *Immunity* **21**, 681–691 (2004).
268. Engelke, M., Engels, N., Dittmann, K., Stork, B. & Wienands, J. Ca(2+) signaling in antigen receptor-activated B lymphocytes. *Nat Rev Immunol* **218**, 778–789 (2007).
269. Horejsí, V., Zhang, W. & Schraven, B. Transmembrane adaptor proteins: Organizers of immunoreceptor signalling. *Nat Rev Immunol* **4**, 603–616 (2004).
270. Ackermann, J. A., Radtke, D., Maurberger, A., Winkler, T. H. & Nitschke, L. Grb2 regulates B-cell maturation, B-cell memory responses and inhibits B-cell Ca2+ signalling. *EMBO J.* **30**, 1621–1633 (2011).
271. Niiro, H. & Clark, E. A. Decision making in the Immune System: Regulation of B-cell fate by antigen-receptor signals. *Nat Rev Immunol* **2**, 945–956 (2002).
272. Gong, Q. *et al.* Disruption of T cell signaling networks and development by Grb2 haploid insufficiency. *Nat Immunol* **2**, 29–36 (2001).
273. Jang, I. K. *et al.* Grb2 functions at the top of the T-cell antigen receptor-induced tyrosine kinase cascade to control thymic selection. *PNAS* **107**, 10620–10625 (2010).
274. Brink, R., Phan, T. G., Paus, D. & Chan, T. D. Visualizing the effects of antigen affinity on T-dependent B-cell differentiation. *Immunol Cell Biol* **86**, 31–39 (2007).
275. Cornall, R. J. *et al.* Polygenic autoimmune traits: Lyn, CD22, and SHP-1 are limiting elements of a biochemical pathway regulating BCR signaling and selection. *Immunity* **8**, 497–508 (1998).
276. Cyster, J. G. *et al.* Regulation of B-lymphocyte negative and positive selection by tyrosine phosphatase CD45. *Nature* **381**, 325–328 (1996).
277. Henson, S. M., Pido-Lopez, J. & Aspinall, R. Reversal of thymic atrophy. *Exp. Gerontol.* **39**, 673–678 (2004).
278. Sempowski, G. D., Gooding, M. E., Liao, H. X., Le, P. T. & Haynes, B. F. T cell receptor excision circle assessment of thymopoiesis in aging mice. *Mol. Immunol.* **38**, 841–848 (2002).
279. Zikherman, J., Parameswaran, R. & Weiss, A. Endogenous antigen tunes the responsiveness of naive B cells but not T cells. *Nature* **489**, 160–164 (2012).
280. Ferry, H., Crockford, T. L., Leung, J. C. H. & Cornall, R. J. Signals

from a self-antigen induce positive selection in early B cell ontogeny but are tolerogenic in adults. ***J. Immunol.*** **176**, 7402–7411 (2006).
281. Zhang, W. ***et al.*** Essential role of LAT in T cell development. ***Immunity*** **10**, 323–332 (1999).
282. Zhu, M., Liu, Y., Koonpaew, S., Granillo, O. & Zhang, W. Positive and negative regulation of FcepsilonRI-mediated signaling by the adaptor protein LAB/NTAL. ***J. Exp. Med.*** **200**, 991–1000 (2004).
283. Cyster, J. Protein tyrosine phosphatase 1C negatively regulates antigen receptor signaling in B lymphocytes and determines thresholds for negative selection. ***Immunity*** **2**, 13–24 (1995).